

Department of Mathematics
University of Fribourg (Switzerland)

New Contributions to Groups of Hyperbolic Isometries

THESIS

presented to the Faculty of Science and Medicine of the University of Fribourg (Switzerland)
in consideration for the award of the academic grade of
Doctor of Philosophy in Mathematics

by

Simon T. Drewitz

from

Germany

Thesis No: 7817
Uniprint Fribourg
2021

Accepted by the Faculty of Science and Medicine of the University of Fribourg (Switzerland)
upon the recommendation of the jury:

Prof. Dr. Christian Mazza
University of Fribourg (Switzerland), President of the jury

Prof. Dr. Ruth Kellerhals
University of Fribourg (Switzerland), Thesis supervisor

Dr. Brent Everitt
York University (United Kingdom), Referee

Prof. Dr. John R. Parker
Durham University (United Kingdom), Referee

Prof. Dr. Alan Reid
Rice University (United States of America), Referee

Fribourg, 5 October 2021

Thesis supervisor

Dean

Prof. Dr. Ruth Kellerhals

Prof. Dr. Gregor Rainer

'You can't mess with geometry, friend. Pyramids?
Dangerous things. Asking for trouble.'

Pthagonal
— Terry Pratchett, Pyramids

Für Nael

Abstract

This thesis contains several new results on hyperbolic geometry.

The main outcome is the identification of the smallest non-arithmetic cusped hyperbolic 3-orbifold as the quotient of hyperbolic 3-space by the Coxeter group $[5, 3, 6]$ using geometric and combinatorial considerations on horoball packings (joint with Ruth Kellerhals).

The same tools are used to establish that the Coxeter group $[5, \infty]$ yields the smallest non-arithmetic cusped hyperbolic 2-orbifold. This gives a Siegel type result by providing a list of all cusped hyperbolic 2-orbifolds with area less than $\frac{\pi}{2}$.

Another perspective concerns compact hyperbolic 2-orbifolds realising minimal area hyperbolic n -gons as a fundamental polygon for $n > 6$. We consider stabiliser subgroups of the Coxeter groups $[n, 3]$ acting on appropriately chosen graphs. Where possible, we describe 2-manifolds by means of torsion-free subgroups thereof. In this way we complete previous work of Matthieu Jacquemet.

These methods are also used to demonstrate that smallest non-arithmetic cusped hyperbolic 3-manifolds covering a Coxeter orbifold cannot be based on $[5, 3, 6]$. In fact, the Coxeter group $[(3^3, 6)]$ yields a smaller manifold cover.

In higher dimensional hyperbolic space we construct right-angled p -gons by utilising the upper half space model based on Clifford vectors (joint with Edoardo Dotti). The main idea of analysing orthogonal geodesics using cross ratios is helpful through most parts of this thesis.

Zusammenfassung

Diese Doktorarbeit behandelt verschiedene neue Resultate der hyperbolischen Geometrie.

Das Haupttheorem identifiziert den Quotienten des hyperbolischen 3-Raumes nach der Coxetergruppe $[5, 3, 6]$ als die kleinste gespitzte nicht-arithmetische hyperbolische 3-Orbifaltigkeit. Diese gemeinsame Arbeit mit Ruth Kellerhals basiert auf geometrischen und kombinatorischen Überlegungen.

Mit Hilfe derselben Methoden beweisen wir, dass die Coxetergruppe $[5, \infty]$ zur kleinsten gespitzten nicht-arithmetischen hyperbolischen 2-Orbifaltigkeit führt. Daraus folgt ein Resultat im Stile Siegels mit einer Liste aller hyperbolischen 2-Orbifaltigkeiten mit Spitze und Fläche kleiner als $\frac{\pi}{2}$.

Des Weiteren betrachten wir kompakte hyperbolische 2-Orbifaltigkeiten, deren Fundamentalpolygone minimale pflasternde n -Ecke sind, dies für $n > 6$. Solche werden von Stabilisatoruntergruppen der Coxetergruppen $[n, 3]$ realisiert, für die wir Gruppenwirkungen auf geeigneten Graphen konstruieren. Wenn möglich, beschreiben wir zugehörige 2-Mannigfaltigkeiten anhand torsionsfreier Untergruppen. Dadurch vervollständigen wir eine frühere Arbeit von Matthieu Jacquemet.

Mit dieser Technik wird auch bewiesen, dass kleinste nicht-arithmetische hyperbolische 3-Mannigfaltigkeiten, die eine Coxeterorbifaltigkeit überlagern, nicht auf der Gruppe $[5, 3, 6]$ basieren können. Wir zeigen, dass es für die Coxetergruppe $[(3^3, 6)]$ eine kleinere überlagernde Mannigfaltigkeit gibt.

Im höherdimensionalen hyperbolischen Raum konstruieren wir rechtwinklige p -Ecke, indem wir das obere Halbraummodell auf Cliffordvektoren aufbauen. Dies ist eine gemeinsame Arbeit mit Edoardo Dotti. Die wesentliche Idee, mit Doppelverhältnissen orthogonale Geodäten zu analysieren, ist für die meisten Teile dieser Dissertation hilfreich.

Résumé

Cette thèse contient de nouveaux résultats en géométrie hyperbolique.

Le résultat principal est l'identification du plus petit 3-orbifold hyperbolique non-compact non-arithmétique avec le quotient de l'espace hyperbolique par le groupe de Coxeter $[5, 3, 6]$. Ce travail est en collaboration avec Ruth Kellerhals où des considérations géométriques et combinatoires sur les empilements d'horoboules sont nos outils principaux.

Les mêmes outils sont utilisés pour établir que le groupe de Coxeter $[5, \infty]$ est le groupe fondamental du plus petit 2-orbifold hyperbolique non-compact non-arithmétique. Le résultat obtenu s'apparente à celui de Siegel donnant lieu à une liste de tous les 2-orbifolds hyperboliques non-compacts d'aire plus petite que $\frac{\pi}{2}$.

Un autre aspect concerne les 2-orbifolds hyperboliques compacts admettant pour polygone fondamental des n -gons hyperboliques d'aire minimale, où $n > 6$. En choisissant de manière stratégique des graphes sur lesquels les groupes de Coxeter $[n, 3]$ agissent, nous considérons les sous-groupes stabilisateurs de ceux-ci. Lorsque cela est possible, nous décrivons des 2-variétés au moyen de leurs sous-groupes sans torsion. Tout ceci vient compléter des travaux antérieurs de Matthieu Jacquemet.

Ces méthodes sont également utilisées pour démontrer que des variétés hyperboliques non-compactes non-arithmétiques de volume minimal revêtant un orbifold de Coxeter ne peuvent pas être basées sur $[5, 3, 6]$. En effet, le groupe de Coxeter $[(3^3, 6)]$ mène à un revêtement par une variété de plus petit volume.

Pour les dimensions supérieures, nous construisons des p -gons à angles droits réalisés dans le modèle du demi-espace supérieur basé sur des vecteurs de Clifford (en collaboration avec Edoardo Dotti). L'analyse des géodésiques orthogonales à l'aide de birapports est utile dans la plupart des parties de cette thèse.

Acknowledgements

First and foremost, I wish to wholeheartedly express my gratitude to my supervisor Ruth Kellerhals for her invaluable support, her persistence on topics that seemed lost, and discussions like tennis matches. Without her experience and support I would never have been able to complete this thesis. I am truly indebted to you.

A special thanks is due to the jury, not only for agreeing to read and comment on my thesis: Brent Everitt, for teaching me useful techniques during two research visits, John Parker, for giving an interesting lecture that prepared me for my PhD studies, and Alan Reid, for giving inspiring talks at several conferences.

I would like to thank everyone in the Maths Department of the University of Fribourg for an unforgettable time and a stimulating atmosphere. My academic siblings are role models, allies, friends, and much more. There are always interesting discussions to be had with fellow PhD students and postdocs. It was a pleasure to work with them.

I thank my former supervisors, professors, motivating teachers, and fellow students in Durham, Mainz and Bad Dürkheim. Their passion for mathematics kept me on the path towards this thesis.

I am grateful to all my friends for keeping my life well balanced wherever I go.

Above all, I am thankful to my family for their everlasting support in everything I do and thank you, Mirjam, for everything that cannot be said with words.

Contents

I. Introduction	1
References	2
II. On Right-Angled Polygons in Hyperbolic Space	3
1. Introduction	3
2. Preliminaries	4
2.1. Clifford Algebra and Clifford Vectors	4
2.2. Cross Ratio and Properties	5
3. The Algorithm	6
3.1. The Start	6
3.2. The Next Geodesics	7
3.3. The Last Geodesic	7
4. Discussion and Remarks	7
4.1. Existence and Isometries	7
4.2. Two Applications	8
References	8
III. The minimal cusped non-arithmetic 3-orbifold	11
1. Introduction	11
2. Non-arithmetic cusped hyperbolic 3-orbifolds	13
2.1. Cusps of hyperbolic orbifolds	13
2.2. Hyperbolic Coxeter orbifolds	14
2.3. Volumes of non-compact hyperbolic tetrahedra	16
2.4. Some horoball geometry	18
3. Proof of the Theorem	20
3.1. The non-rigid and multiply cusped cases	20
3.2. The cusp type $\{3, 3, 3\}$	21
3.3. Some notations	22
3.4. One equivalence class of full-sized horoballs	23
3.5. More than one equivalence class of full-sized horoballs	47
4. Final remarks	54
Appendix III.A. The case $\{2, 3, 6\}$	55
Appendix III.B. The case $\{2, 4, 4\}$	58
References	60
IV. A Small Non-Arithmetic Hyperbolic 3-Manifold	63
1. Introduction	63

2.	Preliminaries	64
2.1.	Group Actions	64
2.2.	Torsion Elements in (Transitive) Group Actions of Coxeter Groups	65
2.3.	Group Actions Given by Graphs	66
3.	A Small Non-Arithmetic Hyperbolic 3-Manifold	67
3.1.	The Base Orbifold	67
3.2.	The Manifold \mathbf{H}^3/Γ_1	68
	References	72
V.	The Minimal Cusped Non-Arithmetic 2-Orbifold	75
1.	Introduction	75
2.	One cusp	76
2.1.	One Equivalence Class of Full-Sized Horoballs	79
2.2.	Two Equivalence Classes of Full-Sized Horoballs	85
2.3.	At Least Three Equivalence Classes of Full-Sized Horoballs	88
3.	Two or More Cusps	88
	References	90
VI.	Minimal Fundamental Polygons	91
1.	Introduction	91
2.	Minimal Hyperbolic N -gon for $N > 6$	91
3.	Surfaces Realising Minimal Polygons	94
	References	95
A.	On Right-Angled Polygons in Hyperbolic Space	99
1.	The real Clifford Algebra and Hyperbolic Space	100
1.1.	The Real Clifford Algebra \mathcal{C}_n	100
1.2.	Square Root of a Clifford Vector	101
1.3.	Clifford Matrices and Hyperbolic Isometries	102
1.4.	The Cross Ratio	103
2.	The Main Theorem	106
2.1.	Preliminaries	106
2.2.	The Theorem	108
2.3.	Proof of Theorem 14	109
3.	Right-Angled Polygons with Full Span	110
3.1.	A Necessary Condition for the Realisation of $(p - 1)$ -Simplices	111
3.2.	Hyperbolic 4-Simplices with an Orthogonal Cyclic Edge Path	111
	References	113
B.	Magma Code	115

I. Introduction

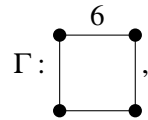
This cumulative thesis treats several different new aspects of hyperbolic geometry. Each chapter contains its own elaborate introduction, bibliography and also some references to other chapters.

The new results mainly concern the hyperbolic plane \mathbf{H}^2 and hyperbolic 3-space \mathbf{H}^3 , but chapter II starts with higher dimensional hyperbolic spaces \mathbf{H}^{n+2} . The model of choice will be the upper half space \mathbf{H}^n , $n \geq 2$, where geodesics are vertical lines or semicircles orthogonal to the boundary. The volume element is given by $\text{dvol} = \frac{1}{x_n^n} dx_1 \cdots dx_n$. All results except for the first chapter concern questions about small volume.

In chapter II, we use generalised cross ratios to construct and analyse the existence of right-angled hyperbolic polygons in higher dimensional hyperbolic space \mathbf{H}^{n+2} . This is joint work with Edoardo Dotti [DD19] motivated by the hexagonal case considered by Delgove and Retailleau [DR14]. The Clifford calculus provides a powerful tool to work with right-angled geodesics and introduce a multiplication on the boundary $\partial\mathbf{H}^{n+2}$ of hyperbolic space. Then, cross ratios of geodesics encode angles of geodesics and their relative position in upper half space. This enables us to encode a right-angled p -gon as a set of Clifford vector parameters q_1, \dots, q_{p-3} and is also useful in later chapters of this thesis. The contributions of both authors to the paper [DD19] are comparable, where my input mostly concerns the construction of the right-angled polygons and counter examples to attempts of a proper parameterisation.

Chapter III is the core of this thesis. We find the smallest non-arithmetic cusped hyperbolic 3-orbifold by utilising horoball geometry. This is joint work with Ruth Kellerhals [DK21]. I contributed a significant share of the research in this paper. By combinatorial considerations we list cusped hyperbolic 3-orbifolds with small volume to be able to argue that the Coxeter group with Coxeter graph $\bullet \overset{5}{\text{---}} \bullet \overset{6}{\text{---}} \bullet$ yields the smallest volume non-arithmetic cusped hyperbolic 3-orbifold. As such, it is unique. The basics of the horoball geometry are due to Adams but we had to extend his arguments from [Ada92] in a considerable way.

This small orbifold obtained from $\bullet \overset{5}{\text{---}} \bullet \overset{6}{\text{---}} \bullet$ does not lead to the smallest non-arithmetic cusped hyperbolic 3-manifold covering a Coxeter orbifold. We prove this in chapter IV by finding a small index torsion-free subgroup G of the Coxeter group



such that the quotient \mathbf{H}^3/G has smaller volume than any manifold cover of $\mathbf{H}^3/\bullet \overset{5}{\text{---}} \bullet \overset{6}{\text{---}} \bullet$.

In the last two chapters, we revisit a famous theorem of Carl Siegel [Sie45] in the hyperbolic plane. In chapter V, we prove a non-compact version by using the techniques of chapter III. This

not only gives the smallest cusped hyperbolic orbifold but also a list of all cusped hyperbolic 2-orbifolds with area smaller than $\frac{\pi}{2}$. In particular, we can prove that the Coxeter group $\bullet \xrightarrow{5} \bullet \xrightarrow{\infty} \bullet$ yields the non-arithmetic cusped hyperbolic 2-orbifold with minimal area.

Chapter VI is a completion of Matthieu Jacquemet's work and concerns compact hyperbolic n -gons tessellating the hyperbolic plane. In his thesis [Jac15], he described the smallest such polygons with $n \leq 6$. Here, we find groups realising the smallest n -gons as fundamental polygons for $n > 6$. This is done using similar methods to those used in chapter IV. Where possible, we also determine smooth hyperbolic surfaces that realise minimal fundamental n -gons.

References

- [Ada92] C. Adams. 'Noncompact hyperbolic 3-orbifolds of small volume'. *Topology '90 (Columbus, OH, 1990)*. Vol. 1. Ohio State Univ. Math. Res. Inst. Publ. de Gruyter, Berlin, 1992, pp. 1–15.
- [DD19] E. Dotti and S. T. Drewitz. 'On right-angled polygons in hyperbolic space'. *Geometriae Dedicata* 200.1 (June 2019), pp. 45–59. DOI: 10.1007/s10711-018-0357-y.
- [DK21] S. T. Drewitz and R. Kellerhals. *The non-arithmetic cusped hyperbolic 3-orbifold of minimal volume*. 2021. arXiv: 2106.12279 [math.GT].
- [DR14] F. Delgove and N. Retailleau. 'Sur la classification des hexagones hyperboliques à angles droits en dimension 5'. eng. *Ann. de la fac. des sci. de Toulouse Math.* 23.5 (2014), pp. 1049–1061. DOI: 10.5802/afst.1435.
- [Jac15] M. Jacquemet. 'New contributions to hyperbolic polyhedra, reflection groups, and their commensurability'. PhD thesis. University of Fribourg, 2015. DOI: 10.13140/RG.2.1.2418.8248.
- [Sie45] C. Siegel. 'Some Remarks on Discontinuous Groups'. *Annals of Mathematics* 46.4 (1945), pp. 708–718. URL: <http://www.jstor.org/stable/1969206>.

II. On Right-Angled Polygons in Hyperbolic Space

1. Introduction

The first part of this thesis is joint work with Edoardo Dotti [DD19]. We generalised work of Delgove and Retailleau [DR14]. They described a classification of right-angled hyperbolic hexagons in \mathbf{H}^5 . We extended this result to right-angled p -gons in higher dimensional hyperbolic space \mathbf{H}^n . In this context, a *right-angled p -gon* is a finite sequence of p geodesics S_0, S_1, \dots, S_{p-1} in hyperbolic space such that consecutive geodesics are orthogonal and $S_{p-1} \perp S_0$.

The model of choice is the *upper half-space model* of hyperbolic space \mathbf{H}^{n+2} where the boundary $\partial\mathbf{H}^{n+2}$ is composed of Clifford vectors $\mathbb{V}^{n+1} \cup \{\infty\} = \partial\mathbf{H}^{n+2}$. The use of Clifford vectors as end points of geodesics admits a new notion of a cross ratio of two or three geodesics. This cross ratio encodes information about the respective orientation of the geodesics to each other. This also proved useful for the remaining chapters of this thesis. For example, in chapter IV, we can use these cross ratio relations to double check other computations.

The cross ratio of the four ideal endpoints of two hyperbolic geodesics encodes their angle if they intersect (see Proposition 4). If three geodesics S_1, S_2 , and S_3 form a so-called *double bridge* (i.e. $S_1 \perp S_2 \perp S_3$), then the cross ratio gives the distance $d(S_1, S_3)$ and additional information on their relative position. Since \mathcal{C}_n is not commutative for $n > 1$, the cross ratio itself is not invariant under hyperbolic isometries in general, but only its norm and real part. In general, the cross ratio can take values in the Clifford group Γ_n generated by the non-zero Clifford vectors. For two given perpendicular geodesics S_1 and S_2 , a third geodesic S_3 cannot make the cross ratio take any arbitrary value in Γ_n but only a subset which depends on the position of the first two geodesics. This can be remedied by considering double bridges of a certain standard configuration, where the cross ratio can take values in $\mathbb{V}^{n+1} \setminus \{0, \pm 1\}$.

This is the central idea of the algorithm. One starts with two geodesics

$$S_0 = (-1, 1), \quad S_1 = (0, \infty) \quad (1.1)$$

in the standard configuration and takes a set of parameters $q_1, \dots, q_{p-3} \in \mathbb{V}^{n+1}$. The third geodesic S_2 is given by the parameter q_1 directly by assuming that S_0, S_1 , and S_2 form a double bridge with cross ratio equal to q_1 . For the geodesic S_3 , one finds a geodesic $S'_3 = (-q_2, q_2)$ which is the third geodesic in a standard configuration with cross ratio q_2 . The geodesic S_3 is then obtained as the image of S'_3 under an isometry mapping

$$(-1, 1) \mapsto S_2, \quad (0, \infty) \mapsto S_3. \quad (1.2)$$

This condition does not uniquely define the isometry but one can define the isometry in a consistent manner. One can continue in this way to obtain the further geodesics up to S_{p-2} which

is given by q_{p-3} . If S_{p-2} and S_0 do not intersect, the common perpendicular yields S_{p-1} and the construction finishes. If they do intersect, then the set of parameters we started with is not valid.

This chapter provides a summary of the paper [DD19] which is attached in Appendix A. Detailed definitions, results, and citations can be found there.

2. Preliminaries

2.1. Clifford Algebra and Clifford Vectors

The crucial step is to use the Clifford algebra \mathcal{C}_n as a generalisation of the real and complex numbers and the quaternions \mathbb{H} . This allows us to multiply and divide points on the boundary of hyperbolic space \mathbf{H}^{n+2} . Let \mathcal{C}_n be the n^{th} Clifford algebra, that is the (anti-)commutative unitary real algebra in n generators i_1, \dots, i_n :

$$\mathcal{C}_n := \langle i_1, \dots, i_n \mid \forall l \neq k : i_l^2 = 1 \text{ and } i_l i_k = -i_k i_l \rangle, n \geq 1.$$

As a real vector space, \mathcal{C}_n is 2^n -dimensional with basis

$$\{i_{k_1} \cdots i_{k_m} \mid 1 \leq k_1 \leq \dots \leq k_m \leq n, 0 \leq m \leq n\}.$$

The coefficient of the empty product $I_0 = 1 =: i_0$ in a Clifford number x is called the *real part* and denoted by $\Re(x)$. We set $\mathcal{C}_0 := \mathbb{R} i_0$. The elements of the vector subspace spanned by 1 and the generators i_1, \dots, i_n are called the *Clifford vectors*. The set is denoted by

$$\mathbb{V}^{n+1} := \langle 1, i_1, \dots, i_n \rangle \subset \mathcal{C}_n.$$

The real numbers are obtained as $\mathcal{C}_0 = \mathbb{R}$, the complex numbers as $\mathcal{C}_1 = \mathbb{C}$ and Hamilton's quaternions as $\mathcal{C}_2 = \mathbb{H}$. There are three standard involutions in the Clifford algebra \mathcal{C}_n , one of them being the reversion, which acts on an element $x \in \mathcal{C}_n$ by reversing the order of the products in the basis elements: $(i_{k_1} \cdots i_{k_m})^* = i_{k_m} \cdots i_{k_1}$. For $n \geq 3$, \mathcal{C}_n contains zero divisors – consider $(1 + i_1 i_2 i_3)(1 - i_1 i_2 i_3)$. However, the non-zero Clifford vectors generate a multiplicative group called the *Clifford group* $\Gamma_n \subset \mathcal{C}_n$.

It is possible to extend the definition of a square root to Clifford vectors that are not both real and negative. By abuse of notation we use the usual symbol for the square root of a real number.

Definition 1. For a Clifford vector $q \in \mathbb{V}^{n+1} \setminus \mathbb{R}_{<0}$ we define

$$\sqrt{q} := \frac{|q| + q}{\sqrt{2(\Re(q) + |q|)}} \in \mathbb{V}^{n+1}.$$

It satisfies the usual properties of a square root, that is $\pm\sqrt{q}$ are the only two Clifford vectors whose square is q .

2.2. Cross Ratio and Properties

In the non-commutative Clifford algebra \mathcal{C}_n , it is necessary to define the exact notion of cross ratio one is using.

Definition 2. For pairwise different Clifford vectors $x, y, z, w \in \mathbb{V}^{n+1}$ define the cross ratio as

$$[x, y, z, w] := (x - z)(x - w)^{-1}(y - w)(y - z)^{-1} \in \Gamma_n.$$

It is possible to extend the definition for one of the variables to be ∞ . The cross ratio has the transformation property

$$[T(x), T(y), T(z), T(w)] = (cz + d)^{* - 1} [x, y, z, w] (cz + d)^*, \quad (2.1)$$

for any $T = \begin{pmatrix} a & b \\ c & d \end{pmatrix} \in \text{SL}(2, \mathcal{C}_n)$. Here,

$$\text{SL}(2, \mathcal{C}_n) = \left\{ A = \begin{pmatrix} a & b \\ c & d \end{pmatrix} \in \text{GL}(2, \mathcal{C}_n) \mid ad^* - bc^* = 1 \right\}$$

denotes the group of Clifford matrices with Ahlfors determinant 1 and the Clifford matrices $\begin{pmatrix} a & b \\ c & d \end{pmatrix} \in \text{GL}(2, \mathcal{C}_n)$ are the matrices satisfying

$$a, b, c, d \in \Gamma_n \cup \{0\}, ab^*, cd^*, c^*a, d^*b \in \mathbb{V}^{n+1}, ad^* - bc^* \in \mathbb{R} \setminus \{0\}.$$

The most important upshot here is the invariance of norm and real part of the cross ratio.

It is useful to calculate details about the relative position of two geodesics $s = (s^-, s^+)$ and $t = (t^-, t^+)$ with endpoints in the boundary $\partial \mathbf{H}^{n+2} = \mathbb{V}^{n+1} \cup \{\infty\}$ of hyperbolic space \mathbf{H}^{n+2} .

Definition 3. We define the cross ratio $\Delta(s, t)$ of two geodesics s and t as

$$\Delta(s, t) := [s^-, s^+, t^-, t^+]. \quad (2.2)$$

Proposition 4. The cross ratio $\Delta(s, t)$ of two geodesics in \mathbf{H}^{n+2} is a negative real number if and only if they intersect. Additionally, $\Delta(s, t) = -1$ if and only if they are orthogonal.

The construction of right-angled polygons will depend on objects Retailleau and Delgove called *double bridges*. They consist of three geodesics r, s , and t in \mathbf{H}^{n+2} such that $r \perp s \perp t$. Also here, the cross ratio encodes valuable information.

Definition 5. For the double bridge (r, s, t) , we call

$$\Delta(r, s, t) := [s^+, s^-, r^+, t^+]$$

the double bridge cross ratio.

Do note, that if the orientation of s is reversed, the double bridge cross ratio becomes the multiplicative inverse. This is one reason why different sets of parameters can lead to the same polygons. One can show that the distance of r and t is given by $|\log(|\Delta(r,s,t)|)|$. The direction $\Delta(r,s,t)|\Delta(r,s,t)|^{-1}$ encodes their relative position in \mathbf{H}^{n+2} .

Remember that the cross ratio is not invariant under isometries. In order to have a sensible representation of the relative position by the cross ratio, we consider a *standard configuration double bridge* (r,s,t) where

$$r = (-1, 1), \quad s = (0, \infty), \text{ and} \quad t = (-q, q). \quad (2.3)$$

In this standard configuration, the cross ratio easily computes as $\Delta(r,s,t) = q$, where $q \in \partial\mathbf{H}^{n+2} \setminus \{\pm 1, 0, \infty\} = \mathbb{V}^{n+1} \setminus \{\pm 1, 0\}$. This is the set of allowed parameters. By restricting the orientation, it is adequate to only consider parameters in the set $\{q \in \mathbb{V}^{n+1} \mid |q| > 1\}$.

We will always start in this standard configuration and then apply an appropriate isometry as desired.

Definition 6. *The set of Clifford vectors $\{q_1, \dots, q_{p-3}\} \subset \mathbb{V}^{p-2} \setminus \{0\}$ gives rise to isometries $\phi_1, \dots, \phi_{p-3}$ as the following Möbius transformations:*

$$\phi_i : x \mapsto \sqrt{-2q_i}^{-1} (x + q_i) (x - q_i)^{-1} \sqrt{-2q_i}, \quad 1 \leq i \leq p-3. \quad (2.4)$$

For a negative number $q_i < 0$, choose $\sqrt{-2q_i} := \sqrt{2q_i} i_1$.

We define the concatenation $\Phi_i := \phi_i \circ \phi_{i-1} \circ \dots \circ \phi_1$.

The isometry ϕ_i^{-1} maps the geodesic $(-1, 1)$ to $(0, \infty)$ and $(0, \infty)$ to $(-q_i, q_i)$.

3. The Algorithm

The aim is to construct a right-angled p -gon in \mathbf{H}^{n+2} , $p \geq 5$, $n \geq 2$, from a set of given parameters $q_1, \dots, q_{p-3} \in \mathbb{V}^{n+1} \setminus \{\pm 1, 0, \infty\}$. We cite the definition of right-angled polygons from [DD19].

Definition 7. *An oriented right-angled polygon with p sides in \mathbf{H}^{n+2} (or p -gon for short), $n \geq 0$, is a p -tuple of oriented geodesics $(S_0, S_1, \dots, S_{p-1})$ with $S_{i-1} \neq S_{i+1}$ for $i \pmod{p}$ and such that S_i is orthogonal to S_{i+1} for $0 \leq i \leq p-2$ and S_{p-1} is orthogonal to S_0 .*

We usually denote it by Π_p .

We call such a p -gon Π_p non-degenerate if consecutive intersections do not coincide (that is $S_{i-1} \cap S_i \neq S_i \cap S_{i+1}$ for $i \pmod{p}$) and the double bridges (S_{i-1}, S_i, S_{i+1}) , $i \pmod{p}$, are properly oriented.

3.1. The Start

As mentioned before, we begin with the two geodesics

$$\begin{aligned} S_0 &= (-1, 1), \text{ and} \\ S_1 &= (0, \infty). \end{aligned}$$

There is a unique geodesic

$$S_2 = (-q_1, q_1)$$

such that the double bridge cross ratio is given by the first parameter $q_1 = \Delta(S_0, S_1, S_2)$.

3.2. The Next Geodesics

Assume we have computed the geodesics S_0, S_1, \dots, S_k from the parameters q_1, \dots, q_{k-1} . The parameter q_k would give a geodesic

$$S'_{k+1} = (-q_k, q_k)$$

in the standard configuration. By applying the isometry Φ_{k-1}^{-1} to S'_{k+1} , we obtain the new geodesic

$$S_{k+1} = \Phi_{k-1}^{-1}(S'_{k+1}) = (\Phi_{k-1}^{-1}(-q_k), \Phi_{k-1}^{-1}(q_k)).$$

3.3. The Last Geodesic

The preceding procedure yields geodesics

$$S_0, S_1, \dots, S_{p-2}.$$

Assuming these geodesics are part of a right-angled p -gon, then the missing geodesic S_{p-1} has to be orthogonal to S_0 and S_{p-2} . The endpoints of S_{p-1} can be calculated by solving the two equations

$$\Delta(S_0, S_{p+2}) = -1, \text{ and} \quad \Delta(S_{p+1}, S_{p+2}) = -1. \quad (3.1)$$

In view of the non-commutative nature of the Clifford algebra, a carefully chosen transformation simplifies this calculation. By using an isometry to map S_0 to $(0, \infty)$ and S_1 to $(1, c)$ for some $c \in \mathbb{V}^{n+1}$, the Clifford vectors in the subspace generated by the endpoints do commute. In this configuration, the missing geodesic can be easily calculated as $(-\sqrt{c}, \sqrt{c})$.

4. Discussion and Remarks

4.1. Existence and Isometries

There are two major questions which are still unanswered:

- Which parameters q_1, \dots, q_{p-3} yield a non-degenerate p -gon?
- What are possible relations between parameters q_1, \dots, q_{p-3} and q'_1, \dots, q'_{p-3} yielding isometric polygons?

The difficulty of calculating S_{p-1} makes those questions hard to answer. Assuming that the parameters q_1, \dots, q_{p-3} yield geodesics S_0, \dots, S_{p-2} , such that the only non-empty intersections are of type $S_i \cap S_{i+1}$ ($0 \leq i \leq p-2$), it is still challenging to calculate the position of S_{p-1} and its intersections with S_0 and S_{p-2} . For example, the parameters $q_1 = 2i, q_2 = 2j \in \mathbb{H}$ might be a good first guess for a non-degenerate pentagon in \mathbf{H}^4 . The first geodesics can be calculated from these parameters as

$$\begin{aligned} S_0 &= (-1, 1), \\ S_1 &= (0, \infty), \\ S_2 &= (-2i, 2i), \text{ and} \\ S_3 &= (\phi_1(-2j), \phi_1(2j)) = \left(\frac{1}{5}(6i - 8j), \frac{1}{5}(6i + 8j) \right). \end{aligned}$$

It can easily be seen without any calculation that the common perpendicular of S_0 and S_3 has to completely lie in the hyperbolic plane defined by its projection $\{xi \mid x \in \mathbb{R}\}$ in the boundary of hyperbolic space. This implies that the intersections of $S_0 \cap S_1$ and $S_4 \cap S_0$ coincide and that the pentagon is degenerate.

By calculating examples, we noticed that orthogonal parameters usually lead to degenerate polygons. It lead us to the conjecture that non-degenerate right-angled pentagons might be constructed by the parameters

$$\{(q_1, q_2) \mid \forall i = 1, 2, |q_i| > 1, \Re(q_1) \neq 0, q_1 \not\perp q_2\}.$$

This set does not ensure that the pentagons are properly oriented or non-isometric but it might assert that they are non-degenerate.

An implementation of our algorithm can be obtained at <https://github.com/drewitz/PiGeonS>.

4.2. Two Applications

We showed in the paper [DD19] that a necessary condition for the intersections of the geodesics in a p -gon Π_p to form a convex $(p-1)$ -simplex is that the parameters q_1, \dots, q_{p-3} together with 1 span the Clifford vector space \mathbb{V}^{p-2} . The idea behind the proof is that each parameter has to introduce another dimension. Above, we have already seen an example that this condition cannot be a sufficient condition.

Furthermore, we considered hyperbolic 4-simplices with a totally orthogonal edge cycle. By using results of Dekster and Wilker [DW91], we were able to show that if there is a 4-simplex containing a totally orthogonal edge cycle where all edge lengths are equal to a , then $\cosh(a) < \frac{1+\sqrt{5}}{2}$.

References

- [DD19] E. Dotti and S. T. Drewitz. ‘On right-angled polygons in hyperbolic space’. *Geometriae Dedicata* 200.1 (June 2019), pp. 45–59. DOI: 10.1007/s10711-018-0357-y.

- [DR14] F. Delgove and N. Retailleau. ‘Sur la classification des hexagones hyperboliques à angles droits en dimension 5’. eng. *Ann. de la fac. des sci. de Toulouse Math.* 23.5 (2014), pp. 1049–1061. DOI: 10.5802/afst.1435.
- [DW91] B. V. Dekster and J. B. Wilker. ‘Simplexes in spaces of constant curvature’. *Geom. Dedicata* 38.1 (1991), pp. 1–12. ISSN: 0046-5755. DOI: 10.1007/BF00147732.

III. The non-arithmetic cusped hyperbolic 3-orbifold of minimal volume

This chapter is the reproduction of the paper [DK21] which is joint work with Ruth Kellerhals. I contributed a substantial part of the research to this paper. The notions and results mentioned here will also be used later in this thesis.

Abstract We show that the 1-cusped quotient of the hyperbolic space \mathbf{H}^3 by the tetrahedral Coxeter group $\Gamma_* = [5, 3, 6]$ has minimal volume among all non-arithmetic cusped hyperbolic 3-orbifolds, and as such it is uniquely determined. Furthermore, the lattice Γ_* is incommensurable to any Gromov-Piatetski-Shapiro type lattice. Our methods have their origin in the work of C. Adams [Ada92a; Ada91]. We extend considerably this approach via the geometry of the underlying horoball configuration induced by a cusp.

1. Introduction

Let \mathbb{H}^3 be the hyperbolic 3-space viewed in the upper half space U^3 of Poincaré, and let $\text{Isom}\mathbb{H}^3$ be its isometry group. A cusped hyperbolic 3-orbifold V is the quotient of \mathbb{H}^3 by a non-cocompact lattice $\Gamma \subset \text{Isom}\mathbb{H}^3$, that is, by a discrete group of hyperbolic isometries with a non-compact fundamental polyhedron of finite volume. In particular, Γ contains a non-trivial parabolic subgroup whose elements fix a point q on the boundary $\partial\mathbb{H}^3$. Without loss of generality, assume that $q = \infty$ with stabiliser $\Gamma_\infty < \Gamma$. The group Γ_∞ gives rise to precisely invariant subsets which are horoballs centred at ∞ . They can be arranged in such a way that there is a maximal horoball B_∞ touching some of its Γ -images, called full-sized horoballs, and which project to a maximal cusp $C \subset V$ of finite volume in V . Hence, the number of non-conjugate parabolic subgroups of Γ equals the number of maximal cusps in V . The orthogonal projection of the full-sized horoballs to the horosphere $\partial B_\infty = H_\infty$ yields a horoball-packing with a characteristic horoball diagram on H_∞ . In this way, a combination of results from crystallography and a density result of K. Böröczky [Bör78, Theorem 4] allows one to deduce lower volume bounds.

Using this picture, R. Meyerhoff [Mey85] identified the 1-cusped quotient space $\mathbf{H}^3/[3, 3, 6]$ as the minimal volume cusped hyperbolic 3-orbifold. The Coxeter group with symbol $[3, 3, 6]$ generates the group of symmetries of an ideal regular tetrahedron S_{reg}^∞ of dihedral angle $\frac{\pi}{3}$. Furthermore, it is an arithmetic group commensurable to the Eisenstein modular group $\text{PSL}(2, \mathbb{Z}[\omega])$ where $\omega = (-1 + \sqrt{-3})/2$ is a primitive cubic root of unity. The orbifold $\mathbf{H}^3/[3, 3, 6]$ is covered by the well-known (non-orientable) 1-cusped Gieseking manifold G which, by a result of Adams [Ada87], is of minimal volume among all cusped hyperbolic 3-manifolds.

The result of Meyerhoff was considerably extended by Adams [Ada92a, Theorem 6.1, Corollary 6.2] who identified the six cusped (orientable and non-orientable) hyperbolic 3-orbifolds of

smallest volume. Crucial in Adams' proof was the assumption of the strict upper volume bound of $\frac{1}{4} \text{vol}(S_{reg}^\infty)$ in the case of orientable orbifolds, implying that such an orbifold has only one cusp and a single orbit of full-sized horoballs modulo the action of the corresponding stabiliser. In [NR92], W. Neumann and A. Reid characterised Adams' spaces and showed that they are all arithmetically defined.

In this work, we consider *non-arithmetic* cusped hyperbolic 3-orbifolds and prove the following result.

Theorem. *Among all non-arithmetic cusped hyperbolic 3-orbifolds, the 1-cusped quotient space V_* of \mathbf{H}^3 by the tetrahedral Coxeter group $[5, 3, 6]$ has minimal volume. As such the orbifold V_* is unique, and its volume v_* is given explicitly by (2.7).*

The Coxeter group $[5, 3, 6]$ gives rise to the group of symmetries of an ideal regular dodecahedron $D_{reg}^\infty \subset \mathbf{H}^3$ of dihedral angle $\frac{\pi}{3}$. By applying different face identifications to D_{reg}^∞ , the orbifold V_* admits several non-isometric non-arithmetic cover manifolds; see [Eve04].

Notice that the non-arithmetic orbifold $V_* = \mathbf{H}^3/[5, 3, 6]$ does not relate to a Gromov–Piatetski-Shapiro construction. In fact, the Coxeter tetrahedron associated to $[5, 3, 6]$ is not *splittable* in the sense of [Fis+18, Section 6.2, Example 6.10]. Therefore, by [Fis+18, Lemma 6.9], the group Γ_* is incommensurable to any Gromov–Piatetski-Shapiro type lattice.

Consider the smooth case of non-arithmetic cusped hyperbolic 3-manifolds. There are many such manifolds. For a list containing small volume examples, we refer to [GMM09] and [MR03, Section 13.6]. Here, we focus on *Coxeter manifolds*, that is, manifolds whose fundamental groups are commensurable with hyperbolic Coxeter groups. Their existence is guaranteed by Selberg's Lemma. The above theorem allows us to deduce the following result in terms of the non-arithmetic tetrahedral Coxeter group $[(3^3, 6)]$.

Proposition. *The fundamental group of a non-arithmetic cusped hyperbolic Coxeter 3-manifold M_* of minimal volume is incommensurable to the Coxeter group $[5, 3, 6]$; the volume of M_* is smaller than or equal to $24 \cdot \text{covol}([(3^3, 6)]) \approx 8.738570$.*

Furthermore and as a by-product of the geometric methods used to prove the Theorem, we obtain the following two-dimensional analogue which has possibly been overlooked so far.

Proposition. *Among all non-arithmetic cusped hyperbolic 2-orbifolds, the 1-cusped quotient space V_* of \mathbf{H}^2 by the triangle Coxeter group $[5, \infty]$ has minimal area. As such the orbifold V_* is unique, and its area is given by $\frac{3\pi}{10}$.*

For fixed dimension n with $2 \leq n \leq 9$, the cusped hyperbolic n -orbifold of minimal volume is known and intimately related to an arithmetic Coxeter simplex group (see [HK07] and [Hil07b; Hil07a]). In comparison to this, it is much more difficult to identify the non-arithmetic cusped hyperbolic n -orbifolds of minimal volume for $n \geq 4$ by providing a presentation of their fundamental groups. In view of the Gromov–Piatetski-Shapiro construction, observe that non-arithmetic non-cocompact hyperbolic Coxeter simplex groups do not exist anymore for $n \geq 4$.

This work is structured as follows. In Section 2 we present the necessary background about cusped hyperbolic orbifolds, their (non-)arithmeticity and the realisation as quotients by hyperbolic Coxeter groups. We provide a short overview about volume computations for hyperbolic

(truncated) tetrahedra and finish by presenting the necessary information about horoball packings and cusp densities. Section 3 contains the proof of our Theorem which consists of several steps. We first show that a non-arithmetic cusped hyperbolic 3-orbifold \mathbf{H}^3/Γ of minimal volume has exactly one cusp C , and then, that C is a rigid cusp of type $\{2,3,6\}$ or $\{2,4,4\}$. We study these two cases separately and have also to distinguish – in contrast to Adams’ work [Ada92a] – whether there is one or more equivalence classes of a full-sized horoball B covering C with respect to Γ_∞ . An essential aspect is the view of the Γ_∞ -periodic horoball packing induced by B by means of its horoball diagram. The possible configurations of full-sized horoballs and their hierarchy allow us to estimate minimal distances of their centres and to derive lower volume bounds. In all cases, we are able to identify fundamental polyhedra for Γ or to exclude groups when they are arithmetic or of a too big covolume. In Section 4, we discuss briefly the related results given by the two propositions above, both due to the first author [Dre21]. In the parts III.A and III.B of the Appendix, we describe certain small volume orientable orbifolds with precisely one cusp of type $\{2,3,6\}$ and $\{2,4,4\}$, respectively, whose associated parabolic groups give rise to only one equivalence class of full-sized horoballs. In the case of $\{2,3,6\}$, we correct the corresponding construction and result of Adams [Ada92a, p. 10].

Acknowledgements

The authors would like to thank Colin Adams and Alan Reid for helpful discussions and comments. The second author was partially supported by Schweizerischer Nationalfonds 200021–172583.

2. Non-arithmetic cusped hyperbolic 3-orbifolds

2.1. Cusps of hyperbolic orbifolds

Consider the hyperbolic space \mathbb{H}^3 in the upper half space $U^3 = \{(x, y, t) \in \mathbb{R}^3 \mid t > 0\}$ equipped with the metric $ds^2 = \frac{dx^2 + dy^2 + dt^2}{t^2}$. Points on the boundary $\partial U^3 = \{(x, y, 0) = (u, 0) \in \mathbb{R}^3\} \cup \{\infty\} = \mathbb{R}^2 \cup \{\infty\}$ are called *ideal* points, and points in \mathbb{R}^3 with $t < 0$ are called *ultraideal*.

Let $\Gamma \subset \text{Isom}\mathbb{H}^3$ be a non-cocompact lattice, that is, Γ is a discrete group with a non-compact fundamental polyhedron $P \subset \mathbf{H}^3$ of finite volume. Then, the quotient space $V = \mathbf{H}^3/\Gamma$ is a *cusped* hyperbolic 3-orbifold of finite volume which is a smooth manifold if the group Γ has no torsion elements. By Selberg’s lemma (see [Rat94, Theorem 7.5.7], for example), Γ always has a finite index subgroup Λ which is torsion-free. In particular, Γ and Λ are *commensurable* groups in $\text{Isom}\mathbb{H}^3$, that is, the intersection of Γ with some conjugate of Λ in $\text{Isom}\mathbb{H}^3$ is of finite index in both groups. Recall that commensurability is an equivalence relation preserving properties such as cocompactness, finite covolume and arithmeticity.

Each cusp C of V is of the form B_q/Γ_q where $B_q \subset \mathbf{H}^3$ is a horoball based at an ideal point $q \in \partial\mathbf{H}^3$ where $\Gamma_q \subset \Gamma$ is the (non-trivial) stabiliser of q in Γ . Enlarge C so that it touches either itself or another cusp of V . Such a cusp is called a *maximal* cusp of V . Without loss of generality, we will assume that a maximal cusp of V is covered by the horoball $B_\infty = \{(x, y, t) \in \mathbb{R}^3 \mid t > 1\}$ based at ∞ , with distance 1 from the ground space $\{t = 0\}$, and bounded by the horosphere $H_\infty = \{(x, y, t) \in \mathbb{R}^3 \mid t = 1\}$. Recall that the induced metric $ds^2|_{t=1}$ on H_∞ coincides with the Euclidean metric with distance function denoted by d_0 . Since the cusp C is maximal, there are

horoball images $\gamma(B_\infty)$ with $\gamma \in \Gamma$ not fixing ∞ whose closures touch B_∞ . These images are called *full-sized* horoballs. By looking at their orthogonal projections onto the horosphere H_∞ , we get horodisks whose centres coincide with the touching points of the corresponding full-sized horoballs. It will be convenient to identify full-sized horoballs and their base points with their horodisks and centres and vice versa. We always suppose, without loss of generality, that one full-sized horoball is based at the origin 0 of $\{t = 0\}$.

The group Γ_∞ is a *crystallographic* group acting cocompactly by Euclidean isometries on $\{t = 0\}$ (and on H_∞). As such it contains a *translation lattice* $L \subset \Gamma_\infty$ of rank two, with minimal translation length $\tau \geq 1$, and a finite subgroup $\phi \subset O(2)$, called the *point group*, which is a subgroup of the automorphism group $\text{Aut}(L)$. The latter group consists of all Euclidean isometries fixing the origin and mapping L onto itself.

The orthogonal projection of the full-sized horoballs onto the horosphere H_∞ provides a sphere packing by balls of diameter 1 of the Euclidean plane $\{t = 1\}$. Recall that the densest packing of the Euclidean plane is achieved by the hexagonal lattice packing where each ball is surrounded by six balls. In the sequel, planar Euclidean and spatial horoball packings of large local densities will play an important role.

The ideal fixed point ∞ can be seen as an ideal vertex of a fundamental polyhedron P of Γ whose vertex link $P \cap H_\infty$ is related either to a triangle $\Delta = \{p, q, r\}$ with angles $\frac{\pi}{p}, \frac{\pi}{q}, \frac{\pi}{r}$ satisfying $(p, q, r) = (2, 3, 6), (2, 4, 4)$ or $(3, 3, 3)$ or to a parallelogram (see [Ada92a, Section 2]).

In this context, a cusp in V is called *rigid* if Dehn filling cannot be performed, and otherwise it is called *non-rigid*. In [Ada91], Adams showed that a cusp is rigid if and only if there are singular curves of order different from 2 going directly out of the cusp.

The *type* of a rigid cusp is denoted by $\{p, q, r\}$ according to the orders p, q and r of its singular axes and the triangular description mentioned above. Assuming that there is at least one non-rigid cusp, Adams found the three (uniquely determined) orientable orbifolds of smallest, second smallest and third smallest (limit) volumes; they all have arithmetic fundamental groups (see [Ada91, Chapter 4, Chapter 7] and the proof of Proposition 6 below).

The (non-)arithmeticity of a discrete group $\Gamma \subset \text{Isom}\mathbb{H}^3$ of finite covolume can be characterised by the following fundamental property due to Margulis (see [MR03, Theorem 10.3.5], for example). Consider the *commensurator*

$$\text{Comm}(\Gamma) = \{ \gamma \in \text{Isom}\mathbb{H}^3 \mid \Gamma \text{ and } \gamma\Gamma\gamma^{-1} \text{ are commensurable} \}$$

of Γ in $\text{Isom}\mathbb{H}^3$. Then, the group $\text{Comm}(\Gamma)$ is a discrete subgroup in $\text{Isom}\mathbb{H}^3$ containing Γ with finite index if and only if Γ is non-arithmetic. In particular, for Γ non-arithmetic, the commensurator $\text{Comm}(\Gamma)$ is the maximal element in the commensurability class of Γ so that all non-arithmetic hyperbolic orbifolds and manifolds with fundamental groups commensurable to Γ cover a smallest common quotient.

2.2. Hyperbolic Coxeter orbifolds

Arithmeticity can be described in a nice way for the class of *hyperbolic Coxeter groups* and the associated quotients called *Coxeter orbifolds*. Consider first a *Coxeter polyhedron* in \mathbb{H}^3 which is a convex polyhedron $P_C \subset \mathbb{H}^3$ of finite volume all of whose dihedral angles are integral

submultiples of π . A hyperbolic Coxeter group $\Gamma_C \subset \text{Isom}\mathbb{H}^3$ (with fundamental polyhedron P_C) is the discrete group generated by the (finitely many) reflections in the facets of P_C . Since the dihedral angles of P_C are non-obtuse, Andreev's theorem (see [And70a], [And70b], [RHD07]) provides necessary and sufficient conditions for its existence. In particular, there are infinitely many non-isometric Coxeter polyhedra in \mathbb{H}^3 but only finitely many Coxeter tetrahedra. In fact, there are precisely 9 compact Coxeter tetrahedra and 23 non-compact ones (for a list with their volumes, see [Joh+99, pp. 347-348]). By Vinberg's seminal work [Vin85], [VS93] about hyperbolic Coxeter polyhedra in any dimension, many of their properties can be read off from their Coxeter graphs and Gram matrices. Let $P_C \subset \mathbb{H}^3$ be a hyperbolic Coxeter polyhedron bounded by $N \geq 4$ geodesic planes H_1, \dots, H_N . Consider the $N \times N$ Gram matrix $G = G(P_C) = (g_{ij})$ of P_C which is a real symmetric matrix with $g_{ii} = 1$ and, for $i \neq j$,

$$-g_{ij} = \begin{cases} \cos \frac{\pi}{m_{ij}} & \text{if } H_i, H_j \text{ intersect at the angle } \frac{\pi}{m_{ij}} \text{ in } \mathbb{H}^3, \\ 1 & \text{if } H_i, H_j \text{ meet at } \partial\mathbb{H}^3, \\ \cosh l_{ij} & \text{if } H_i, H_j \text{ are at distance } l_{ij} \text{ in } \mathbb{H}^3. \end{cases} \quad (2.1)$$

In case of many orthogonal bounding planes and small N it is convenient to represent P_C by means of its *Coxeter graph* which is a (weighted) graph $\Sigma = \Sigma(P_C)$ of order N defined as follows. To each bounding plane H of P_C we associate a node v in Σ . Two different nodes v_i, v_j are connected by an edge with a weight if the planes H_i, H_j are not orthogonal. The weight equals m_{ij} if $g_{ij} = -\cos \frac{\pi}{m_{ij}}$. In the special (and frequent) case $m_{ij} = 3$, however, the edge carries no label. An edge will be decorated by the symbol ∞ if $g_{ij} = -1$. Edges related to disjoint planes with $g_{ij} < -1$ are replaced by dotted edges, and the weights are usually omitted. In order to describe a Coxeter graph in an abbreviated way, we use the *Coxeter symbol*. In particular, $[p, q, r]$ with integral components is associated to a linear Coxeter graph describing a *hyperbolic Coxeter orthoscheme* with dihedral angles $\frac{\pi}{p}, \frac{\pi}{q}, \frac{\pi}{r}$, and the Coxeter symbol $[(p^r, q^s)]$ describes a polyhedron with cyclic Coxeter graph having $r \geq 1$ consecutive weights p followed by s consecutive weights q (see [Joh+99, Appendix], for example). In the sequel, we often represent a Coxeter group by quoting the Coxeter symbol of its Coxeter polyhedron.

For the arithmeticity of hyperbolic Coxeter groups, there is a very efficient criterion due to Vinberg (see [VS93, pp. 226-227]). We quote it in the special case of a non-compact Coxeter polyhedron $P_C \subset \mathbb{H}^3$ with Gram matrix $G = (g_{ij})$ and with associated reflection group $\Gamma_C \subset \text{Isom}\mathbb{H}^3$. Write $2G =: (h_{ij})$ and form *cycles (of length k)* of the form

$$h_{i_1 i_2} h_{i_2 i_3} \cdots h_{i_{k-1} i_k} h_{i_k i_1}, \quad (2.2)$$

with distinct indices i_j in $2G$. Then, Γ_C is arithmetic with field of definition \mathbb{Q} if and only if all the cycles of $2G$ are rational integers. Furthermore, if the Coxeter graph $\Sigma(P_C)$ contains no dotted edges, then, by a result of Guglielmetti [Gug15, Proposition 1.13], Γ_C is arithmetic if and only if all weights of $\Sigma(P_C)$ lie in $\{\infty, 2, 3, 4, 6\}$, and each cycle of length at least 3 in $2G$ lies in \mathbb{Z} .

Examples.

1. Among all non-compact Coxeter orthoschemes $[p, q, r]$ in \mathbb{H}^3 , only $[5, 3, 6]$ defines a non-arithmetic reflection group, which we denote by Γ_* . The associated Coxeter orbifold V_* has one cusp.

2. The Coxeter tetrahedron P_\circ with the cyclic graph $[(3^3, 6)]$ yields a non-arithmetic reflection group, denoted Γ_\circ . The associated Coxeter orbifold V_\circ has 2 cusps.

Remark 1. By [Joh+02, Theorem 3], the groups $[5, 3, 6]$ and $[(3^3, 6)]$ are not commensurable; in particular, their invariant trace fields are different (see [MR03, Section 13.2]). Due to the graph symmetry $[(3^3, 6)]$, the Coxeter tetrahedron P_\circ has a symmetry plane H_r along which it can be dissected into 2 isometric tetrahedra (of non-Coxeter type), each with one cusp. The group extension $\Gamma_\circ^r := [(3^3, 6)] * C_r$ by the cyclic group C_r generated by the half-turn r with respect to H_r is a non-arithmetic discrete group containing $[(3^3, 6)]$ with index 2 and giving rise to the 1-cusped quotient space V_\circ^r .

2.3. Volumes of non-compact hyperbolic tetrahedra

Consider a finite volume orthoscheme $R = R(\alpha, \beta) \subset \mathbb{H}^3$ with one ideal vertex q and dihedral angles $\alpha, \beta, \beta' = \frac{\pi}{2} - \beta$ such that $\beta' \leq \alpha < \frac{\pi}{2}$ (see Figure III.1). More precisely, R is a tetrahedron bounded by geodesic planes H_1, \dots, H_4 with opposite vertices $p_1 = q, p_2, p_3, p_4$ such that the Gram matrix $G(R) = (g_{ij})$ is given by

$$G(R) = \begin{pmatrix} 1 & -\cos \alpha & 0 & 0 \\ -\cos \alpha & 1 & -\cos \beta & 0 \\ 0 & -\cos \beta & 1 & -\cos \beta' \\ 0 & 0 & -\cos \beta' & 1 \end{pmatrix}.$$

The matrix $G(R)$ is of signature $(3, 1)$ and has – beside positive definite principal submatrices – exactly one positive semi-definite principal submatrix of rank 2 (at the lower right) characterising the ideal vertex q of R .

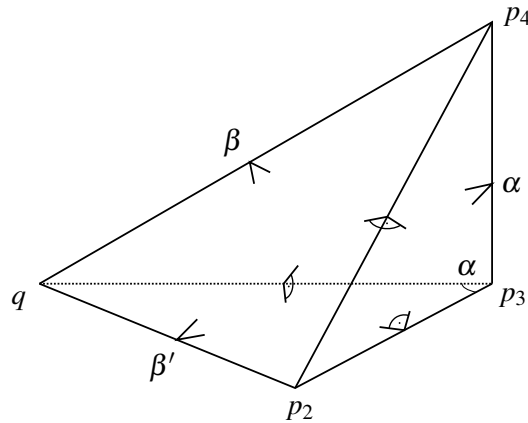


Figure III.1.: An orthoscheme $R(\alpha, \beta)$ with ideal vertex q

It is well-known that the scissors congruence group $\mathcal{P}(\mathbb{H}^3)$ is generated by the classes of orthoschemes $R(\alpha, \beta)$ (see [Kel12, Chapter 3], for example). Hence, the volume of any polyhedron $P \subset \mathbb{H}^3$ is a linear combination of volumes of orthoschemes of type $R(\alpha, \beta)$.

The volume of $R(\alpha, \beta)$ is given by the expression (see [Kel89], for example)

$$\text{vol}(R(\alpha, \beta)) = \frac{1}{4} \left\{ \mathbb{I}\left(\frac{\pi}{2} + \alpha - \beta\right) - \mathbb{I}\left(\frac{\pi}{2} + \alpha + \beta\right) + 2\mathbb{I}(\beta) \right\}, \quad (2.3)$$

where $\mathbb{I}(x) = \frac{1}{2} \sum_{r=1}^{\infty} \frac{\sin(2rx)}{r^2} = -\int_0^x \log |2 \sin t| dt$, $x \in \mathbb{R}$, is Lobachevsky's function. The function $\mathbb{I}(x)$ is odd, π -periodic and satisfies the distribution formula (see [Joh+99, Appendix], for example)

$$\frac{1}{k} \mathbb{I}(kx) = \sum_{r=0}^{k-1} \mathbb{I}\left(x + \frac{r\pi}{k}\right), \quad k \in \mathbb{N}.$$

As a consequence, for the volume of an ideal tetrahedron $T(\alpha, \beta, \gamma)$ with dihedral angles α, β, γ along edges emanating from an ideal vertex such that $\alpha + \beta + \gamma = \pi$, one deduces that

$$\text{vol}(T(\alpha, \beta, \gamma)) = \mathbb{I}(\alpha) + \mathbb{I}(\beta) + \mathbb{I}(\gamma). \quad (2.4)$$

As a special case, an ideal regular tetrahedron S_{reg}^{∞} (of dihedral angle $\frac{\pi}{3}$) is of volume $\mu_3 = \text{vol}(S_{reg}^{\infty}) = 24 \text{vol}(R(\frac{\pi}{3}, \frac{\pi}{3}))$. An ideal regular octahedron O_{reg}^{∞} (of dihedral angle $\frac{\pi}{2}$) can be dissected into 48 orthoschemes $R(\frac{\pi}{3}, \frac{\pi}{4})$ so that the volume ω_3 of O_{reg}^{∞} is given by $\omega_3 = 48 \text{vol}(R(\frac{\pi}{3}, \frac{\pi}{4}))$.

Examples.

The volume of the (arithmetic) Coxeter orthoscheme $R(\frac{\pi}{3}, \frac{\pi}{3}) = [3, 3, 6]$ equals

$$\frac{1}{8} \mathbb{I}\left(\frac{\pi}{3}\right) \approx 0.042289. \quad (2.5)$$

In particular, we deduce that $\mu_3 = \text{vol}(S_{reg}^{\infty}) = 3 \mathbb{I}(\frac{\pi}{3}) \approx 1.014942$.

The volume of the (arithmetic) Coxeter orthoscheme $R(\frac{\pi}{3}, \frac{\pi}{4}) = [3, 4, 4]$ equals

$$\frac{1}{6} \mathbb{I}\left(\frac{\pi}{4}\right) \approx 0.076330. \quad (2.6)$$

As a consequence, we have that $\omega_3 = \text{vol}(O_{reg}^{\infty}) = 8 \mathbb{I}(\frac{\pi}{4}) \approx 3.663862$.

The volume of the (non-arithmetic) Coxeter orthoscheme $R(\frac{\pi}{5}, \frac{\pi}{3}) = [5, 3, 6]$ equals

$$\frac{1}{2} \mathbb{I}\left(\frac{\pi}{3}\right) + \frac{1}{4} \left\{ \mathbb{I}\left(\frac{\pi}{6} + \frac{\pi}{5}\right) + \mathbb{I}\left(\frac{\pi}{6} - \frac{\pi}{5}\right) \right\} \approx 0.171502. \quad (2.7)$$

By dissection, the volume of the four Coxeter tetrahedra with cyclic Coxeter symbol $[(3, 6, 3, m)]$, $3 \leq m \leq 6$, can be determined quite easily. In particular, the volume of the non-arithmetic Coxeter tetrahedron $[(3^3, 6)]$ equals

$$\frac{5}{8} \mathbb{I}\left(\frac{\pi}{3}\right) + \frac{1}{3} \mathbb{I}\left(\frac{\pi}{4}\right) \approx 0.364107, \quad (2.8)$$

which is the smallest one among the four.

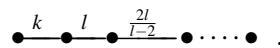
For the volumes of *all* hyperbolic Coxeter tetrahedra, we refer to [Joh+99, Appendix].

A generalisation of the volume formula (2.3) for orthoschemes $R(\alpha, \beta)$ with one ideal vertex can be obtained by allowing that $\alpha + \beta < \frac{\pi}{2}$. This condition is equivalent to the assumption

that the vertex p_4 as depicted in Figure III.1 is ultraideal, that is, the face planes H_q, H_2 and H_3 opposite to q, p_2 and p_3 intersect (in p_4) outside of $\mathbb{H}^3 \cup \partial\mathbb{H}^3$. In this situation, $R(\alpha, \beta)$ is of infinite volume. However, there is a unique hyperbolic plane H intersecting orthogonally H_q, H_2 and H_3 . In fact, in the projective model of \mathbb{H}^3 , the plane H is the *polar plane* associated to p_4 . By truncating $R(\alpha, \beta)$ by means of H , we obtain a *simply truncated orthoscheme* denoted by $R_t(\alpha, \beta)$. By [Kel89, (34)], the volume of $R_t(\alpha, \beta)$ is given analytically by the same formula (2.3), however under the constraint $\alpha + \beta < \frac{\pi}{2}$. This fact combined with suitable dissection procedures can be applied to determine the volumes of various families of truncated polyhedra in \mathbb{H}^3 .

Example.

For $k, l \in \mathbb{N}$ with $\frac{1}{k} + \frac{1}{l} < \frac{1}{2}$, consider a simply truncated Coxeter orthoscheme $R_t(\frac{\pi}{k}, \frac{\pi}{l})$ with one ideal vertex q . Its Coxeter graph is given by



In particular, the volume of the simply truncated Coxeter orthoscheme $R_t(\frac{\pi}{k}, \frac{\pi}{3})$, $k \geq 7$, is given by

$$\frac{1}{2} \mathbb{J}(\frac{\pi}{3}) + \frac{1}{4} \left\{ \mathbb{J}(\frac{\pi}{6} + \frac{\pi}{k}) + \mathbb{J}(\frac{\pi}{6} - \frac{\pi}{k}) \right\}, \tag{2.9}$$

while the volumes of the Coxeter family $R_t(\frac{\pi}{k}, \frac{\pi}{6})$, $k \geq 4$, are equal to

$$\frac{1}{2} \mathbb{J}(\frac{\pi}{6}) + \frac{1}{4} \left\{ \mathbb{J}(\frac{\pi}{3} + \frac{\pi}{k}) + \mathbb{J}(\frac{\pi}{3} - \frac{\pi}{k}) \right\}. \tag{2.10}$$

In both cases, for $k \rightarrow \infty$, the limiting Coxeter polyhedron is a pyramid with two ideal vertices and Coxeter symbol $[\infty, 3, 6, \infty]$ and has volume $\frac{5}{4} \mathbb{J}(\frac{\pi}{3}) \approx 0.42289$.

Remark 2. Notice that for the infinite families of polyhedra $R(\alpha, \beta)$ and $R_t(\alpha, \beta)$ with fixed angle β , the volume is strictly increasing when the dihedral angle α decreases. This is a direct consequence of Schläfli’s formula for the volume differential; see [Kel89, Section 2].

2.4. Some horoball geometry

Let $V = \mathbf{H}^3/\Gamma$ be a finite volume hyperbolic 3-orbifold with a set $\mathcal{C} = \{C_1, \dots, C_m\}$, $m \geq 1$, of disjoint cusps. Let $C \in \mathcal{C}$ be a maximal cusp such that $C = B_\infty/\Gamma_\infty$. Consider the image horoballs $\gamma(B_\infty)$ with $\gamma \notin \Gamma_\infty$ and project them orthogonally to the horosphere $H_\infty = \{t = 1\}$. The full-sized horoballs project onto Euclidean balls of diameter 1 and yield a periodic packing of the Euclidean plane by equal balls. Any minimal configuration of them providing the entire information (about translational and finite order symmetries) of the crystallographic group Γ_∞ yields a *horoball diagram* or *cuspid diagram* $D \subset H_\infty$ (see [Ada92a, Figure 1 or Figure 6], for example, and Section 3.3).

Denote by $F \subset \mathbb{R}^2$ a fundamental polygon for the action of Γ_∞ on the horosphere H_∞ , and let $\text{vol}_0(F)$ be its Euclidean area. Then, the volume of C can be expressed by (see [Cox54, Section 5])

$$\text{vol}(C) = \frac{1}{2} \text{vol}_0(F). \tag{2.11}$$

Notice that if Γ_∞ is a reflection group, its index two subgroup Γ_∞^+ of orientation preserving rotations yields twice the volume of (2.11).

The concept of local density of a horoball B covering C with respect to its Dirichlet-Voronoi cell $D(B)$ leads to the following lower volume bound for V in comparison with the total cusp volume $\text{vol}(\mathcal{C}) = \sum_{r=1}^m \text{vol}(C_r)$ (see [Mey86] and [Kel98, Lemma 3.2]).

$$\text{vol}(V) \geq \frac{\text{vol}(\mathcal{C})}{d_3(\infty)}, \quad (2.12)$$

where $d_3(\infty) = \frac{\sqrt{3}}{2\mu_3} \approx 0.853276$ is the simplicial horoball density related to an ideal regular tetrahedron S_{reg}^∞ of volume $3\mathbb{I}(\frac{\pi}{3})$.

Observe that the bound (2.12) is sharp if the lift of each element of \mathcal{C} to \mathbf{H}^3 induces a *regular* horoball packing (see [Kel98, Section 2]).

In the case of a 1-cusped orbifold with maximal cusp C , the cusp density $\delta(C) = \frac{\text{vol}(C)}{\text{vol}(V)} < 1$ is bounded from above by (see (2.12))

$$\delta(C) \leq d_3(\infty). \quad (2.13)$$

The following facts will be useful when studying horoball diagrams.

Lemma 1. [Ada91, Lemma 4.4] *The centres of two tangent horoballs of radii r_1 and r_2 are at Euclidean distance $2\sqrt{r_1 r_2}$.*

Lemma 2. [Ada91, Lemma 4.3], [HK07, Lemma 1] *Consider the horoball B_∞ and a full-sized horoball B_u based at $u \in \mathbb{R}^2$. Denote by l a geodesic with endpoints u and $v \in \mathbb{R}^2 \setminus \{u\}$, and let $\delta_0 = d_0(u, v)$ be the Euclidean distance from u to v . Put $a = (u, 1)$, and let p be the intersection point of l with $H_u = \partial B_u$. Then, the induced distance $d(a, p)$ from a to p on H_u is given by $d(a, p) = \frac{1}{\delta_0}$.*

Corollary 3. [HK07, Lemma 2] *Consider a horoball $B_u(h)$ of diameter h in \mathbf{H}^3 . Then, the interior of its upper hemisphere is an open disk of radius 1 with respect to the induced metric on the boundary $H_u(h)$.*

Corollary 4. [Hil07a, Corollary 7] *Let $B_u(h)$ and $B_v(k)$ be two horoballs with common touching point p and of Euclidean diameter h and k , respectively. Denote by δ_0 the Euclidean distance $d_0(u, v)$ and by $\delta = \delta_0/h$ the induced distance $d((u, h), (v, h))$ on the horosphere based at ∞ and at Euclidean height h . Then, the following identity holds.*

$$\frac{\sqrt{h}}{\sqrt{k}} = \frac{\delta_0}{k} = \frac{h}{\delta_0} = \frac{h\delta}{k} = \frac{1}{\delta}.$$

Corollary 5. *Consider a full-sized horoball B_u and a horoball $B_v(k)$ of diameter k based at $v \in \mathbb{R}^2$ which touches B_u . Denote by δ_0 the Euclidean distance $d_0(u, v)$. Then, the diameter k of B_v equals δ_0^2 .*

Lemma 3. [Ada91, Lemma 4.6], [Ada92a, Lemma 1.2] Consider two horoballs $B_u(h)$ and $B_v(k)$ based at $u, v \in \mathbb{R}^2$ of diameter h and k , respectively, which cover the cusp C of V . Suppose that $B_u(h)$ and $B_v(k)$ are not tangent, and denote by $d_0(u, v) =: r$ the Euclidean distance between their base points u and v . Then, there exists a horoball of diameter $\frac{hk}{r^2}$ covering C .

Consider the action of the crystallographic subgroup $\Gamma_\infty \subset \Gamma$ on the set of all full-sized horoballs. The following facts are fairly obvious (see [Ada92a, Lemma 3.1 and Lemma 2.1]).

Lemma 4. Suppose that Γ_∞ identifies all full-sized horoballs. If the shortest translation length satisfies $\tau > 1$, then there cannot be a set of three full-sized horoballs which are pairwise tangent.

Lemma 5. Suppose that Γ_∞ identifies all full-sized horoballs. Then, every point of tangency between two Γ -equivalent horoballs lies on the axis of an order two elliptic isometry in Γ such that its axis is tangent to both horoballs.

3. Proof of the Theorem

In this section, we provide a proof in several steps of our main result stated as follows.

Theorem. Among all non-arithmetic cusped hyperbolic 3-orbifolds, the 1-cusped quotient space V_* of \mathbf{H}^3 by the tetrahedral Coxeter group [5, 3, 6] has minimal volume. As such the orbifold V_* is unique, and its volume v_* is given explicitly by (2.7).

For the proof, we adapt and generalise the strategies and results of Adams as developed in [Ada92a], [Ada91] and [Ada92b].

3.1. The non-rigid and multiply cusped cases

Let $\mu_3 = \text{vol}(S_{reg}^\infty) = 3\text{JI}(\frac{\pi}{3}) \approx 1.014942$ and $\omega_3 = \text{vol}(O_{reg}^\infty) = 8\text{JI}(\frac{\pi}{4}) \approx 3.663862$ be the volumes of an ideal regular tetrahedron and of an ideal regular octahedron, respectively (see (2.5) and (2.6)).

Denote by $V = \mathbf{H}^3/\Gamma$ a non-arithmetic cusped orbifold of minimal volume. By a result of Meyerhoff [Mey85], the smallest volume of any cusped hyperbolic 3-orbifold equals $\frac{\mu_3}{24}$ and is realised in a unique way by the volume of the quotient of \mathbf{H}^3 by the arithmetic tetrahedral Coxeter group [3, 3, 6]. Therefore, the volume of V has to satisfy the inequalities

$$0.042289 \approx \frac{\mu_3}{24} < \text{vol}(V) \leq \text{vol}(V_*) = v_* \approx 0.171502. \quad (3.1)$$

Proposition 6. A non-arithmetic cusped hyperbolic 3-orbifold V of minimal volume has precisely one cusp, and this cusp is a rigid one.

Proof. In [Ada92b], Adams considered the small volume spectrum of hyperbolic 3-orbifolds with $m \geq 2$ cusps. He proved that the four smallest (non-orientable) orbifolds of this sort have volumes equal to

$$\frac{\mu_3}{6}, \frac{5\mu_3}{24}, \frac{\omega_3}{16} \quad \text{and} \quad \frac{\mu_3}{4} \quad (3.2)$$

(see [Ada92b, Corollary 2.6]). Comparing the four values in (3.2) with the volume bound in (3.1) shows that all values except the first one given by $\frac{\mu_3}{6}$ are strictly bigger than $\text{vol}(V_*)$. Furthermore, in [Ada92b, Lemma 2.2], Adams identified the individual multiply-cusped orbifolds with small volumes and proved their uniqueness. According to his proof [Ada92b, pp. 155-156], one easily deduces that the value $\frac{\mu_3}{6}$ is the volume of the quotient space of \mathbf{H}^3 by the *arithmetic* tetrahedral Coxeter group $[3, 6, 3]$. Therefore, V can have only one cusp.

Suppose that a hyperbolic 3-orbifold V has a single cusp C , and that C is non-rigid. By the results of Adams [Ada91, Corollary 4.2 and Section 7] about limit volumes of orientable hyperbolic 3-orbifolds, the three smallest volumes are $\frac{\omega_3}{12} \approx 0.305322$, 0.444457 and 0.457983 . These values are realised in a unique way by orientable orbifolds which are explicitly described in the proof of [Ada91, Lemma 7.1]. In fact, their fundamental groups are all arithmetic and related to Bianchi groups $\text{PSL}(2, \mathcal{O}_d)$ where \mathcal{O}_d is the ring of integers of the imaginary quadratic number field $\mathbb{Q}(\sqrt{-d})$. In particular, the fundamental group of the orbifold with volume $\frac{\omega_3}{12}$ is the Bianchi group $\text{PSL}(2, \mathcal{O}_1)$ which is commensurable to the tetrahedral Coxeter group $[3, 4, 4]$ and to the fundamental group of the Borromean Rings complement (see also [MR03, Section 9.2]). As a consequence, a non-orientable hyperbolic 3-orbifold with a single, non-rigid cusp of volume smaller than or equal to $\text{vol}(V_*)$ is arithmetic. \square

3.2. The cusp type $\{3, 3, 3\}$

By Proposition 6, a non-arithmetic non-compact orbifold $V = \mathbf{H}^3/\Gamma$ of minimal volume has only one cusp, and the cusp is a rigid one of type $\{2, 3, 6\}$, $\{2, 4, 4\}$ or $\{3, 3, 3\}$. The next result allows us to exclude the type $\{3, 3, 3\}$ from further consideration.

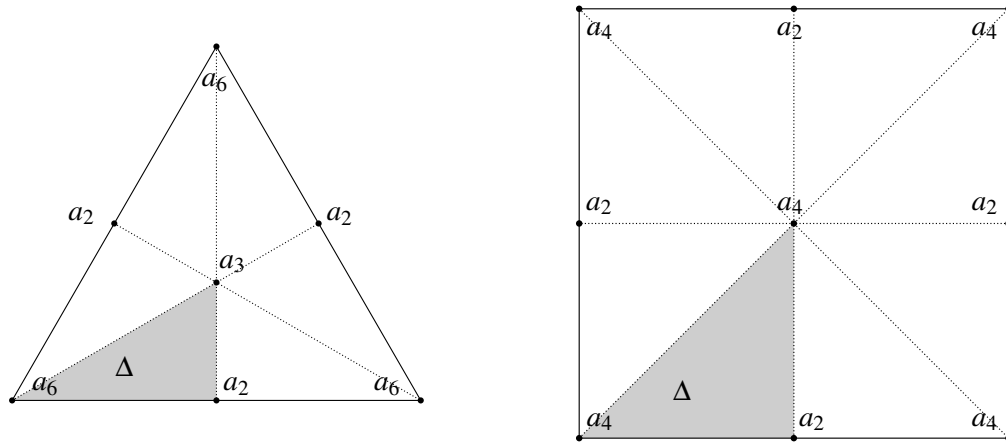
Proposition 7. *A non-arithmetic cusped hyperbolic 3-orbifold V of minimal volume cannot have a cusp of type $\{3, 3, 3\}$.*

Proof. In [Ada92a, Theorem 4.2], Adams proved that an orientable hyperbolic 3-orbifold with a cusp of type $\{3, 3, 3\}$ has volume either $\frac{\mu_3}{6}$, $\frac{\mu_3}{3}$, $\frac{5\mu_3}{12}$ or at least $\frac{\mu_3}{2}$. Furthermore, he showed that there are unique orbifolds whose volumes equal these first three values, and that they are the double covers of certain *unique* orientable orbifolds with one cusp of type $\{2, 3, 6\}$ of small volume. He provides an explicit description of the latter orbifolds as follows (see [Ada92a, p. 10]).

The unique orientable orbifold with one cusp of type $\{2, 3, 6\}$ and of volume $\frac{\mu_3}{12}$ is the orientable double cover of the arithmetic orbifold $\mathbf{H}^3/[3, 3, 6]$ implying that the orbifold with cusp of type $\{3, 3, 3\}$ and of volume $\frac{\mu_3}{6}$ is the quotient of \mathbf{H}^3 by the rotation subgroup of the arithmetic tetrahedral Coxeter group with symbol $[3, 3^{[3]}]$.

The unique orientable orbifold with one cusp of type $\{2, 3, 6\}$ and of volume $\frac{\mu_3}{6}$ is the orientable double cover of the quotient space of \mathbf{H}^3 by the \mathbb{Z}_2 -extension of the arithmetic Coxeter group $[3, 6, 3]$. Let us add that this orbifold as well as its double cover with one cusp of type $\{3, 3, 3\}$ are *not* Coxeter orbifolds anymore.

Finally, observe that the third smallest value $\frac{5\mu_3}{12} \approx 0.422892$ in the above sequence is strictly bigger than the covolume $2\text{vol}(V_*)$ of the rotation subgroup of $[5, 3, 6]$. As a consequence, a non-arithmetic cusped orbifold V of minimal volume cannot have a cusp of type $\{3, 3, 3\}$. \square


 Figure III.2.: Tiling of D into copies of its characteristic triangle Δ

3.3. Some notations

Before we continue with the proof, let us fix some notations. Consider a non-compact orbifold $V = \mathbf{H}^3/\Gamma$ with precisely one (maximal) cusp, denoted by C , such that C is a rigid one. We assume that the *cuspidal point* (or *parabolic fixed point*) associated to C is based at ∞ and that $C = B_\infty/\Gamma_\infty$ with B_∞ the horoball at height 1 from the ground plane $\{t = 0\}$. Denote by $\tau \geq 1$ the minimal translation length induced by the translation lattice $L \subset \Gamma_\infty$.

Suppose that C is of type $\{p, q, r\}$ with $(p, q, r) = (2, 3, 6)$ or $(2, 4, 4)$ (see Section 2.1). In particular, C contains 3 singular (rotation) axes of orders 2, q, r , respectively. By Proposition 7, these assumptions do hold if V is non-arithmetic of minimal volume.

Consider a cuspidal diagram $D \subset H_\infty$ of Γ_∞ . If C is of type $\{2, 3, 6\}$, then D is a Euclidean regular triangle of edge length τ , and if C is of type $\{2, 4, 4\}$, then D is given by a Euclidean square of edge length τ . In particular, the singular axes of C give rise to singular points a_2, a_q and a_r in D in the following way. The midpoint of each edge of D is a singular point a_2 of order 2, the centre of D is a singular point a_q of order q , and each vertex of D is a singular point a_r of order r . Since the horoballs covering C do not intersect in their interiors, the vertical axis l_s in the upper half space U^3 passing through a singular point a_s , $s \in \{2, q, r\}$, can lie in the interior of a full-sized horoball B_u only if the horoball B_u is centred at the intersection u of l_s with $\{t = 0\}$, that is, if $a_s = (u, 1)$. We say that B_u is *centred at* a_s and write B omitting the index u , for short. By barycentric decomposition, D is tiled into copies of its *characteristic triangle* Δ with vertices a_s , $s \in \{2, q, r\}$, and which is either a right-angled triangle $[3, 6]$ or a right-angled triangle $[4, 4]$; see Figure III.2. The aim is to determine or estimate in terms of τ or – more easily – by means of the smallest distance d of full-sized horoballs the cathetus length $d_0(a_2, a_p)$ or $d_0(a_2, a_q)$ of Δ . The position of the full-sized horoballs, projecting to full-sized horodisks (of radius $\frac{1}{2}$) in H_∞ , will play a crucial role. These investigations will allow us to bound the volume of V by the expression (see (2.11) and (2.12))

$$\text{vol}(V) \geq \frac{\text{vol}(C)}{d_3(\infty)} = \frac{\mu_3}{\sqrt{3}} \cdot \text{vol}_0(\Delta). \quad (3.3)$$

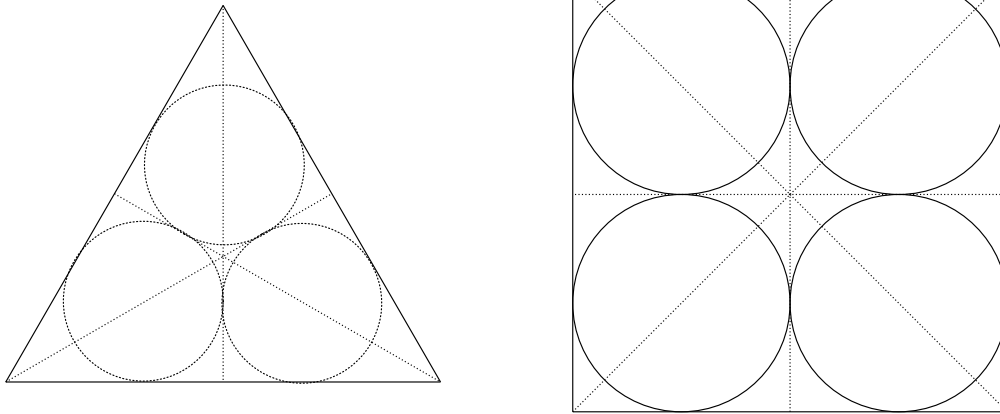


Figure III.3.: Full-sized horoballs not centred at singular points

3.4. One equivalence class of full-sized horoballs

Assume that the crystallographic group Γ_∞ gives rise to only one equivalence class of full-sized horoballs. If there is a full-sized horoball which is *not* centred at any of the singular points a_s , $s \in \{2, q, r\}$, in the cusp diagram D , then the least cusp volume $\text{vol}(C)$ is given by (see also [Ada92a, Figure 1(a), p. 4, and Figure 6(a), p. 12] and Figure III.3)

$$\text{vol}(C) = \begin{cases} \frac{\sqrt{3}}{12} \left(1 + \frac{\sqrt{3}}{2}\right) \approx 0.269338 & \text{if } C \text{ is of type } \{2, 3, 6\}, \\ \frac{1}{4} & \text{if } C \text{ is of type } \{2, 4, 4\}. \end{cases} \quad (3.4)$$

As a consequence, the volume of V is strictly bigger than $v_* = \text{vol}(\mathbf{H}^3/[5, 3, 6])$ (compare with (3.1)).

From now on, we assume that there is a full-sized horoball centred at one of the singular points a_s , $s \in \{2, q, r\}$, in the cusp diagram D . We treat the cases $s \in \{2, 3, 6\}$ and $s \in \{2, 4, 4\}$ separately.

The case $\{2, 3, 6\}$

(i) First we assume that there are at least two full-sized horoballs which touch one another, that is, the minimal distance d of the centres of full-sized horoballs equals 1. In particular, in the cusp diagram D , there will be at least two full-sized disks, centred at equivalent singular points, which touch one another; see Figure III.4.

Order 6. If there is a full-sized horoball (of radius $\frac{1}{2}$) centred at the singular point a_6 in Δ , then $d_0(a_2, a_6) = \frac{1}{2}$, and the cusp volume $\text{vol}(C)$ equals $\frac{\sqrt{3}}{48}$. Since there are exactly three full-sized horoballs touching one another and the horoball B_∞ , it is easy to see that the (up to isometry) unique orbifold V_0 corresponding to this configuration is given by the quotient of \mathbf{H}^3 modulo the arithmetic Coxeter group $[3, 3, 6]$ (see [Mey86], [Mey85]). The orbifold is covered by Gieseking's manifold and is known to be the cusped hyperbolic 3-orbifold of minimal volume (which equals

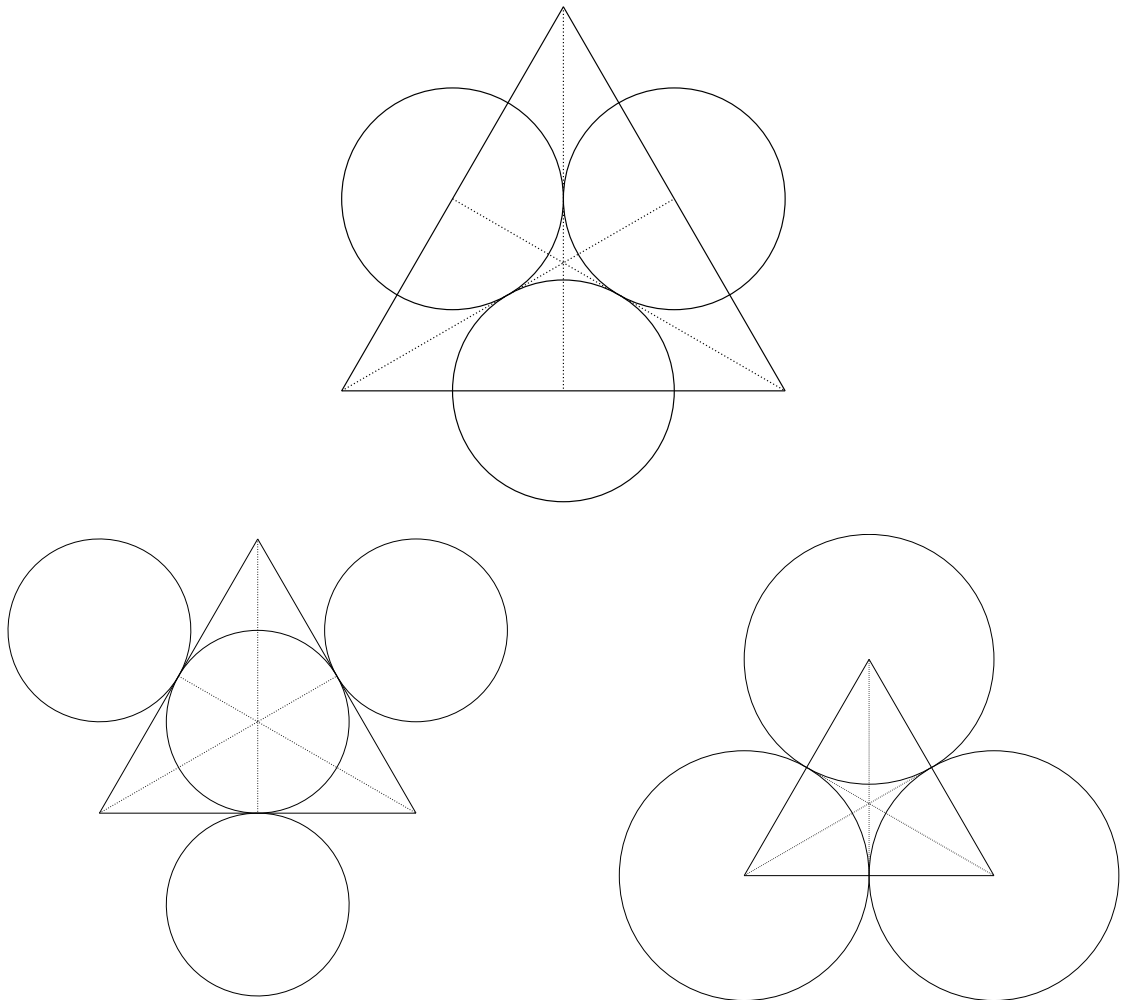


Figure III.4.: A $\{2, 3, 6\}$ -cusp with full-sized horoballs centred at equivalent singular points

$\frac{\mu_3}{24} = \frac{1}{8} \mathbb{I}(\frac{\pi}{3}) \approx 0.042289$). In particular, the cusp density $\delta(C)$ satisfies $\text{vol}(C)/\text{vol}(V_0) = d_3(\infty)$ (see also (2.13)).

Order 3. Suppose that there is a full-sized horoball centred at the singular point a_3 in Δ . Then, $d_0(a_2, a_3) = \frac{1}{2}$ and $d_0(a_2, a_6) = \frac{\sqrt{3}}{2}$ so that the cusp volume equals $\frac{\sqrt{3}}{16}$ [Ada92a, Figure 1(c), p. 4]. By Lemma 5, it is not difficult to see that there is a unique orbifold which corresponds to this configuration. Its fundamental group is given by the \mathbb{Z}_2 -extension of the *arithmetic* Coxeter group $[3, 6, 3]$ (and has covolume $\frac{1}{4} \mathbb{I}(\frac{\pi}{3}) \approx 0.084579$).

Order 2. Suppose that there is a full-sized horoball centred at the vertex $a_2 \in \Delta$. Then, $d_0(a_2, a_3) = \frac{1}{\sqrt{3}}$ and $d_0(a_2, a_6) = 1$, and the cusp volume is given by $\frac{\sqrt{3}}{12} \approx 0.144338$ (see [Ada92a, Figure 1(b), p. 4]). Note that this volume is also the smallest cusp volume for the case that we have full-sized horoballs at both the singular points a_2 and a_6 . There is a unique orbifold which corresponds to this configuration, and it is given by the *arithmetic* Coxeter simplex with symbol $[3^{1,1}, 6]$ and 2 cusps. By cutting along the symmetry plane of $[3^{1,1}, 6]$, we get an orbifold whose fundamental group is commensurable to $[3^{1,1}, 6]$ and isomorphic to the arithmetic Coxeter group $[4, 3, 6]$ of covolume $\frac{5}{16} \mathbb{I}(\frac{\pi}{3}) \approx 0.105723$ (see [Joh+99, p. 347], for example).

(ii) Suppose now that the full-sized horoballs do *not* touch another. Then, the minimal distance d of their centres satisfies $d > 1$. Assume that one full-sized horoball is centred at the singular point a_s , $s \in \{2, 3, 6\}$, in Δ . Since Γ_∞ identifies all full-sized horoballs, Lemma 5 yields an order two elliptic element $\gamma_s \in \Gamma$ with axis perpendicular at $a_s =: (u_s, 1)$ to the order s axis l_s . The element γ_s sends the horoball B_∞ to the full-sized horoball B_{u_s} and vice versa. Furthermore, γ_s sends the s neighboring full-sized horoballs – each at distance d from u_s – to s smaller horoballs. By the proof of Lemma 3, these smaller horoballs are of Euclidean diameter $\frac{1}{d^2}$, and by Corollary 4, their base points are at a distance $\frac{1}{d}$ from u_s . Following the terminology of Adams [Ada92a, p. 5], call each of these balls a $(\frac{1}{d})$ -ball. By construction, the $(\frac{1}{d})$ -balls are the biggest horoballs of diameter less than 1 that are tangent to full-sized horoballs.

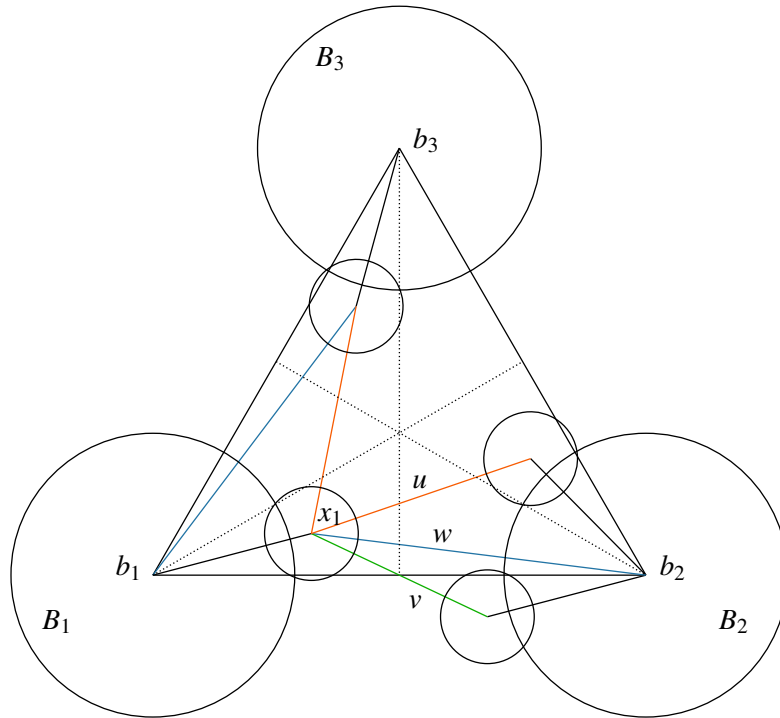
Let $B(h)$ be a horoball of diameter h such that $\frac{1}{d^2} \leq h < 1$ covering C which is *not* tangent to any larger horoball covering C . Then, in the interior of its upper hemisphere, there are no points of tangency with horoballs covering C . By Corollary 3, this upper hemisphere is an open disk of radius 1 with respect to the induced metric on its boundary. By mapping $B(h)$ to B_∞ by means of an element in Γ , we obtain a disk of radius 1 on the horosphere H_∞ which contains no point of tangency with full-sized horoballs. Such a disk is called a *disk of no tangency*. Notice that the existence of a disk of no tangency in the cusp diagram on H_∞ for C has the same effect as an extra full-sized horoball touching the centre of the disk would have.

Furthermore, by Corollary 4, one can deduce the following fact for a cusp of any type (for a proof, see [Ada92a, pp. 5–6]).

Lemma 6. *Let B be a full-sized horoball covering the cusp C , and let $B_{\frac{1}{d}}$ be a $(\frac{1}{d})$ -ball touching B . If the base point x of $B_{\frac{1}{d}}$ has Euclidean distance $d_0(x, y) < 1$ from the base point y of another full-sized horoball B' or if $d_0(x, z) < \frac{1}{d}$ with z a base point of another $(\frac{1}{d})$ -ball $B'_{\frac{1}{d}}$, without $B_{\frac{1}{d}}$ touching B' or $B'_{\frac{1}{d}}$, then there is a disk of no tangency in the cusp diagram of C .*

With these preliminary remarks, we investigate in detail each of the cases $s \in \{2, 3, 6\}$.

Order 6. Suppose that a full-sized disk $B = B_1$ is centred at the singular point $b_1 = a_6$ in D ,


 Figure III.5.: $(\frac{1}{d})$ -balls in the $\{2, 3, 6\}$ -cusp triangle D

and that B_2, B_3 are full-sized disks centred at the vertices b_2, b_3 at distance d from B_1 in the cusp triangle D . For $1 \leq i \leq 3$, let x_i denote the center (at height 1) of the $(\frac{1}{d})$ -ball touching B_i in D . Following Adams [Ada92a, Figure 2], we define the Euclidean distances $u = d_0(x_i, x_j)$, v and w as in Figure III.5.

Consider the triangle $\Delta(b_1, x_1, b_2)$ with edge lengths $d_0(b_1, x_1) = \frac{1}{d}$, $d_0(x_1, b_2) = w$ as well as $d_0(b_1, b_2) = d$, and denote by $\theta = \angle(x_1, b_2)$ the angle at $b = b_1$. By symmetry of D , we may suppose that $0 \leq \theta \leq \frac{\pi}{6}$. The elementary law of cosines allows one to deduce the following identities (see [Ada92a, (1)–(3)])

$$u^2 = d^2 + \frac{3}{d^2} - \sqrt{3} \sin \theta - 3 \cos \theta = d^2 + \frac{3}{d^2} - 2\sqrt{3} \cos(\frac{\pi}{6} - \theta) \quad (3.5)$$

$$v^2 = d^2 + \frac{4}{d^2} - 4 \cos \theta \quad (3.6)$$

$$w^2 = d^2 + \frac{1}{d^2} - 2 \cos \theta. \quad (3.7)$$

The strategy as developed in detail by Adams [Ada92a, pp. 6–10] consists now in analysing the different tangency possibilities of the $(\frac{1}{d})$ -balls with respect to one or several full-sized horoballs and among themselves.

A crucial point will be the dichotomy of Γ_∞ preserving orientation, or not. If Γ_∞ contains a reflection, then we say that the horoball configuration in the cusp diagram D has a *mirror symmetry*.

Altogether, we will be able to determine or estimate explicitly the lengths d and τ , the associated cusp volume $\text{vol}(C) = \frac{\sqrt{3}d^2}{48}$ (in case of no mirror symmetry) and to describe the corresponding orbifold V under the volume constraint $\text{vol}(V) \leq \text{vol}(V_*) = v_*$ (see (3.1)). Furthermore, one has to check whether the resulting orbifold V is arithmetic or not. This is not difficult if its fundamental group is given by a hyperbolic Coxeter group (see Section 2.2) or by an explicit presentation in $\text{PSL}_2(\mathbb{C})$ (see [MR03, Section 8]).

Remark 8. Assuming the rough volume estimate (see (2.7), (2.12))

$$\text{vol}(V) \geq \frac{\text{vol}(C)}{d_3(\infty)} = \frac{\sqrt{3}d^2}{48d_3(\infty)} > \text{vol}(V_*) = v_* \approx 0.171502,$$

where $d_3(\infty) \approx 0.853276$, we obtain $d > 2.013813$. Hence, we only have to consider values for $d > 1$ with $d \leq 2.013813$ or – in the case that Γ_∞ is orientation-preserving – values for d with $d \leq 1.423982$.

We start with the easy case of $(\frac{1}{d})$ -balls touching at least two full-sized horoballs. This case has a complete answer showing that the resulting orbifold is arithmetic (see [Ada92a, p. 3 and p. 10] and [NR92]). We provide one illustrating example and suppose that a single $(\frac{1}{d})$ -ball touches three full-sized horoballs giving a cusp diagram as depicted in [Ada92a, Figure 3(b)]. It easily follows that $d = \sqrt[4]{3}$ yielding a cusp volume of $\frac{1}{16}$. Associated to this configuration is a unique orbifold with fundamental group that is commensurable to the arithmetic Coxeter group $[3, 6, 3]$ (see [Ada92a, p. 10] in the corresponding oriented case).

The delicate case is when each $(\frac{1}{d})$ -ball touches a unique full-sized horoball. Let us consider the mutual position of the $(\frac{1}{d})$ -balls. By Lemma 4, we can exclude the case that three $(\frac{1}{d})$ -balls touch each other.

Next, observe that we can assume that the distance w as depicted in Figure III.5 satisfies

$$w \geq 1 \quad \text{implying that} \quad d \geq \frac{1}{2}(\sigma + \sqrt{\sigma^2 - 4}) \approx 1.515464 \quad \text{for} \quad \sigma = \sqrt{3 + \sqrt{3}}. \quad (3.8)$$

In fact, if there is *no* disk of no tangency, this is a direct consequence of Lemma 6. If there is a disk of no tangency in D , then $d \geq \sqrt{3}$. Since $0 \leq \theta \leq \frac{\pi}{6}$, equation (3.7) for w implies that $w \geq \frac{2}{\sqrt{3}} > 1$ and the asserted estimate for d .

Consequence. If Γ_∞ is orientation-preserving, the bound $d \geq 1.515464$ from (3.8) yields a too big cusp estimate $\frac{\text{vol}(C)}{d_3(\infty)}$ in comparison with v_* . In particular, we do not have to analyse in depth cusp diagrams D with no mirror symmetry.

Now, if two $(\frac{1}{d})$ -balls touch one another but no further $(\frac{1}{d})$ -ball touches this pair, then the point of tangency created by this pair must coincide with a 2-fold singular point a_2 in D . Since the tangency point is the midpoint of an edge e of D , one has $v = \frac{1}{d^2}$ with v given by equation (3.6). Implementing this identity into the equation (3.7) for w , the property $w \geq 1$ yields the inequality

$$d^6 - 2d^4 - 2d^2 + 1 \geq 0, \quad (3.9)$$

and hence $d \geq 2 \cos \frac{\pi}{5} > 1.6$. One can conclude the case by different considerations (for Adams' conclusion, see [Ada92a, pp. 7-8]). First, assume that the centres of the two $(\frac{1}{d})$ -balls are *not*

aligned with b_1 and b_2 on the edge e of D . Then, the group Γ_∞ consists of rotations, only, and we are done.

Next, assume that the centres of the two $(\frac{1}{d})$ -balls lie on the edge e . Then,

$$d = \frac{2}{d} + \frac{1}{d^2},$$

and hence, $d = 2 \cos \frac{\pi}{5}$. There is a unique orbifold associated to this situation, which is based on an orthoscheme $R(\frac{\pi}{5}, \frac{\pi}{3})$ and its reflection group (see Section 2.3). Indeed, the orbifold equals V_* with non-arithmetic fundamental group [5, 3, 6] (see [Ada92a, pp. 6-8]).

Assume now that the $(\frac{1}{d})$ -balls *do not touch* each other. Following [Ada92a, p. 8], and by Lemma 5, there is an order 2 elliptic element exchanging the horoball B_∞ and a full-sized horoball B_j while sending a neighbouring full-sized horoball B_k to a $(\frac{1}{d})$ -ball B_x , say (compare Figure III.6). Then, the $(\frac{1}{d})$ -ball B_y (at distance w from B_j) touching B_k gets sent to a ball B_x (at distance $\frac{1}{w}$ from B_j) touching B_x . Like in [Ada92a] we call this ball a $(\frac{1}{w})$ -ball. Its diameter equals $\frac{1}{w^2 d^2}$ by Lemma 3. We study now the positions of the $(\frac{1}{w})$ -balls and distinguish several cases.

- Suppose that the $(\frac{1}{w})$ -balls of the three $(\frac{1}{d})$ -balls in D coincide. This implies that the $(\frac{1}{w})$ -ball is centred in the 3-fold singular point $p = a_3$ in D yielding $w = \frac{\sqrt{3}}{d}$. Knowing all the side lengths of the triangle $\Delta(j, k, x)$ one can calculate the angle θ with the law of cosines as $\cos \theta = \frac{5}{2\sqrt{7}}$ which yields $d = \sqrt[4]{7} > 1.6$ by means of (3.7). Furthermore, one can derive that the points j, x and y are aligned. The situation is sketched in Figure III.6.

As a consequence, the horoball configuration in the cusp diagram D has no mirror symmetry. Hence, the cusp volume equals

$$\text{vol}(C) = \frac{\sqrt{21}}{24} > 0.19 > v_*,$$

and we can exclude this case from our considerations.

Remark 9. Adams considered the case above for an oriented orbifold $O = \mathbb{H}^3/\Gamma$ and calculated the corresponding cusp volume correctly as $\frac{\sqrt{21}}{24}$. However, in [Ada92a, p. 10], he gives a wrong fundamental polyhedron for Γ and a volume which is too big. In the Appendix III.A, we correct Adams' analysis, compute the volume and prove the arithmeticity of the orbifold O .

- Suppose that two $(\frac{1}{w})$ -balls of two $(\frac{1}{d})$ -balls coincide, having center x , say, and that no further $(\frac{1}{w})$ -ball touches them. If D has no mirror symmetry, then by means of the estimate $d \geq 1.515464$ given by (3.8), we obtain

$$\frac{\text{vol}(C)}{d_3(\infty)} = \frac{\sqrt{3}d^2}{24d_3(\infty)} > 0.19 > v_*.$$

Hence, we may assume that the center x coincides with an edge center a_2 of D . It follows that $d = \frac{2}{w}$ which, by means of (3.7) and with $\theta = 0$, yields $d^4 - 2d^2 - 3 = 0$ with solution $d = \sqrt{3}$. There is a unique orbifold realising this configuration. It is arithmetic and of volume $\frac{3}{8}\mathbb{II}(\frac{\pi}{3})$, being commensurable to the 2-cusped quotient space by the Coxeter group [6, 3, 6].

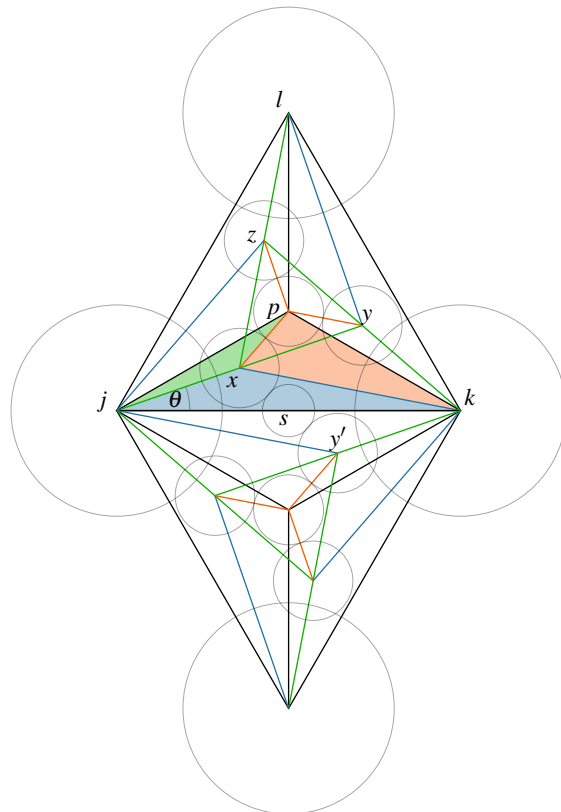


Figure III.6.: A single $(\frac{1}{w})$ -ball in a $\{2, 3, 6\}$ -cusp triangle D

• Suppose that the $(\frac{1}{w})$ -balls are distinct and that D has a mirror symmetry. In general, the $(\frac{1}{w})$ -balls cannot touch full-sized balls since then two $(\frac{1}{d})$ -balls touch another, in contrast to our assumption above. Furthermore, three $(\frac{1}{w})$ -balls cannot touch one another pairwise by Lemma 4.

Since D has a mirror symmetry, the group Γ_∞ is a reflection group. As a consequence, the centres of the $(\frac{1}{d})$ -balls lie either on the edges or on the angle bisectors of D .

Assume first that the centres of the $(\frac{1}{d})$ -balls lie on the edges of D . The situation is depicted in Figure III.7. Consider the horoballs smaller than the full-sized horoballs in a hierarchical way as

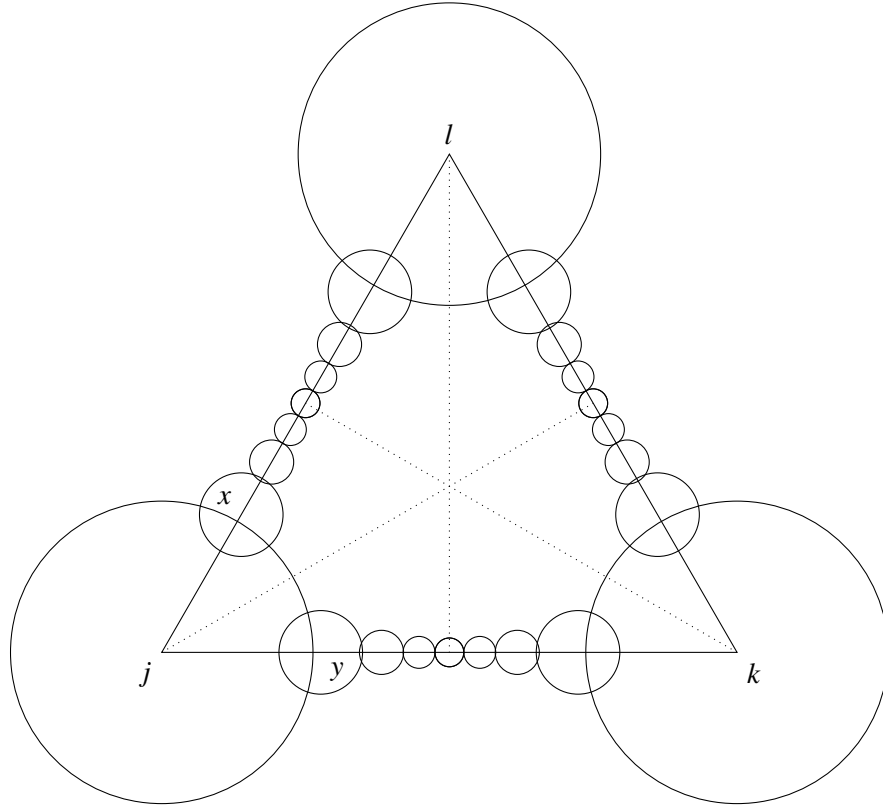


Figure III.7.: $(\frac{1}{d})$ -balls aligned along the edges of D

follows. For the $(\frac{1}{d})$ -balls, we have the following three possibilities

- (i) Each $(\frac{1}{d})$ -ball touches two full-sized balls.
- (ii) Each $(\frac{1}{d})$ -ball touches one full-sized ball and one other $(\frac{1}{d})$ -ball.
- (iii) Each $(\frac{1}{d})$ -ball touches one full-sized ball and *no* other $(\frac{1}{d})$ -ball.

In the third case, there are $(\frac{1}{w})$ -balls which are smaller images of the $(\frac{1}{d})$ -balls under an order 2 elliptic element r which maps B_∞ to a full-sized horoball according to Lemma 5. For those $(\frac{1}{w})$ -balls, there are the analogous three cases as above, and so on. This defines a sequence of horoball diagrams whose first elements are depicted in Figure III.8. Note that Adams [Ada92a]

discussed the depicted horoball diagrams in detail (see above). In particular, the third horoball diagram corresponds to the group $[5, 3, 6]$ while the fourth and the two first ones correspond to arithmetic groups.

For a given horoball diagram of this type, define a sequence

$$d_1 := d, d_2 := w = d - \frac{1}{d_1}, \dots$$

in the sense that in the third case where the $(\frac{1}{d_k})$ -balls do not touch, there are $(\frac{1}{d_{k+1}})$ -balls which are the smaller images of the $(\frac{1}{d_k})$ -balls under the isometry r . This implies the recursion

$$d_{k+1} = d - \frac{1}{d_k}, k \geq 1. \quad (3.10)$$

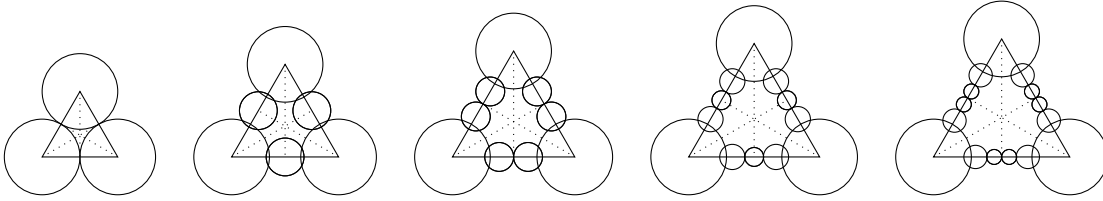


Figure III.8.: The beginning of the sequence of horoball diagrams with aligned $(\frac{1}{d})$ -balls.

Let $k_{\max} := \max \{k \mid \text{the horoball diagram } D \text{ contains a } \frac{1}{d_k}\text{-ball}\}$. There are two cases.

If one $(\frac{1}{d_{k_{\max}}})$ -ball touches two $(\frac{1}{d_{k_{\max}-1}})$ -balls, the centre of the $(\frac{1}{d_{k_{\max}}})$ -ball lies in the midpoint a_2 between two neighbouring full-sized balls, leading to the equation

$$\frac{1}{d_{k_{\max}}} = \frac{d}{2}. \quad (3.11)$$

If there is a pair of touching $(\frac{1}{d_{k_{\max}}})$ -balls, it implies that one of those $(\frac{1}{d_{k_{\max}}})$ -balls is fixed by r because otherwise r sends $(\frac{1}{d_k})$ -balls to $(\frac{1}{d_{k-1}})$ -balls or to $(\frac{1}{d_{k+1}})$ -balls but there is no $(\frac{1}{d_{k_{\max}+1}})$ -ball. This yields the equation

$$1 = d - \frac{1}{d_{k_{\max}}}. \quad (3.12)$$

The recursion (3.10) together with the end conditions (3.11) or (3.12) prove that d has to be the root of a polynomial related to the Chebyshev polynomials of the first kind or of the second kind, respectively. In case (3.11), this implies

$$d = 2 \cos \left(\frac{\pi}{2k_{\max} + 2} \right), \quad (3.13)$$

and in case (3.12), it implies

$$d = 2 \cos \left(\frac{\pi}{2k_{\max} + 3} \right). \quad (3.14)$$

Details can be found in [Dre21]. This recursion allows us to investigate the horoball diagrams and to characterise the group Γ assuming that Γ_{∞} is a reflection group.

Proposition 10. *In the case of the $\{2, 3, 6\}$ -cusp where Γ_∞ is a reflection group and the full-sized horoballs are centred in the singular points a_6 , the group Γ having a horoball diagram according to Figure III.7 contains the Coxeter group*

$$\bullet \overset{6}{\text{---}} \bullet \text{---} \bullet \overset{\alpha_k}{\text{---}} \bullet$$

where $d =: 2 \cos \alpha_k$ is given according to (3.13) and (3.14), respectively.

Proof. Since the Coxeter group $\Gamma_\infty = \bullet \overset{6}{\text{---}} \bullet \text{---} \bullet$ is contained in Γ , it only remains to prove the existence of the last generator in Γ . Consider an elliptic isometry r of order 2 mapping B_∞ to a full-sized horoball and vice versa.

If r is a reflection, we can see that it is the desired one: Its reflection plane R is a hemisphere orthogonal to the two reflection planes of Γ_∞ passing through a_6 . The hemisphere has radius 1, and its centre has distance $\frac{d}{2}$ to the last reflection plane of Γ_∞ implying that the angle of intersection α satisfies $\cos \alpha = \frac{d}{2}$, that is, $\alpha = \alpha_k$.

In the case where r is a rotation of order 2, we can choose it such that the full-sized ball B_k is mapped to the $(\frac{1}{d})$ -ball B_x , and B_l is mapped to B_y ; see Figure III.7. Then, r is the rotation in the edge ab of the orthoscheme defined by the planes mentioned above; see Figure III.9. If $s \in \Gamma_\infty$ is the reflection in the face (a, b, ∞) , then $rs = sr$ is the reflection in the hemisphere R as above and belongs to Γ . \square

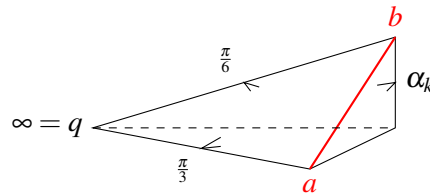


Figure III.9.: Fundamental orthoscheme

As a consequence of Proposition 10, the groups Γ with distances $\sqrt{2} \leq d \leq \sqrt{3}$ between full-sized horoballs are of smallest covolume if Γ coincides with (a finite index subgroup of) the arithmetic Coxeter group $[l, 3, 6]$ for $l = 3, 4$ or 6 , or with the non-arithmetic Coxeter group $[5, 3, 6]$.

If the distance d between full-sized horoballs satisfies $d > \sqrt{3}$, then the hyperbolic Coxeter group $\bullet \overset{6}{\text{---}} \bullet \text{---} \bullet \overset{\alpha_k}{\text{---}} \bullet$ with $2 \cos \alpha_k = d$ of Proposition 10 has infinite covolume since the orthoscheme $R(\alpha_k, \frac{\pi}{3})$ has an ultraideal vertex given by the graph $\bullet \text{---} \bullet \overset{\alpha_k}{\text{---}} \bullet$ (see Section 2.3). In order to construct an orbifold with finite volume from it, its fundamental group Γ has to contain additional isometries.

Proposition 11. *In the case of Proposition 10 with $\sqrt{3} < d \leq 2$, the minimal possible orbifold volume is obtained from the truncated Coxeter orthoscheme $R_t(\alpha_k, \frac{\pi}{3})$ with Coxeter graph*

$$\bullet \overset{6}{\text{---}} \bullet \text{---} \bullet \overset{\alpha_k}{\text{---}} \bullet \dots \bullet \quad \text{where} \quad d = 2 \cos \alpha_k .$$

Proof. If the horoball diagram appears as in Figure III.7 with $d > \sqrt{3}$, then the orthoscheme $\bullet \xrightarrow{6} \bullet \xrightarrow{\alpha_k} \bullet$ has an ultraideal vertex v_0 . Hence, there has to be an additional horoball B_+ close to the centre of D in order to obtain finite volume. In view of the realisations of the horoball B_+ , Proposition 10 guarantees the existence of reflections mapping B_∞ to the full-sized balls B_j , B_k , and B_l . Denote the associated reflection planes by P_j , P_k , and P_l , respectively. The horoball B_+ cannot intersect any of those planes because otherwise it would intersect its image under the corresponding reflection. The biggest possible horoball B_+ (yielding the minimal volume orbifold) hence *touches* all three planes P_j , P_k , and P_l . Those three planes are orthogonal to the polar plane P_0 of v_0 . Therefore, P_j , P_k , and P_l are left invariant under the reflection r_0 in the plane P_0 . The horoballs B_∞ and B_+ are the only ones touching all three planes at once, implying that one is the image of the other under r_0 . Thus, the polar plane P_0 is the bisector of B_∞ and B_+ .

In our constructions, a fundamental polyhedron of Γ can be found by considering the Dirichlet-Voronoi cell of B_∞ modulo Γ_∞ . The previous arguments show that a fundamental polyhedron of Γ has to include at least the truncated orthoscheme $R_t(\alpha_k, \frac{\pi}{3})$ as asserted.

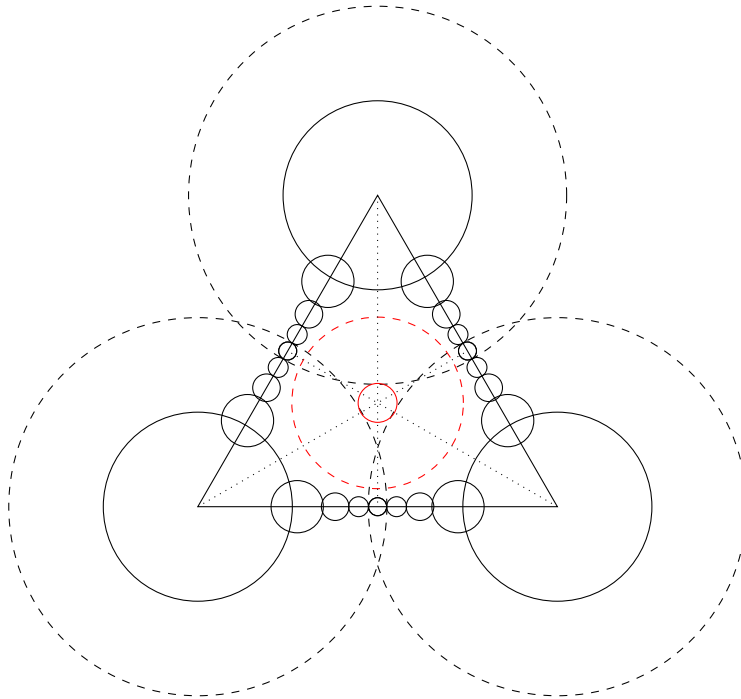


Figure III.10.: $(\frac{1}{d})$ -balls in line

□

By Proposition 11, the minimal possible orbifold volume in the case $\sqrt{3} < d = 2 \cos \alpha_k \leq 2$ is given by the volume of the truncated Coxeter orthoscheme $R_t(\alpha_k, \frac{\pi}{3})$. In Section 2.3, an explicit formula for $\text{vol}(R_t(\alpha_k, \frac{\pi}{3}))$ is given by (2.9). Furthermore, by Remark 2, $\text{vol}(R_t(\alpha_k, \frac{\pi}{3}))$ is strictly increasing when α_k decreases, that is, when d increases. In particular, for $\sqrt{3} < d \leq 2$, we get

the lower volume bound

$$\text{vol}(R_t(\alpha_k, \frac{\pi}{3})) \geq \text{vol}(R_t(\frac{\pi}{7}, \frac{\pi}{3})) > 0.317811 > v_* .$$

In view of Proposition 11, it remains to identify groups Γ with full-sized horoballs satisfying $2 < d \leq 2.013813$ (see Remark 8). It turns out that Γ has the same basic structure as before, and truncation of its fundamental orthoscheme with the polar plane P_0 gives a polyhedron R_t of smallest volume because of the following proposition.

Proposition 12. *For any horoball on an angle bisector as depicted in Figure III.12, its bisector with B_∞ intersects the polar plane P_0 exactly below the boundary of the triangle D at height 1 in the upper half space U^3 . Any other cutting plane leads to a bigger volume than the volume of R_t .*

Proof. The proof is basic trigonometry. If the centre of a horoball B on an angle bisector of D has distance a from the boundary of D and touches the bisector of the two closest full-sized horoballs, then its radius r satisfies

$$(1+r)^2 = l^2 + r^2 = \frac{d^2}{4} + a^2 + r^2, \quad (3.15)$$

where l is the distance between the centres of B and of the next full-sized horoball. Figure III.11 depicts a vertical cut in U^3 through the centres of the two horoballs. The identity (3.15) implies

$$2r = \frac{d^2}{4} + a^2 - 1.$$

Using that the radius of the bisector is $\sqrt{2r}$, the height h of the bisector is then independent of the distance a :

$$h^2 = (\sqrt{2r})^2 - a^2 = \frac{d^2}{4} - 1.$$

□

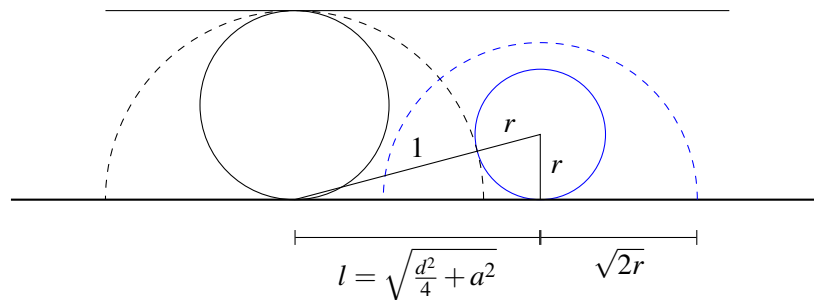


Figure III.11.: Vertical cut along l through the centres of the two horoballs in U^3

By means of Proposition 12 and as a final step in the analysis of horoball diagrams D with $(\frac{1}{d_k})$ -balls aligned on the edges of D according to Figure III.7, we can state the following result.

Proposition 13. Under the assumptions of Proposition 10 with $d > 2$, the minimal possible volume is obtained by an orbifold related to a truncated orthoscheme $R_t(\beta, \frac{\pi}{6})$ with Vinberg graph

$$\bullet \xrightarrow{\beta} \bullet \xrightarrow{6} \bullet \cdots \bullet \quad \text{where } 0 < \beta < \frac{\pi}{15} .$$

Proof. We have to verify the bound $\beta < \frac{\pi}{15}$, only. In fact, we are assuming the upper bound $d \leq 2.013813$ according to Remark 8. By a similar trigonometrical computation in the upper half space U^3 as in the proof of Proposition 12 above, one can relate β and d according to

$$\cos \beta = \frac{d}{2\sqrt{d^2 - 3}} .$$

In this way, we get the estimate $\beta < \frac{\pi}{15}$. □

By Proposition 13, the minimal possible orbifold volume in the case $d > 2$ is given by the volume of the truncated Coxeter orthoscheme $R_t(\beta, \frac{\pi}{6})$. By (2.10) of Section 2.3, we have an explicit formula for $\text{vol}(R_t(\beta, \frac{\pi}{6}))$ which, by its strict monotonicity behavior with respect to $\beta < \frac{\pi}{15}$, yields the lower volume bound

$$\text{vol}(R_t(\beta, \frac{\pi}{6})) \geq \text{vol}(R_t(\frac{\pi}{15}, \frac{\pi}{6})) > 0.416491 > v_* .$$

These investigations complete the analysis of the case that the centres of the $(\frac{1}{d})$ -balls lie on the edges of D .

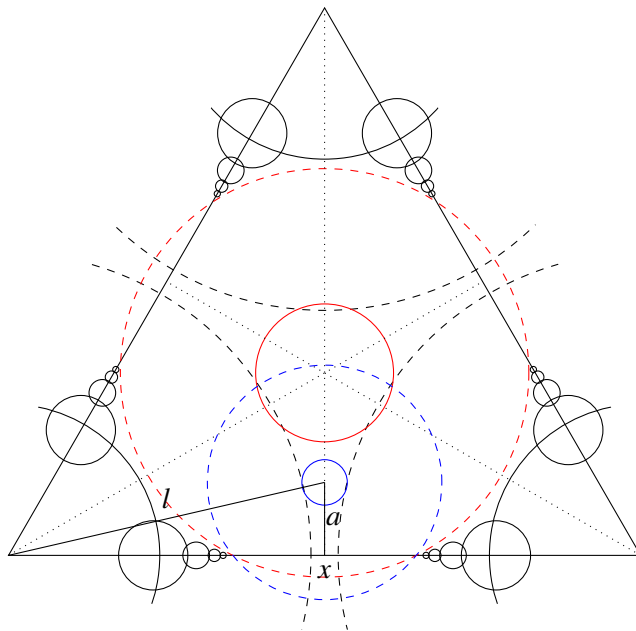


Figure III.12.: $(\frac{1}{d})$ -balls on the edges of D with $d > 2$

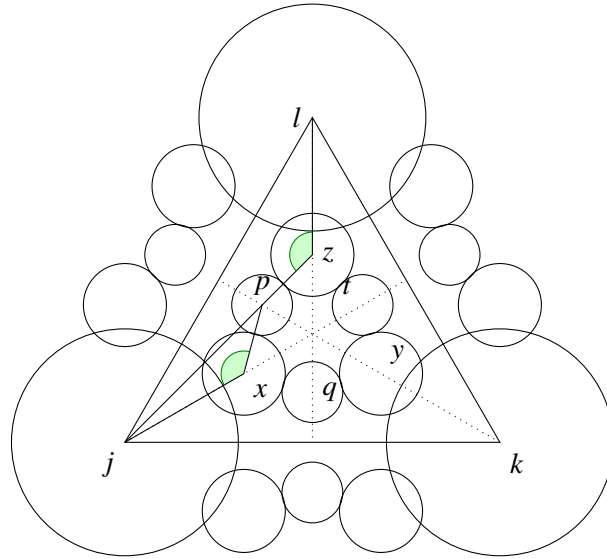


Figure III.13.: Horoball diagram D with $d = \sqrt{1 + \sqrt{3}}$

In order to finish the part of full-sized horoballs centred at singular points of order 6 and of distance $d > 1$, we need to study the case when the centres of the $(\frac{1}{d})$ -balls lie on the angle bisectors of D . We are still assuming that Γ_∞ is a reflection group.

The $(\frac{1}{d})$ -balls cannot touch each other because then three balls would touch pairwise which is impossible because the full-sized balls do not touch. This implies the existence of $(\frac{1}{w})$ -balls. For a fixed distance d , the position of the $(\frac{1}{w})$ -balls is given by the similarity of the two triangles (j, z, l) and (j, x, p) . See Figure III.13 for the labels. This similarity and the reflection symmetry of the horoball diagram D also prove that the centre of the full-sized horoball B_j is on a common line with those of the $(\frac{1}{d})$ -ball B_z and the $(\frac{1}{w})$ -ball B_p .

Note that Figure III.13 depicts the case where the $(\frac{1}{w})$ -balls touch two $(\frac{1}{d})$ -balls but the above statement about the alignment of their centres stays true if the $(\frac{1}{w})$ -balls do not touch two $(\frac{1}{d})$ -balls. This in turn means that each $(\frac{1}{d})$ -ball touches two $(\frac{1}{w})$ -balls because of the present symmetries. Hence, there are twelve $(\frac{1}{w})$ -balls around a full-sized horoball.

Knowing that the centres j , p , and z are on the same line, we can calculate d by using

$$w = \frac{1}{w} + \frac{1}{wd^2}$$

and the identity $w^2 = d^2 + \frac{1}{d^2} - 2 \cos \frac{\pi}{6}$ according to (3.7). This implies $d^2 = 1 + \sqrt{3}$.

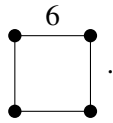
The following considerations allow us to describe the orbifold associated to this horoball diagram. They are also valid if d is bigger, that is, if each of the $(\frac{1}{w})$ -balls touches only one $(\frac{1}{d})$ -ball. Since we assume that Γ_∞ is a reflection group, there is a reflection $s \in \Gamma_\infty$ which exchanges B_j and B_k . By Lemma 5, there is an order 2 elliptic element r in Γ which swaps

$$B_j \leftrightarrow B_\infty \quad , \quad B_k \leftrightarrow B_x .$$

Hence, rsr is the reflection in the bisector of B_∞ and B_x and an element of the group Γ . This proves the following result.

Proposition 14. *In the case of a $\{2, 3, 6\}$ -cusp where Γ_∞ is a reflection group and where the $(\frac{1}{d})$ -balls are centred on the angle bisectors of the horoball diagram D , there are reflections in Γ mapping B_∞ to any $(\frac{1}{d})$ -ball.*

In the situation of Figure III.13, the distance u between two neighbouring $(\frac{1}{d})$ -balls can be calculated as $\frac{1}{d}$. Using this information, one can consider the polyhedron created from the triangular cone with apex ∞ and angles $\frac{\pi}{2}, \frac{\pi}{3}, \frac{\pi}{6}$ by cutting with the bisector/reflection plane of rsr . The bisector is orthogonal to one side of the cone and has angle $\frac{\pi}{3}$ with the other two because its centre has (Euclidean) distance $\frac{1}{2d}$ from the hyperplanes and the radius of the bisector is $\frac{1}{d}$. Thus, it can be seen that this polyhedron is the fundamental polyhedron of the (non-arithmetic) reflection group $[(3^3, 6)]$ with Coxeter graph



One can see that r induces the internal symmetry of that polyhedron (and its graph). Hence, Γ is equal to the group extension $\Gamma_\circ^r = [(3^3, 6)] * C_r$ of $[(3^3, 6)]$ by means of the cyclic group generated by r ; see Remark 1. The volume of the tetrahedron $[(3^3, 6)]$ as given by (2.8) is bigger than 0.36 so that $\text{vol}(\mathbb{H}^3/\Gamma_\circ^r) > v_*$.

If we do not assume that the $(\frac{1}{w})$ -balls touch two $(\frac{1}{d})$ -balls, we have basically the same case distinction as when the $(\frac{1}{d_k})$ -balls are centred on the edges D .

- (i) There is a single $(\frac{1}{d_{k_{\max}}})$ -ball, or
- (ii) there are two touching $(\frac{1}{d_{k_{\max}}})$ -balls,

where $k_{\max} := \max \left\{ k \mid \text{the horoball diagram } D \text{ contains a } (\frac{1}{d_k})\text{-ball} \right\}$. See Figure III.14 for a sketch of the first couple of horoball diagrams in that sequence.

In the part above, we discussed the first case with $k_{\max} = 2$, $d_2 = w$ and a horoball diagram D depicted in Figure III.13. There, the isometry r maps the full-sized horoball B_k to the $(\frac{1}{d_1})$ -ball B_x and the $(\frac{1}{d_1})$ -ball B_y to the $(\frac{1}{d_2})$ -ball B_q .

In general, there is a similar pattern as follows. A $(\frac{1}{d_k})$ -ball close to the full-sized ball B_k gets mapped to a $(\frac{1}{d_{k+1}})$ -ball closer to the full-sized ball B_j .

- (a) If there is a unique $(\frac{1}{d_{k_{\max}}})$ -ball in the corresponding part of the horoball diagram D , then a $(\frac{1}{d_{k_{\max}-1}})$ -ball on the right gets mapped to this $(\frac{1}{d_{k_{\max}}})$ -ball.
- (b) If there are two $(\frac{1}{d_{k_{\max}}})$ -ball in this part of the D , then a $(\frac{1}{d_{k_{\max}-1}})$ -ball on the right gets mapped to the left $(\frac{1}{d_{k_{\max}}})$ -ball. This implies that in the second case the right-hand $(\frac{1}{d_{k_{\max}}})$ -ball is *fixed*.

In both cases, the reflection rsr then maps a $(\frac{1}{d_k})$ -ball on the right to a $(\frac{1}{d_{k+2}})$ -ball on the left as long is $k \leq k_{\max} - 2$. In the case (a), a $(\frac{1}{d_{k_{\max}-1}})$ -ball on the right is fixed by rsr because it is

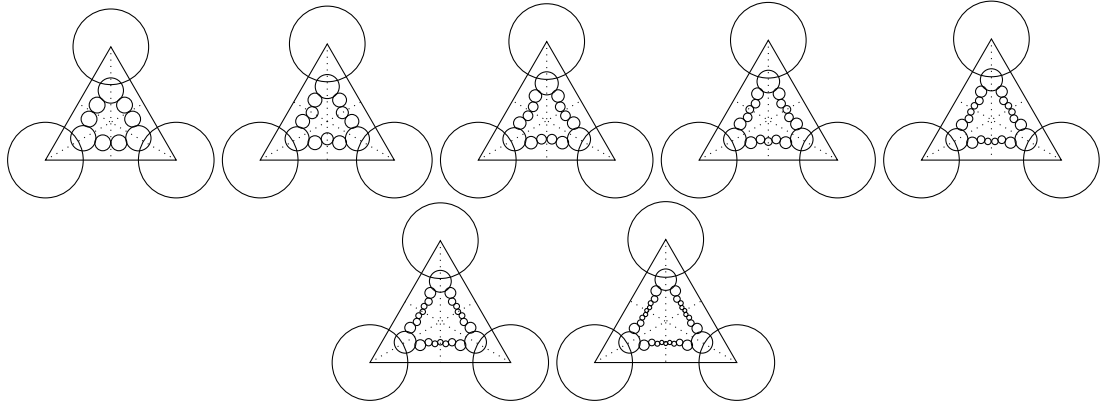


Figure III.14.: Horoball diagrams with angle $\theta = \frac{\pi}{6}$

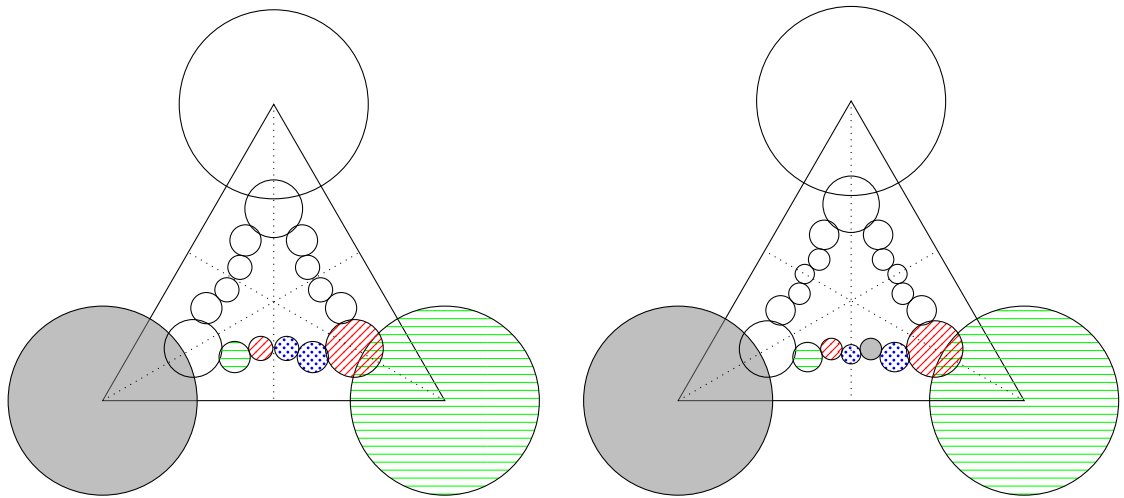


Figure III.15.: Action of rsr on some horoballs according to the cases (a) and (b)

the only ball left. In the case (b), the $(\frac{1}{d_{k_{\max}-1}})$ -ball on the right has to be mapped to the right $(\frac{1}{d_{k_{\max}}})$ -ball. Refer to Figure III.15 for a sketch of illustrative examples for the cases (a) and (b). Each pair of horoballs with matching colour and pattern is exchanged by rsr . Those horoballs with a solid fill are fixed.

Lemma 7. *The case (b) is impossible.*

Proof. The previously discussed fact that rsr maps $(\frac{1}{d_k})$ -balls to $(\frac{1}{d_{k+2}})$ -balls proves that the $(\frac{1}{d_{2k+1}})$ -balls are on one line with the $(\frac{1}{d_1})$ -balls. We already showed that a neighboring pair of a $(\frac{1}{d_1})$ -ball and a $(\frac{1}{d_2})$ -ball are on a line with a full-sized horoball. This implies that the $(\frac{1}{d_{2k}})$ -balls are not on the same line as the $(\frac{1}{d_{2k+1}})$ -balls. However, this means that the right-hand $(\frac{1}{d_{k_{\max}}})$ -ball is not on the same line as the right-hand $(\frac{1}{d_{k_{\max}-1}})$ -ball. Thus it cannot be true that they get mapped to one another by rsr , proving the statement. \square

Hence, it remains to discuss the general case (a) with a single $(\frac{1}{d_{k_{\max}}})$ -ball. It turns out to be helpful to consider the subgroup Γ' of Γ generated by Γ_∞ and rsr . In fact, this move allows us to drop the rotation r and to purge the full-sized horoballs as well as the $(\frac{1}{d_{2k}})$ -balls from the horoball diagram D . Then, the $(\frac{1}{d_{2k+1}})$ -balls can be increased to yield a cusp which is a maximal cusp again. More precisely, the $(\frac{1}{d})$ -balls become full-sized horoballs (of diameter $\frac{1}{d}$), and then, the horoball diagram D is renormalised in order to have the horosphere $H_\infty = \partial B_\infty$ at distance 1 from ∂U^3 . Figure III.16 depicts the cases with small k_{\max} .

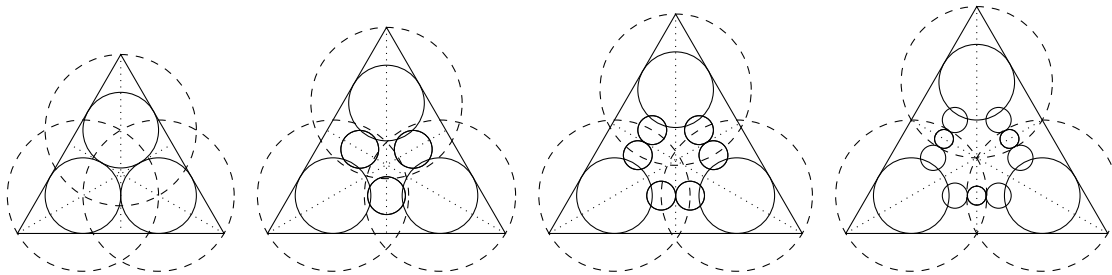
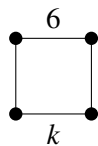


Figure III.16.: Horoball diagrams of the reflection subgroups generated by Γ_∞ and rsr

As a consequence, the group Γ' is a hyperbolic Coxeter group, and by the same methods as above, one can identify Γ' by means of the Coxeter graph describing a Coxeter polyhedron $P = P(\frac{\pi}{k})$, with an order 2 internal symmetry plane, according to



where k is an integer with $k \geq 3$. For $3 \leq k \leq 6$, the volume of $P(\frac{\pi}{k})$ satisfies $\text{vol}(P(\frac{\pi}{k})) \geq \text{vol}([3^3, 6]) > 2v_*$ by (2.8).

In the case $k = 6$, the fundamental polyhedron P of Γ' has four cusps, and for $k > 7$, there are two ultraideal vertices. We do not have to consider those cases because we can easily estimate the orbifold volume using the cusp volume. If $k = 6$, the distance between two full-sized horoballs is $d = \sqrt{3}$ as calculated above in Equation (3.13). For this case and for $d \geq \sqrt{3}$, the side length of D is $e = d + \sqrt{3} \geq 2\sqrt{3}$ (compare Figure III.17). The cusp volume can then be bounded by

$$\text{vol}(C) = \frac{e^2 \sqrt{3}}{48} \geq \frac{\sqrt{3}}{4} > 0.43 > 2v_*. \quad (3.16)$$

Order 3. Suppose that a full-sized disk $B = B_1$ is centred at the singular point $b = a_3$ in the barycenter of the triangle D . Consider a full-sized horoball B_2 whose center is at distance d from b . It follows that the inradius of the cusp triangle D equals $\frac{d}{2}$ and that the edge length of D equals $\sqrt{3}d$. In particular, the cusp volume $\text{vol}(C)$ is given by $\frac{\sqrt{3}d^2}{16}$. In the case that Γ_∞ is orientation-preserving, the assumption $d > 1$ yields the cusp volume estimate

$$\frac{\sqrt{3}d^2}{8} > 0.21 > v_* .$$

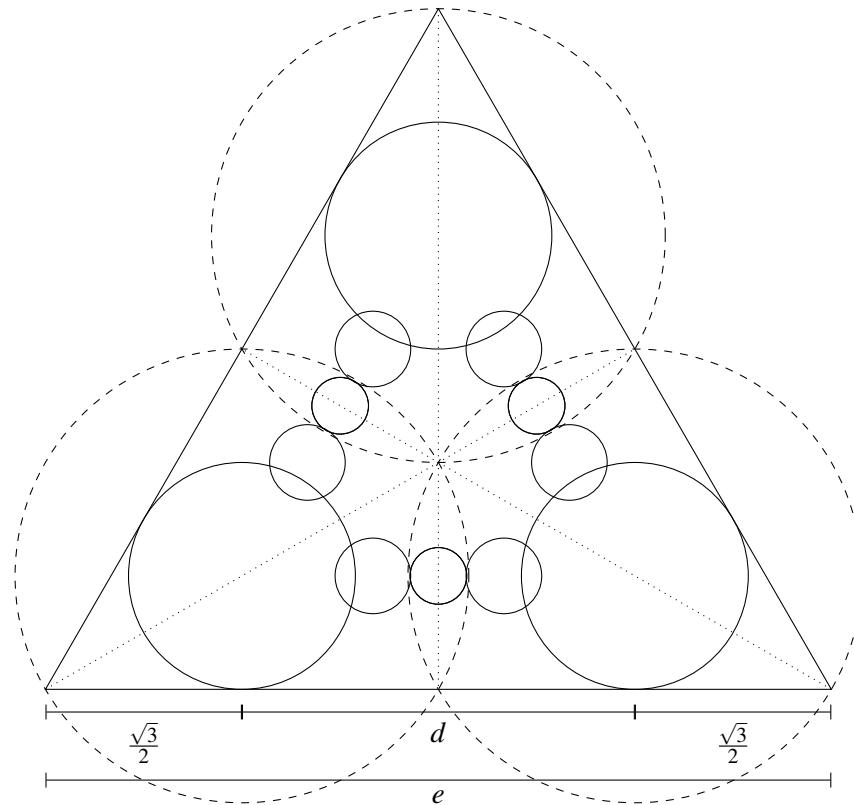


Figure III.17.: Horoball diagram of the reflection subgroup Γ' with $k = 6$

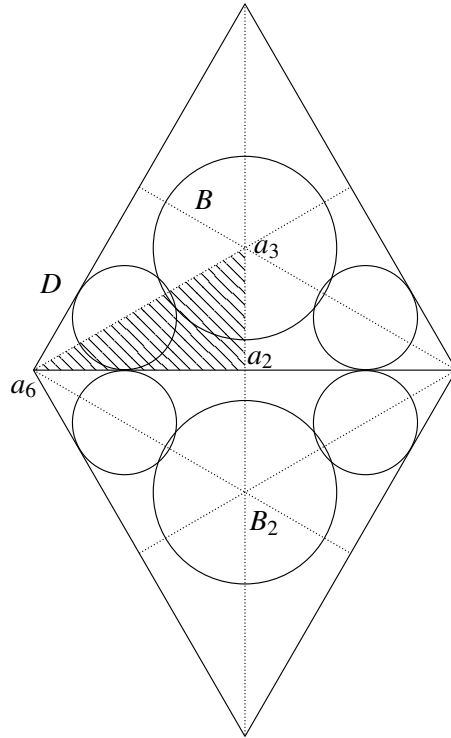


Figure III.18.: A $\{2, 3, 6\}$ -cusp triangle D with a full-sized horoball B centred in a_3

Hence, we assume that the cusp triangle D has a mirror symmetry. Since $d > 1$, there are three $(\frac{1}{d})$ -balls, each of diameter $\frac{1}{d^2}$, touching B in D in a symmetrically arranged way. Denote by x the centre of one of these $(\frac{1}{d})$ -balls. The distance $d_0(b, x)$ equals $\frac{1}{d}$.

- If x lies on the edge e_{23} defined by $b = a_3$ and the midpoint a_2 of an edge of D , then the bound

$$\frac{d}{2} = d_0(b, a_2) \geq d_0(b, x) = \frac{1}{d}$$

yields $d \geq \sqrt{2}$ and, hence, $\text{vol}(C) \geq \frac{\sqrt{3}}{8} \simeq 0.216506$, which is too big in comparison with $v_* = \text{vol}(\mathbb{H}^3/[5, 3, 6]) \approx 0.171502$ (see (3.1)).

- If $x \notin e_{23}$, then x lies on the edge segment e_{36} of Δ defined by $b = a_3$ and a vertex a_6 of D . Since $d > 1$, the center x is different from a_6 . Furthermore, it is easy to see that d and hence $\text{vol}(C)$ take minimal values if the $(\frac{1}{d})$ -ball B_x is internally tangent to the border of D (see Figure III.18). In this situation, and since the radius of B_x equals $\frac{1}{2d^2}$, we deduce the inequality

$$d \geq \frac{1}{d^2} + \frac{1}{d},$$

whose solution $d \geq 1.324718$ yields the cusp volume bound

$$\text{vol}(C) \geq 0.189971 > v_*.$$

Order 2. Suppose that a full-sized horoball $B = B_1$ is centred at the singular point $b_1 = a_2$ in D , and let B_2, B_3 be full-sized horoballs centred at b_2, b_3 in D , both at distance d from b_1 . Then, the edge length of the cusp triangle D equals $2d$ while the distance from b_1 to the centre of D is given by $r = \frac{d}{\sqrt{3}}$ (representing the inradius of D). In particular, we have $\text{vol}(C) = \frac{\sqrt{3}d^2}{12}$, and there are disks of no tangency centred at the vertices of D . Hence, we cannot assume that $w \geq 1$.

However, the case that Γ_∞ is orientation-preserving can be excluded since the corresponding cusp volume for $d > 1$ immediately yields the estimate

$$\text{vol}(C) = \frac{\sqrt{3}d^2}{6} > \frac{\sqrt{3}}{6} > v_* .$$

Assume that D has a mirror symmetry. We analyse the different tangency possibilities of the $(\frac{1}{d})$ -balls with respect to one or several full-sized horoballs and among themselves. To this end, the following fact is very useful.

Fact. The centres of the four $(\frac{1}{d})$ -balls touching one full-sized horoball form a rectangle whose diagonals intersect at the angle $\frac{\pi}{3}$.

- If a single $(\frac{1}{d})$ -ball touches three full-sized horoballs in D , then it is centred at a_3 . It follows that $r = \frac{1}{d}$, and hence, $d = \sqrt[4]{3}$ so that $\text{vol}(C) = \frac{1}{4} > v_*$.

- If a single $(\frac{1}{d})$ -ball touches a pair of neighboring full-sized horoballs but does not touch a third full-sized one, then the smallest cusp volume arises if the centres of the $(\frac{1}{d})$ -ball and of the full-sized horoballs which it touches are aligned. This follows easily from the above *fact*. We deduce that $d = \sqrt{2}$ and that $\text{vol}(C) = \frac{\sqrt{3}}{6} > v_*$.

- Suppose that each $(\frac{1}{d})$ -ball touches a unique full-sized horoball. As in the case when a full-sized horoball B is centred at a singular point a_6 of order 6 in D with distance w from a_6 to the centre x of a $(\frac{1}{d})$ -ball not touching it (see Figure III.5), we obtain the identical equation (3.7) for w when the full-sized horoball B is centered at a singular point a_2 in D with the condition $0 \leq \theta \leq \frac{\pi}{3}$ (see Figure III.19).

There are again several cases to consider. The case that three $(\frac{1}{d})$ -balls are mutually tangent in D can be excluded by Lemma 4. If two $(\frac{1}{d})$ -balls are tangent and do not touch the third one in D , then the smallest volume arises if their centres and the centres of the associated full-sized horoballs form an isosceles trapezoid; see Figure III.19. In this case, by Ptolemy's theorem, the square of the diagonal of the trapezoid equals

$$w^2 = \frac{1}{d} + \frac{1}{d^2} .$$

By means of equation (3.7) with $0 \leq \theta \leq \frac{\pi}{3}$, we deduce that $d^3 - d - 1 \geq 0$ and $d \geq 1.32471$. Hence, $\text{vol}(C) > \frac{1}{4} > v_*$.

Suppose that the $(\frac{1}{d})$ -balls do not touch each other. In particular, the minimum distance μ of their centres is bigger than $\frac{1}{d^2}$. Since D has mirror symmetry, we get a (possibly degenerate) isosceles trapezoid formed by the centres of two closest $(\frac{1}{d})$ -balls in D and the centres of the two full-sized horoballs which they touch. By Ptolemy's theorem, we deduce that

$$w^2 = \mu d + \frac{1}{d^2} > \frac{1}{d} + \frac{1}{d^2} , \tag{3.17}$$

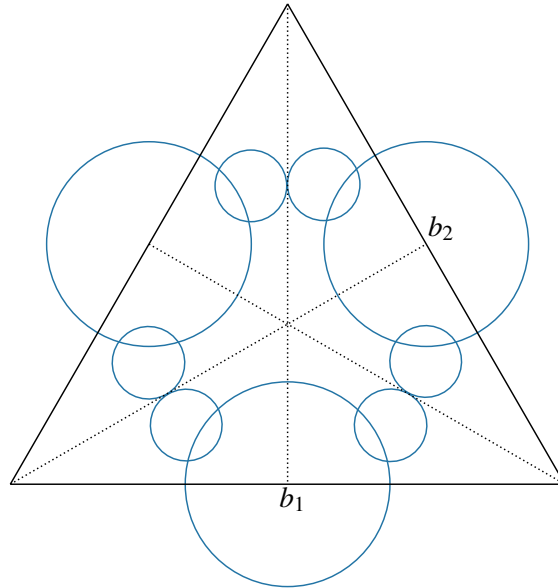


Figure III.19.: Full-sized horoballs centred at singular points of order 2

and hence $\text{vol}(C) > \frac{1}{4} > v_*$ in a similar way as above.

As a summary of all the investigations in Section 3.4, we obtain the following result.

Proposition 15. *Let V be a non-arithmetic hyperbolic 3-orbifold with a single cusp $C = B_\infty/\Gamma_\infty$ which is rigid of type $\{2, 3, 6\}$. Suppose that Γ_∞ gives rise to only one equivalence class of full-sized horoballs. Then,*

$$\text{vol}(V) \geq \text{vol}(V_*),$$

and equality holds if and only if the orbifold V is isometric to $V_* = \mathbf{H}^3/[5, 3, 6]$.

The case $\{2, 4, 4\}$

(i) As in Section 3.4, (i), we start by assuming that there are at least two full-sized horoballs, which are centred at equivalent singular points and which touch one another in the (square) cusp diagram D . That is, the minimal distance d of the centres of full-sized horoballs equals 1 (see also [Ada92a, Section 5, p. 11]).

Order 4. Suppose that there is a full-sized horoball centred at one of the two singular points a_4 of order 4 in Δ . Then, $d_0(a_2, a_4) = \frac{1}{2}$, and the associated cusp volume $\text{vol}(C)$ equals $\frac{1}{16}$. Similarly to the case of Section 3.4, one can check that there is a unique orbifold V related to this cusp configuration. In fact, it is the quotient of \mathbf{H}^3 by the *arithmetic* Coxeter group $[3, 4, 4]$ (see also [Ada92a, p. 13]). The quotient space $V = \mathbb{H}^3/[3, 4, 4]$ has volume $\frac{\omega_3}{48} = \frac{1}{6} \mathbb{J}(\frac{\pi}{4}) \approx 0.0763304$ (see Section 2.3). By [Ada92a, Theorem 5.2 and Theorem 6.1], we know that the space $\mathbb{H}^3/[3, 4, 4]$ has minimal volume among *all* hyperbolic 3-orbifolds with at least one cusp of type $\{2, 4, 4\}$.

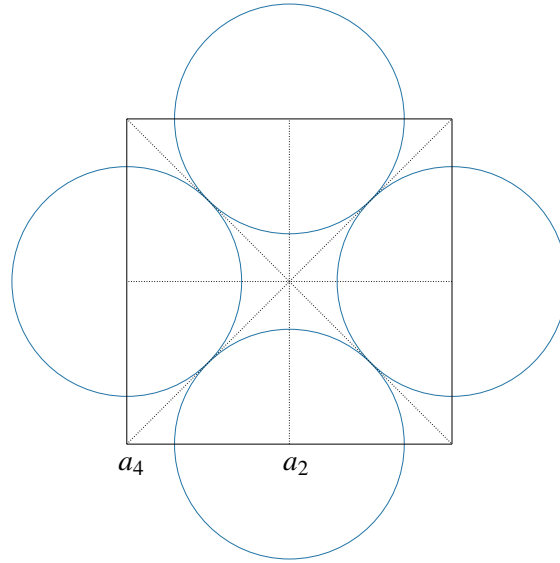


Figure III.20.: A full-sized horoball centred at a_2

Order 2. If there is a full-sized horoball centred at $a_2 \in \Delta$, then we get $d_0(a_2, a_4) = \frac{1}{\sqrt{2}}$, and the cusp volume equals $\frac{1}{8}$ (see [Ada92a, Figure 6(b), p. 12] and Figure III.20). Again, there is a unique orbifold corresponding to this configuration. Its fundamental group is given by the Coxeter group $[4^{1,1}, 3]$ and therefore commensurable to the arithmetic Coxeter group $[3, 4, 4]$ (see [Joh+02, p. 130]).

(ii) Suppose now that the full-sized horoballs do *not* touch one another implying that the minimal distance d between the centres a_s (for $s = 2$ or $s = 4$) of full-sized horoballs satisfies $d > 1$.

Notice that if the stabiliser Γ_∞ is orientation-preserving, then the cusp volume equals

$$\text{vol}(C) = \frac{d^2}{2s} > \frac{1}{2s}. \quad (3.18)$$

In particular, for $s = 2$, we deduce that the cusp volume yields $\text{vol}(C) > \frac{1}{4} > v_*$. Moreover, the case $s = 4$ can also be excluded as follows. If there is a disk of no tangency, then $d \geq \sqrt{2}$ and $\text{vol}(C) > v_*$. If there is *no* disk of no tangency, then by Lemma 6 we have that the distance w of the centre of a $(\frac{1}{d})$ -ball touching B to the centre of a neighboring full-sized horoball satisfies $w \geq 1$. The equation (3.7) for w remains valid under the adapted constraint $0 \leq \theta \leq \frac{\pi}{4}$ in the square diagram D . The inequality $w \geq 1$ now implies that

$$d^4 - (1 + \sqrt{2})d^2 + 1 \geq 0,$$

and hence $\text{vol}(C) = \frac{d^2}{8} > \frac{1.88}{8} > 0.2 > v_*$.

Consequence. We can assume that the cusp diagram D has a mirror symmetry.

As in the case 3.4, (ii), we study the $(\frac{1}{d})$ -balls and their tangency behavior with respect to the full-sized horoballs centred at a singular point a_s . Observe that for each full-sized horoball B ,

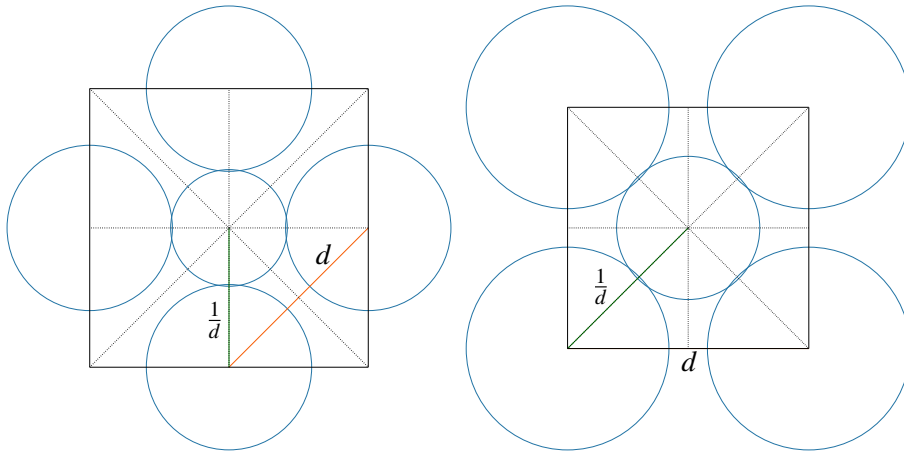


Figure III.21.: $(\frac{1}{d})$ -balls touching four full-sized balls

there are four $(\frac{1}{d})$ -balls touching B . The angles formed by their centres measured from the center B is a multiple of $\frac{\pi}{4}$. This leads to the following first cases; see Figure III.21.

(a) Suppose that one $(\frac{1}{d})$ -ball B_x is touching four full-sized horoballs so that the center x coincides with a singular point of order $s = 4$. By symmetry, we can suppose that x is the center of the cusp diagram D .

- Assume first that the centres of the full-sized horoballs lie at the singular points of order 2 in D , that is, D has circumradius d . Since the distance between the center x and the centre of each of the full-sized horoballs equals $\frac{1}{d}$, we deduce that $d = \sqrt[4]{2}$. Hence, for the cusp volume, we get $\text{vol}(C) = \frac{d^2}{8} = \frac{\sqrt{2}}{8} \approx 0.176777$ and therefore $\text{vol}(C) > v_*$ (see (3.18)).

- Assume next that the centres of the full-sized horoballs lie at the vertices (of order 4) of D . Hence, D has circumradius $\frac{1}{d}$. We deduce that $d = \sqrt[4]{2}$ as well. However, for the cusp volume, we obtain $\text{vol}(C) = \frac{\sqrt{2}}{16}$. As shown by [Ada92a, p. 13] in the oriented case, there is a unique orbifold corresponding to this configuration. It is the arithmetic quotient of an ideal Coxeter tetrahedron with dihedral angles $\frac{\pi}{4}$, $\frac{\pi}{4}$ and $\frac{\pi}{2}$ by its orientation-preserving symmetry group. Hence, in the non-oriented case, a hyperbolic orbifold with cusp volume $\frac{\sqrt{2}}{16}$ would have a fundamental group commensurable to the arithmetic Coxeter group $[4^{[4]}]$ and therefore can be excluded from our consideration.

(b) Suppose that one $(\frac{1}{d})$ -ball B_x is touching exactly two full-sized horoballs.

- If these full-sized ones are centred at singular points of order 2 in D , then the circumradius of D equals d . Since the center x is aligned with the centres of the full-sized horoballs which B_x touches, we deduce that $d = \sqrt{2}$ and $\text{vol}(C) = \frac{d^2}{8} = \frac{1}{4} > v_*$.

- If the two full-sized horoballs are centred at vertices (of order 4) of D , then again $d = \sqrt{2}$. It follows that $\text{vol}(C) = \frac{1}{8}$. Observe that there is a disk of no tangency based at the centre of D and touching the full-sized horoballs. Given this, the only possible such configuration, and which leads to a singly cusped orbifold, arises by halving the Coxeter orthoscheme $[4, 4, 4]$ with vertices q, p_1, p_2, p_3 by means of the plane P passing through the edge p_2p_3 and orthogonal to the (doubly infinite) edge qp_4 (see Figure III.1). However, a simple computation shows that the

horoball sector $B_\infty \cap [4, 4, 4]$ associated to q , has non-empty intersection with P in contradiction to the maximality of the cusp. Hence, this configuration can not be realised.

(c) Suppose that a $(\frac{1}{d})$ -ball is touching only one full-sized horoball B .

Observe that, and similarly to the distance w , the distance v of the centre of B to the centre of its neighboring $(\frac{1}{d})$ -balls as given by (3.6) remains valid under the constraint $0 \leq \theta \leq \frac{\pi}{4}$ (the distance u between the centres of two $(\frac{1}{d})$ -balls needs a slight modification, though).

- Assume that B is centred at a singular point of order 2 in D . As in the case of the cusp of type $\{2, 3, 6\}$, and by symmetry, we get a (possibly degenerate) isosceles trapezoid formed by the centres of two neighboring $(\frac{1}{d})$ -balls at distance $\mu \geq \frac{1}{d^2}$ and by the centres of the full-sized horoballs which they touch. We obtain the identity (3.17) which, combined with the equation (3.7) for w^2 and the condition $0 \leq \theta \leq \frac{\pi}{4}$, yields $d^3 - \sqrt{2}d - 1 \geq 0$ and the estimate $d \geq 1.450405 > \sqrt{2}$. As a consequence, the volume of the cusp C satisfies $\text{vol}(C) = \frac{d^2}{8} > \frac{1}{4} > v_*$.

- More delicate is the case when B is centred at a singular point of order 4. By symmetry, we can suppose that the centre of B coincides with a vertex of D . For the cusp volume, we obtain $\text{vol}(C) = \frac{d^2}{16}$.

As in [Ada92b, Section 5], we consider the mutual positions of the $(\frac{1}{d})$ -balls associated to the full-sized horoballs. The case that four $(\frac{1}{d})$ -balls are closest to one another, that is, each one is tangent to two other ones and they all are symmetrically arranged around the centre of D , can be excluded by applying verbatim Adams' corresponding argument.

Suppose next that two $(\frac{1}{d})$ -balls are tangent, and no other $(\frac{1}{d})$ -ball is tangent to them. Since D has a mirror symmetry, this can only happen if they are tangent at a singular point a_2 of order 2 with centres being aligned with the centres of the corresponding full-sized horoballs. We deduce that $d = \frac{2}{d} + \frac{1}{d^2}$ and hence $d = 2 \cos \frac{\pi}{5}$. It follows that

$$\frac{\text{vol}(C)}{d_3(\infty)} > 0.19 > v_* .$$

It remains to investigate the case when the $(\frac{1}{d})$ -balls do not touch. As in the analogous case of a cusp of type $\{2, 3, 6\}$, we consider the $(\frac{1}{w})$ -balls with their position relative to the $(\frac{1}{d})$ -balls. Assume first that four $(\frac{1}{w})$ -balls coincide and, hence, have center equal to the centre of the square D . Then, the circumradius of D equals $\frac{1}{w}$ so that $w = \frac{\sqrt{2}}{d}$. By means of (3.7), one can compute that $d = \sqrt[4]{5}$ and $\cos \theta = \frac{2}{\sqrt{5}}$; see Figure III.31. Hence, the cusp diagram D has no mirror symmetry, and the corresponding cusp volume yields $\text{vol}(C) = \frac{\sqrt{5}}{8} > \frac{1}{4} > v_*$. By performing analogous computations as in the case of a type $\{2, 3, 6\}$ -cusp, we can show furthermore that there is a unique corresponding oriented orbifold that is arithmetic. For more details, see Appendix III.B.

The case that two of the $(\frac{1}{w})$ -balls coincide in the interior of D can be excluded by symmetry.

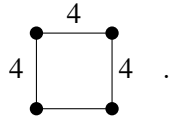
Hence, it remains to investigate the situation when all $(\frac{1}{w})$ -balls are distinct. In order to finish this case, it is sufficient to check the following two extremal possibilities for a $(\frac{1}{w})$ -ball touching two $(\frac{1}{d})$ -balls associated to two different full-sized balls.

- Suppose first that a $(\frac{1}{w})$ -ball touches two $(\frac{1}{d})$ -balls in such a way that their centres are aligned on an edge of D . Then, $\frac{1}{w} = \frac{d}{2}$ which by means of (3.8) and $\theta = 0$ implies that $d^4 - 2d^2 - 3 = 0$ with solution $d = \sqrt{3}$. Hence, $\text{vol}(C) = \frac{3}{16} > v_*$.

- Suppose next that a $(\frac{1}{w})$ -ball touches two $(\frac{1}{d})$ -balls whose centres lie on the diagonals of D . Notice that there are eight $(\frac{1}{w})$ -balls around each full-sized horoball. Then, one can show

in a similar way as in the case of a cusp of type $\{2, 3, 6\}$ that $d = \sqrt{1 + \sqrt{2}}$. It follows that $\frac{\text{vol}(C)}{d_3(\infty)} = \frac{1 + \sqrt{2}}{16d_3(\infty)} > 0.176 > v_*$.

Furthermore, we can describe the associated 1-cusped orbifold in an analogous way as in the case of a cusp of type $\{2, 3, 6\}$ and the explanations referring to Figure III.13. The orbifold has a non-arithmetic fundamental group and is built upon a polyhedron arising from halving the Coxeter tetrahedron with cyclic Coxeter symbol $[(4^3, 3)]$ and Coxeter graph with internal symmetry as given by



As a result, and by [Joh+99, p. 348], the volume of the orbifold is about 0.27814 and hence too large.

Summarising the investigations in Section 3.4, we can state the following result.

Proposition 16. *Let V be a non-arithmetic hyperbolic 3-orbifold with a single cusp $C = B_\infty/\Gamma_\infty$ which is rigid of type $\{2, 4, 4\}$. Suppose that Γ_∞ gives rise to only one equivalence class of full-sized horoballs. Then,*

$$\text{vol}(V) > \text{vol}(V_*).$$

3.5. More than one equivalence class of full-sized horoballs

Assume that the crystallographic group Γ_∞ gives rise to more than one equivalence class of full-sized horoballs. We show that the corresponding orbifold has volume strictly bigger than $v_* = \text{vol}(\mathbb{H}^3/[5, 3, 6])$ (if it exists) by treating the cases of a cusp C of type $\{2, 3, 6\}$ or of type $\{2, 4, 4\}$ separately. For simplicity, we assume that the group Γ is *orientation-preserving* by passing to its orientation-preserving subgroup of index 2 if necessary.

The case $\{2, 3, 6\}$

As in the case of one equivalence class, inequivalent horoballs have to be centred in the singular points $a_s, s \in \{2, 3, 6\}$ of the cusp diagram D because otherwise already the cusp volume becomes too big (see Section 3.4 and (3.4)).

Suppose first that there are three equivalence classes of full-sized horoballs with respect to the action of Γ_∞ . The smallest volume then arises if $d_0(a_2, a_3) = 1$. It follows that the (oriented) cusp volume satisfies $\text{vol}(C) = \frac{\sqrt{3}}{2} > 2v_*$, and that the orbifold volume is too big.

Consider the case of exactly two equivalence classes of full-sized horoballs. Continue to denote by τ the shortest translation length in Γ_∞ and by d the shortest distance between two equivalent full-sized horoballs. In the case where the full-sized horoballs are centred in singular points of order 2 and 3, we get $\tau \geq 2$ which leads to a cusp volume of at least $\text{vol}(C) \geq \frac{\sqrt{3}}{2} > 2v_*$.

Using the fact that the full-sized horoballs are centred in singular points a_s , we can deduce the following slightly generalised version of Adams' Lemma 5 in the case of a (oriented) cusp C of type $\{2, 3, 6\}$.

Lemma 8. *Suppose that the full-sized horoballs of a $\{2, 3, 6\}$ -cusp are centred in singular points a_s in the cusp diagram D . Then, there is a rotation of order 2 in Γ whose axis is tangent to a full-sized horoball and the horoball B_∞ .*

Proof. Take a full-sized horoball centred at a singular point $a_s = (u, 1)$ where $u \in \mathbb{R}^2$ belongs to the boundary ∂U^3 . Since the group Γ acts transitively on the set of horoballs covering C , there is an isometry $\gamma \in \Gamma$ mapping u to ∞ . Since the axis l_s formed by u and ∞ is the rotational axis of an isometry in Γ_∞ , the image geodesic $\gamma(l_s)$ is also the axis of a rotation of the same order. Thus, by composing γ with a suitable isometry in Γ_∞ , we can assume that γ maps ∞ back to u . It follows that the element γ has to be a rotation of order 2 in Γ whose axis is tangent to the full-sized horoball and B_∞ . \square

There are two cases to consider for a possible placement of the centres of the full-sized horoballs.

Centres at a_6 and a_3 . Assume that the full-sized horoballs are centred in singular points a_s of order 6 and 3, respectively. Denote by $e = \frac{\tau}{\sqrt{3}}$ the distance between a_6 and a_3 in the cusp diagram D .

In the minimal case, $e = 1$; see Figure III.22. By Lemma 8, we have the existence of rotations

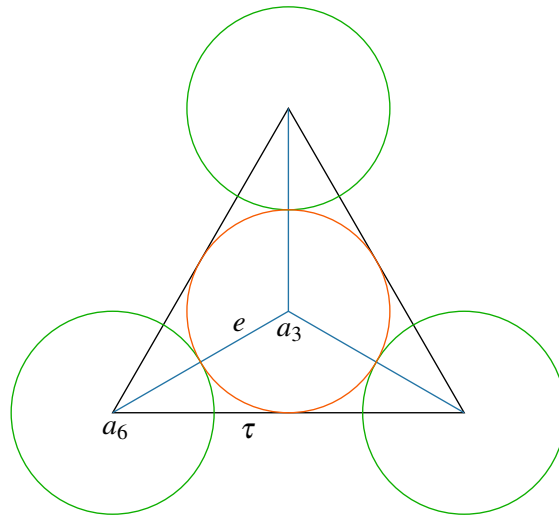


Figure III.22.: Inequivalent full-sized horoballs touch one another

of order 2 which exchange the full-sized horoballs centred at $a_6 = (u_6, 1)$ and at $a_3 = (u_3, 1)$ with the horoball B_∞ . It is not difficult to see that the rotation which sends ∞ to u_3 and fixes u_6 , together with the rotations in the singular axes of order 2, give a face identification of the ideal regular tetrahedron S_{reg}^∞ with ideal vertices defined by the 3 vertices of the regular triangle D and ∞ . One can also see that the above rotations are generated by reflections in the sides of the characteristic orthoscheme $[3, 3, 6]$ associated to S_{reg}^∞ . That implies that these rotations generate an arithmetic subgroup of finite index in Γ so that Γ itself is arithmetic. The rotations around the singular axis of order 3 and the rotation of order 2 mapping u_6 to ∞ generate 6 isometries of S_{reg}^∞ .

As a by-product, we can calculate the volume by means of (2.5) and obtain

$$\text{vol}(\mathbb{H}^3/\Gamma) = \frac{1}{6} \text{vol}(\mathcal{S}_{\text{reg}}^\infty) = \frac{1}{2} \mathbb{I}\left(\frac{\pi}{3}\right).$$

In the case $e > 1$, there is a similar notion to a $(\frac{1}{d})$ -ball in the case of one equivalence class. More precisely, the rotations of Lemma 8 map full-sized horoballs at distance e from a full-sized horoball to horoballs of diameter $\frac{1}{e^2}$ at distance $\frac{1}{e}$ from the full-sized image of B_∞ . Accordingly, we call these balls $(\frac{1}{e})$ -balls. The general situation is depicted in Figure III.23.

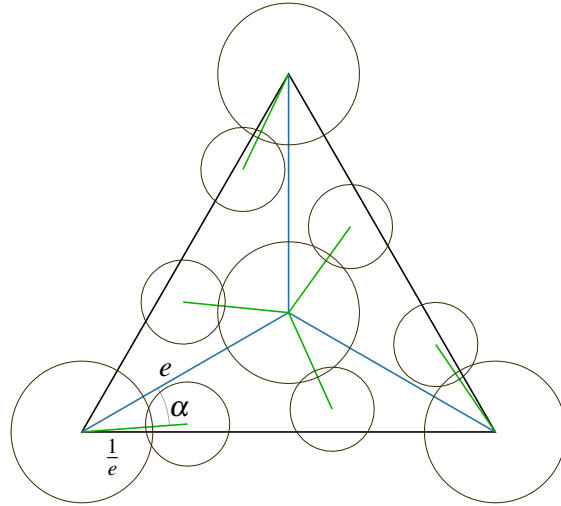


Figure III.23.: Inequivalent full-sized horoballs at distance $e > 1$

The minimal distance e is obtained by decreasing e to the point where the $(\frac{1}{e})$ -balls touch simultaneously both inequivalent full-sized horoballs; see Figure III.24. For a given angle $\alpha \in [0, \frac{\pi}{6}]$ as defined in Figure III.23, one can calculate the minimal possible e by using the isosceles triangle with base e , opposite angle α and sides $\frac{1}{e}$. This implies that $\cos \alpha = \frac{e^2}{2}$ and that

$$e = \sqrt{2 \cos \alpha} \geq \sqrt{2 \cos \frac{\pi}{6}} = \sqrt[4]{3}. \quad (3.19)$$

The lower bound on e yields a lower bound for the (oriented) cusp volume. It follows that

$$\text{vol}(C) = \frac{\tau e}{8} = \frac{\sqrt{3} e^2}{8} \geq \frac{3}{8} > 2v_*,$$

which is enough to exclude this case this from our considerations.

Centres at a_6 and a_2 . Assume that the full-sized horoballs are centred in singular points a_6 and a_2 , of order 6 and 2, respectively. Denote by $e \geq 1$ the shortest distance between a_6 and a_2 in the diagram D . The next result shows that $e > 1$.

Proposition 17. *Suppose that a 1-cusped oriented hyperbolic 3-orbifold has a cusp of type $\{2, 3, 6\}$ with precisely two equivalence classes of full-sized horoballs centred in the singular*

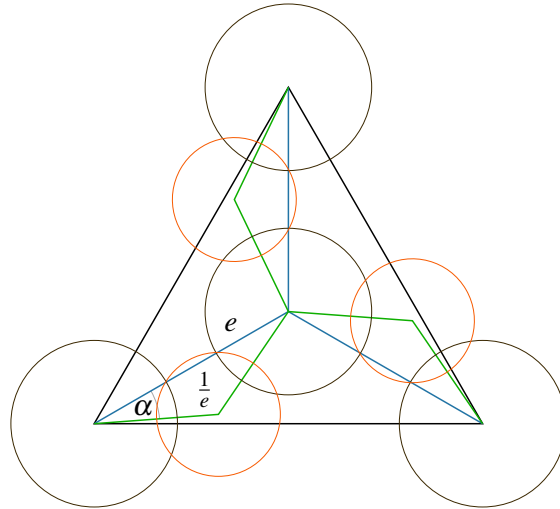


Figure III.24.: A $(\frac{1}{e})$ -ball touching two inequivalent full-sized horoballs

points a_6 and a_2 of the horoball diagram D . Then, $d_0(a_6, a_2) > 1$, and the full-sized horoballs cannot touch each other.

Proof. On the contrary, assume there is such an orbifold with touching full-sized horoballs giving rise to a horoball configuration as in Figure III.25. By Lemma 8, there is a rotation of order 2 exchanging the horoball B_1 centred in the singular point $b_1 = (u_1, 1)$ of order 6 and the horoball B_∞ at infinity. This rotation sends the touching full-sized horoballs around B_1 onto each other. After possibly using a rotation around the axis $l_1 = (u_1, \infty)$, we can assume that there is such a rotation r exchanging B_1 and B_∞ while fixing B_2 and B'_2 centred in $b_2 = (u_2, 1)$ and $b'_2 = (u'_2, 1)$, respectively. This implies that the image geodesic (u_1, u_2) of the order 2 axis $l_2 = (u_2, \infty)$ is also a rotation axis of order 2.

Using Lemma 8 again, there has to be a rotation r' around a common tangent of B_2 and B_∞ . Denote by s the rotation of order 2 around the axis l_2 . Then sr' is also a rotation through a common tangent of B_2 and B_∞ . The axis of sr' is perpendicular to the rotation axis of r' . Both rotations r' and sr' have to map full-sized horoballs touching B_2 to full-sized horoballs touching B_2 . Hence one of these rotations has to fix two of the touching full-sized horoballs. (If r' does not fix two full-sized horoballs touching B_2 , then it has to map two neighbouring full-sized horoballs touching B_2 onto each other. The rotational axis of r' then has to pass between those horoballs. Since the rotational axis of sr' is orthogonal, it has to pass through the centres of two full-sized horoballs touching B_2 .) Due to symmetry it is enough to consider the cases where B_1 or B_3 is fixed. Assuming that r' fixes B_1 , then the axis (u_1, u_2) has to have order 6 because of its image (u_1, ∞) . However, we already noted that it has order 2. Assuming that r' fixes B_3 centred at $b_3 = (u_3, 1)$, then the axis (u_2, u_3) has to have order 2 – the same as its image (u_3, ∞) . The geodesic (u_2, u_4) related to b_2 and $b_4 = (u_4, 1)$, has to have order 6 as its image (u_1, ∞) . However, they have to have the same order as they get mapped to each other by rotations around the singular point a_3 representing the centre of the cusp diagram D . \square

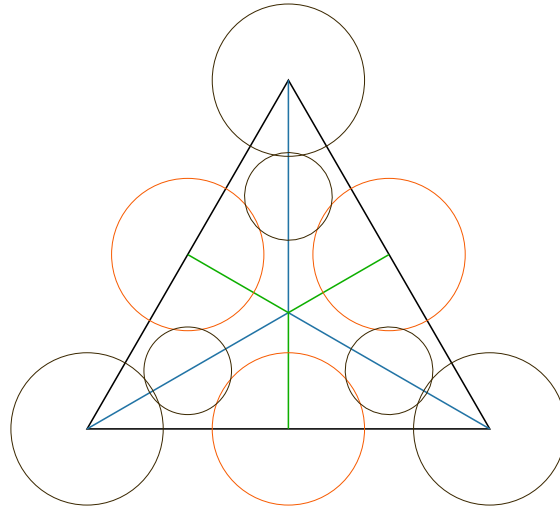


Figure III.26.: A $(\frac{1}{e})$ -ball centred on the angle bisector in D

However, for a cusp of type $\{2, 4, 4\}$, there is no equivalent of Lemma 8 since there are non-conjugate rotations of the same order in Γ_∞ . This is the reason why there are two cases to distinguish if one assumes that the full-sized horoballs, representing different equivalence classes, touch each other. We analyse this situation first.

- Suppose that $e = 1$. There is an (orientation preserving) isometry $r \in \Gamma$ mapping the full-sized horoball B_1 centred at $b_1 = (u_1, 1)$ to B_∞ . After possibly using an isometry in Γ_∞ , we can assume that r maps B_∞ to B_1 or to B_2 where B_2 is an inequivalent full-sized horoball centred in $b_2 = (u_2, 1)$ in D , respectively; see Figure III.27.

Case 1. If r sends ∞ to u_1 , then r is a rotation of order 2 and has to map the 4 touching full-sized horoballs onto each other. There are 4 such rotations, and any one of them helps us. In fact, the order 2 rotations around the midpoints a_2 of the sides of the square diagram D with side lengths τ and their conjugates by r give a side pairing of the ideal regular octahedron O_{reg}^∞ formed by the ideal points defined by the 4 vertices and the in-centre of the square diagram D and ∞ . Since this side pairing generates a finite index subgroup of Γ as well as a finite index subgroup of the arithmetic reflection group $[4, 4, 4]$, they are all commensurable. In particular, Γ has to be arithmetic.

Case 2. If r sends ∞ to u_2 , we can assume that $r(u_2) = u_1$. That implies that r is a rotation of order 3, which permutes ∞ , u_1 and u_2 . It also permutes the centres b'_1, b'_2 of neighbouring full-sized horoballs and a $(\frac{1}{e})$ -ball touching all of them as depicted in Figure III.27. Denote by s the rotation of order 2 around the vertical axis defined by the centre of this $(\frac{1}{e})$ -ball in \mathbb{H}^3 . Then, rsr^{-1} is a rotation of order 2 exchanging B_∞ and the $(\frac{1}{e})$ -ball. It follows that the two rotations of order 4 around the axes associated to b_1 and b'_1 , together with their conjugates by rsr^{-1} , give a side-pairing of the ideal regular octahedron O_{reg}^∞ . With the same reasoning as above, Γ turns out to be arithmetic.

- Suppose that $e > 1$. We can use the ideas from the proofs of Lemma 8 and Adams' Lemma 5 as follows. A full-sized horoball B_u centred at $u \in \partial\mathbf{H}^3 \setminus \{\infty\}$ can be mapped to B_∞ , and B_∞

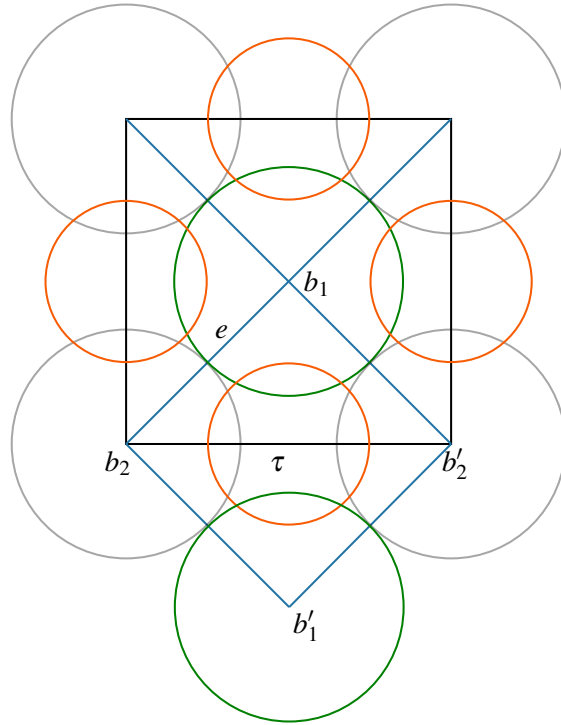


Figure III.27.: Two equivalence classes of full-sized horoballs in the diagram of a cusp of type $\{2,4,4\}$

gets mapped to a horoball B_v centred at v . By hypothesis, there is a full-sized horoball at distance e from B_u which gets mapped to a horoball touching B_v and of diameter $\frac{1}{e^2}$. This is the equivalent of the $(\frac{1}{e})$ -ball as above.

The minimal possible distance e is obtained if the $(\frac{1}{e})$ -ball touches inequivalent full-sized horoballs as illustrated in Figure III.28. We can perform the same calculation which led to equation (3.19) by using the isosceles triangle with angle α satisfying $\alpha \in [0, \frac{\pi}{4}]$. We obtain the lower bound according to

$$e = \sqrt{2 \cos \alpha} \geq \sqrt{2 \cos \frac{\pi}{4}} = \sqrt[4]{2}.$$

Hence, the (oriented) cusp volume yields the estimate

$$\text{vol}(C) = \frac{e^2}{4} \geq \frac{\sqrt{2}}{4} > 0.35 > 2v_*.$$

As a summary of the investigations in Sections 3.5 and 3.5, we can formulate the following result.

Proposition 18. *A non-arithmetic cusped hyperbolic 3-orbifold \mathbb{H}^3/Γ of minimal volume with cusp of the form $C = B_\infty/\Gamma_\infty$ has the property that Γ_∞ permutes all full-sized horoballs.*

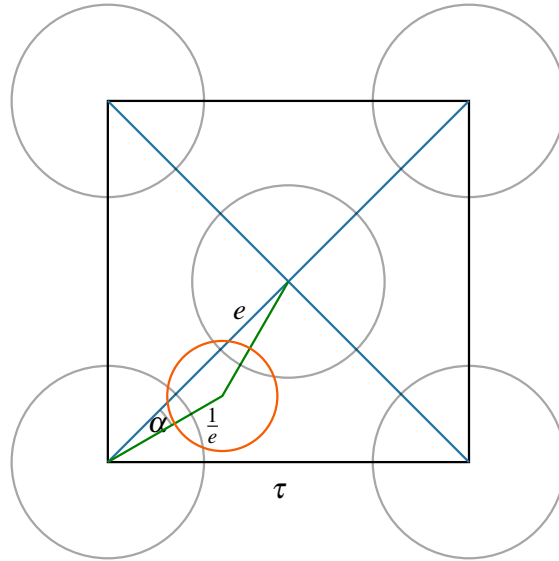


Figure III.28.: Two inequivalent full-sized horoballs at distance e with $(\frac{1}{e})$ -ball in the diagram of a cusp of type $\{2, 4, 4\}$

In combination with Proposition 6, Proposition 7, Proposition 15 and Proposition 16, Proposition 18 is the final step in the proof of the Theorem as stated in Section 1 and in Section 3.

4. Final remarks

The theory and investigations exploited in this work are valid for cusped hyperbolic n -orbifolds of dimensions $n \geq 2$. While for $n \geq 4$ the adaption becomes very cumbersome, one can derive in a fairly easy way the following corresponding result for $n = 2$ mentioned in Section 1 (for details, see [Dre21]).

Proposition 19. *Among all non-arithmetic cusped hyperbolic 2-orbifolds, the 1-cusped quotient space of \mathbf{H}^2 by the triangle Coxeter group $[5, \infty]$ has minimal area. As such the orbifold is unique, and its area is given by $\frac{3\pi}{10}$.*

By Selberg's Lemma, any hyperbolic orbifold has a finite sheeted (smooth) cover manifold. In the following, we are interested in cusped hyperbolic 3-manifolds of small volume. These manifolds form a large family of spaces. For a list of smallest ones, see [GMM09] and [MR03, Section 13.6]. Here, we focus on the subclass of *non-arithmetic Coxeter manifolds*, that is, manifolds whose fundamental groups are commensurable with non-arithmetic hyperbolic Coxeter groups. Consider the 1-cusped orbifold $V_* = \mathbf{H}^3/[5, 3, 6]$ of smallest volume among all non-arithmetic cusped hyperbolic 3-orbifolds. The minimal index of a torsion-free subgroup of $[5, 3, 6]$ is given by the l.c.m. of the orders of finite subgroups of $[5, 3, 6]$ and equals 120. In [Eve04], it is shown that there are 10 such subgroups which are non-conjugate in $[5, 3, 6]$, yielding non-

isometric non-arithmetic hyperbolic Coxeter 3-manifolds, all orientable with one or two cusps, covering the orbifold V_* . Each of these manifolds is of volume $120 \cdot \text{vol}([5, 3, 6]) \approx 20.580199$.

Compare V_* with the non-arithmetic 2-cusped orbifold V_\circ of volume

$$\frac{5}{8} \mathbb{I}\left(\frac{\pi}{3}\right) + \frac{1}{3} \mathbb{I}\left(\frac{\pi}{4}\right) \approx 0.364107$$

whose fundamental group is given by the tetrahedral Coxeter group $[(3^3, 6)]$ (see Example 2.2 and (2.8)). There is a torsion-free subgroup Λ of $[(3^3, 6)]$ of minimal possible index equal to 24 so that the resulting Coxeter manifold $M = \mathbf{H}^3/\Lambda$ is of volume ≈ 8.738570 . Moreover, the manifold M is non-orientable and multiply-cusped. Since the groups $[5, 3, 6]$ and $[(3^3, 6)]$ are incommensurable (see Remark 1), the manifold M does not have a common covering manifold with V_* . As a consequence, one gets the following result stated in Section 1.

Proposition 20. *The fundamental group of a non-arithmetic cusped hyperbolic Coxeter 3-manifold M_* of minimal volume is incommensurable to the Coxeter group $[5, 3, 6]$; the volume of M_* is smaller than or equal to $24 \cdot \text{vol}([(3^3, 6)]) \approx 8.738570$.*

Let us add that there are precisely four conjugacy classes of torsion-free subgroups of index 24 in $[(3^3, 6)]$. The related quotient manifolds are non-orientable and have 2, 2, 3 and 4 cusps. It is an open question whether these spaces are the smallest ones among all non-arithmetic cusped hyperbolic Coxeter 3-manifolds. For more details and the proof of Proposition 20, we refer to [Dre21, Chapter IV].

Appendix III.A The case $\{2, 3, 6\}$

Consider a discrete group $\Gamma \subset \text{Isom}^+ \mathbb{H}^3$ of orientation preserving isometries whose quotient space O has exactly one cusp of the form $C = B_\infty/\Gamma_\infty$ giving rise to full-sized horoballs of diameter 1 in the upper half space U^3 .

Suppose that C is of type $\{2, 3, 6\}$ and that the group Γ_∞ induces only one equivalence class of full-sized horoballs, all centred at singular points of order 6 in the cusp diagram D .

In the sequel, we consider the special case when the full-sized horoballs are at distance $d > 1$ from one another and when the associated $(\frac{1}{d})$ -balls do not touch one another. In particular, these $(\frac{1}{d})$ -balls give rise to $(\frac{1}{w})$ -balls. Suppose that the $(\frac{1}{w})$ -balls of the three $(\frac{1}{d})$ -balls in D coincide with center at the singular point $p = a_3$ of order 3 in D ; see Figure III.29. As explained in Section 3.4, one obtains $w = \frac{\sqrt{3}}{d}$, $\cos \theta = \frac{5}{2\sqrt{7}}$ and $d = \sqrt[4]{7}$. In particular, $\text{vol}(C) = \frac{\sqrt{21}}{24}$.

In the following, we correct Adams' determination of a fundamental polyhedron for Γ and the volume computation for O as given in [Ada92a, p. 10]. Furthermore, we show that O is arithmetic (see Remark 9 in Section 3.4).

Consider the full-sized horoballs B_j , B_k and B_l , as well as the $(\frac{1}{d})$ -balls centred at x , y and z as depicted in Figure III.29. Identify all horoball centres at height $t = 1$ in D with the corresponding points in the plane $\{t = 0\}$. Recall that the centres j , x , and y are located on one line. Denote by r the order 2 rotation which interchanges the horoballs B_∞ and B_j as well as B_k and B_x .

The $(\frac{1}{w})$ -ball B_s is actually the image of B_y under this rotation r and centred in a_2 . It is fixed by a rotation $s \in \Gamma_\infty$ of order 2 around a singular point a_2 .

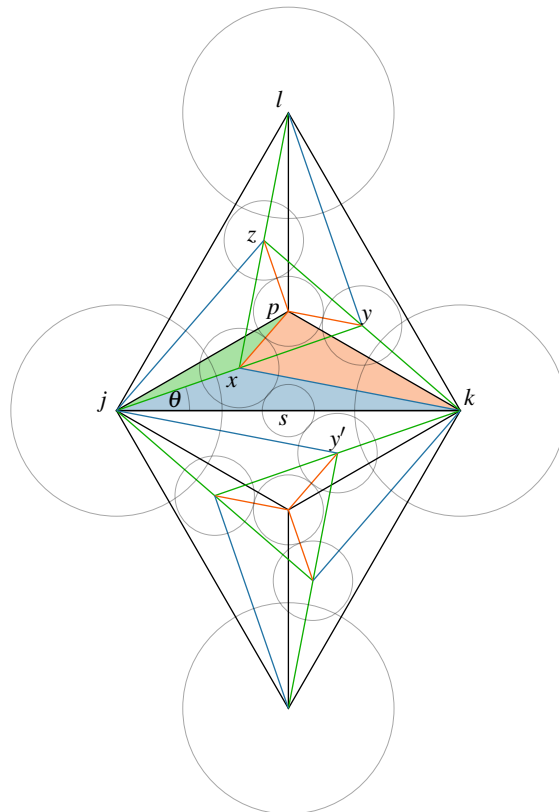
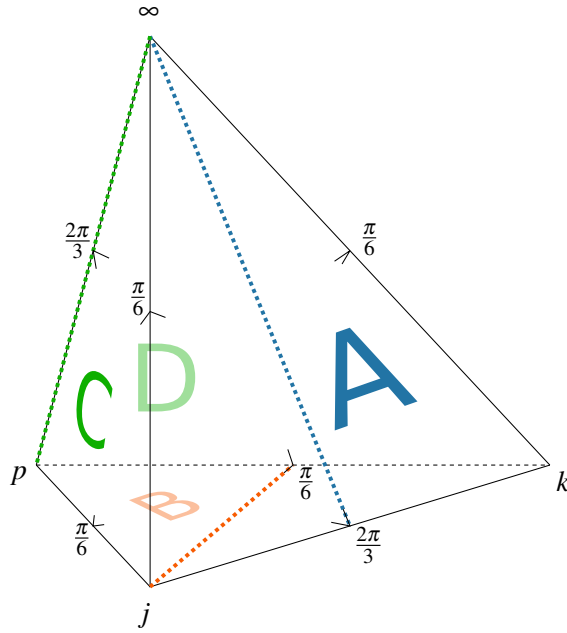


Figure III.29.: A single $(\frac{1}{w})$ -ball in a $\{2,3,6\}$ -cusp triangle D


 Figure III.30.: Side pairings of P for a subgroup of Γ

The image of the axis connecting B_∞ and B_p under the rotation r is the geodesic connecting B_j and B_y . Hence the conjugate rotation $s' := rsr$ swaps B_x and B_∞ while fixing B_j and B_y .

It is easy enough to find a fundamental polyhedron for a subgroup of Γ described by the cusp diagram. Consider the ideal tetrahedron with vertices ∞ , j , k , and p . Each of its ideal vertex triangles has angles $\frac{\pi}{6}$, $\frac{\pi}{6}$ and $\frac{2\pi}{3}$. Denote by ρ the clockwise rotation of order 3 around the singular axis connecting the centres of B_∞ and B_p . The symmetries s , s' , and ρ give face identifications which are visualised in Figure III.30. The faces A and B are identified with themselves by the appropriate rotation around the given axes. The face C gets mapped to D by ρ . This gives a *subproper side pairing* according to [Rat94, Section 13.4] implying that P is a fundamental polyhedron for a subgroup of finite index in Γ . Denote this subgroup by Θ .

From this we can deduce the arithmeticity of Γ as follows. A representation of Θ in $\mathrm{PSL}_2(\mathbb{C})$ is given by

$$s \mapsto \begin{pmatrix} i & -i \\ 0 & -i \end{pmatrix}, \quad \rho \mapsto \begin{pmatrix} -\omega & \omega^2 \\ 0 & \omega^2 \end{pmatrix}, \quad s' \mapsto \begin{pmatrix} i & 0 \\ id^2 e^{-i\beta} & -i \end{pmatrix} = \begin{pmatrix} i & 0 \\ -\frac{\sqrt{3}}{2} + i\frac{5}{2} & -i \end{pmatrix},$$

where $\omega = \frac{1}{2} + i\frac{\sqrt{3}}{2}$ is a primitive sixth root of unity. The trace field is $k\Gamma = \mathbb{Q}(\omega)$. This can be seen by utilising [MR03, Theorem 3.5.9] and by taking ρ^{-1} , $\rho^{-1}s$, and $srsr$ as generators for the subgroup Θ . By means of [MR03, Theorem 8.3.2], it follows that Γ is arithmetic, and the result [MR03, Theorem 8.4.1] in conjunction with [MR03, Theorem 3.3.8] allows us to deduce that Γ is even commensurable to the $[3, 3, 6]$.

In order to obtain Γ , one needs to add r as a generator to Θ . Replacing the generator ρ by $s\rho$ (a rotation around the axis connecting ∞ and j) makes it easy to show that $\Gamma = \Theta \rtimes \langle r \rangle$ is a semidirect product. The subgroup Θ has index 2 in Γ , so half of P is a fundamental polyhedron

for Γ . This allows us to calculate the volume of the fundamental polyhedron P and of the orbifold O as follows (see Section 2.3).

$$\text{vol}(O) = \text{vol}(P) = \frac{1}{2} \left\{ \mathbb{I} \left(\frac{2\pi}{3} \right) + 2\mathbb{I} \left(\frac{\pi}{6} \right) \right\} = \mathbb{I} \left(\frac{\pi}{3} \right) \approx 0.338314.$$

Remark 21. Based on Adams' original explanation [Ada92a, p. 10], there is a dissection of the polyhedron P and its image under rsr into three ideal tetrahedra $T(\infty, j, k, x)$, $T(\infty, j, p, x)$, and $T(\infty, k, p, x)$. They are represented by the coloured triangles in Figure III.29. The blue and green tetrahedra have angles θ , $\frac{\pi}{6} - \theta$ and $\frac{5\pi}{6}$, where $\cos \theta = \frac{5}{2\sqrt{7}}$ as above. The red tetrahedron has angles θ , $\frac{\pi}{3} - \theta$, and $\frac{2\pi}{3}$. This is useful in order to obtain the following new identity¹ for the Lobachevsky function evaluated at $\frac{\pi}{3}$.

$$\begin{aligned} \mathbb{I} \left(\frac{\pi}{3} \right) &= \frac{1}{4} \left(2 \left(\mathbb{I}(\theta) + \mathbb{I} \left(\frac{\pi}{6} - \theta \right) + \mathbb{I} \left(\frac{5\pi}{6} \right) \right) + \mathbb{I}(\theta) + \mathbb{I} \left(\frac{2\pi}{3} - \theta \right) + \mathbb{I} \left(\frac{\pi}{6} \right) \right) \\ &= \frac{3}{4} \mathbb{I}(\theta) + \frac{1}{2} \mathbb{I} \left(\frac{\pi}{6} - \theta \right) + \frac{1}{4} \mathbb{I} \left(\frac{2\pi}{3} - \theta \right) - \frac{1}{4} \mathbb{I} \left(\frac{\pi}{6} \right) \quad \text{with} \quad \cos \theta = \frac{5}{2\sqrt{7}}. \end{aligned}$$

Appendix III.B The case $\{2, 4, 4\}$

As in Appendix III.A, consider a discrete group $\Gamma \subset \text{Isom}^+ \mathbb{H}^3$ of orientation preserving isometries whose quotient space O has exactly one cusp of the form $C = B_\infty / \Gamma_\infty$ giving rise to full-sized horoballs of diameter 1 in the upper half space U^3 .

Suppose that C is of type $\{2, 4, 4\}$ and that the group Γ_∞ has only one equivalence class of full-sized horoballs, all centred at singular points of order 4 in the cusp diagram D , and at distance $d > 1$ from one another. Assume that the associated $(\frac{1}{d})$ -balls do not touch one another so that each $(\frac{1}{d})$ -ball yields $(\frac{1}{w})$ -balls.

Suppose that the four $(\frac{1}{w})$ -balls associated to the four $(\frac{1}{d})$ -balls in D coincide and, hence, have centre equal to the centre of the square D . Furthermore, the circumradius of D coincides with $\frac{1}{w}$ so that $w = \frac{\sqrt{2}}{d}$.

In a completely analogous manner as in Appendix III.A, and by means of (3.7), one can show that $d = \sqrt[4]{5}$ and $\cos \theta = \frac{2}{\sqrt{5}}$. Since the cusp diagram D has no mirror symmetry, the cusp volume yields the large value $\text{vol}(C) = \frac{\sqrt{5}}{8} > v_*$; see Figure III.31.

Furthermore, by performing similar computations as in Appendix III.A, one can deduce that this configuration gives rise to a unique oriented orbifold $O = \mathbb{H}^3 / \Gamma$ that is arithmetic and in fact commensurable to the Coxeter group $[3, 4, 4]$.

Remark 22. By a suitable decomposition of a fundamental polyhedron for Γ as above, a similar identity for the value $\mathbb{I} \left(\frac{\pi}{4} \right)$ of the Lobachevsky function in terms of the angle $0 < \theta < \frac{\pi}{4}$ satisfying

¹To the best of the authors knowledge, this identity is new.

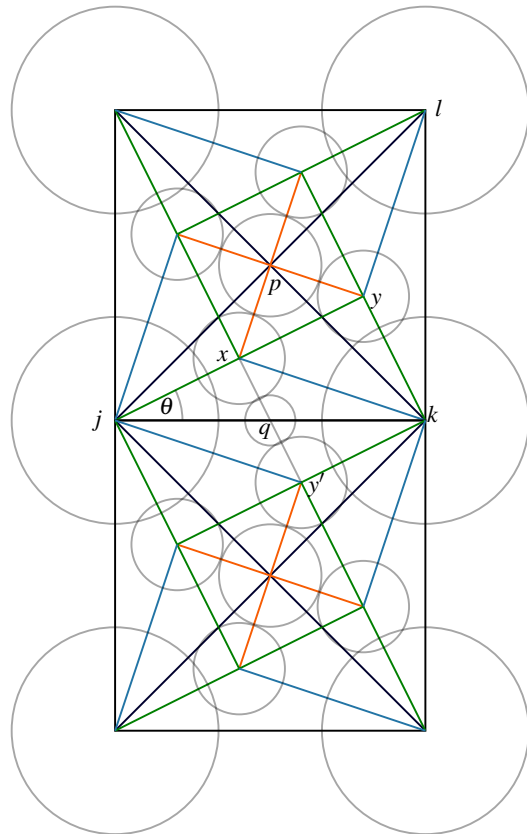


Figure III.31.: The cusp diagram D for the cusp of type $\{2,4,4\}$ with a single $(\frac{1}{w})$ -ball at its centre

$\cos \theta = \frac{2}{\sqrt{5}}$ is obtained. This value also gives the volume of the orbifold O as follows.

$$\begin{aligned} \mathbb{II}\left(\frac{\pi}{4}\right) &= \frac{1}{4} \left\{ 2 \left(\mathbb{II}(\theta) + \mathbb{II}\left(\frac{\pi}{4} - \theta\right) + \mathbb{II}\left(\frac{3\pi}{4}\right) \right) + \mathbb{II}(\theta) + \mathbb{II}\left(\frac{\pi}{2} - \theta\right) + \mathbb{II}\left(\frac{\pi}{2}\right) \right\} \\ &= \frac{3}{4} \mathbb{II}(\theta) + \frac{1}{2} \mathbb{II}\left(\frac{\pi}{4} - \theta\right) + \frac{1}{4} \mathbb{II}\left(\frac{\pi}{2} - \theta\right) - \frac{1}{4} \mathbb{II}\left(\frac{\pi}{4}\right) \\ &\approx 0.45983 \quad \text{with} \quad \cos \theta = \frac{2}{\sqrt{5}}. \end{aligned}$$

References

- [Ada87] C. Adams. ‘The noncompact hyperbolic 3-manifold of minimal volume’. *Proc. Amer. Math. Soc.* 100 (1987), pp. 601–606.
- [Ada91] C. Adams. ‘Limit volumes of hyperbolic three-orbifolds’. *J. Differential Geom.* 34 (1991), pp. 115–141.
- [Ada92a] C. Adams. ‘Noncompact hyperbolic 3-orbifolds of small volume’. *Topology ’90 (Columbus, OH, 1990)*. Vol. 1. Ohio State Univ. Math. Res. Inst. Publ. de Gruyter, Berlin, 1992, pp. 1–15.
- [Ada92b] C. Adams. ‘Volumes of hyperbolic 3-orbifolds with multiple cusps’. *Indiana Univ. Math. J.* 41 (1992), pp. 149–172.
- [And70a] E. Andreev. ‘Convex polyhedra in Lobachevski spaces’. *Mat. Sb. (N.S.)* 81 (123) (1970), pp. 445–478.
- [And70b] E. Andreev. ‘Convex polyhedra of finite volume in Lobachevski space’. *Mat. Sb. (N.S.)* 83 (125) (1970), pp. 256–260.
- [Bör78] K. Böröczky. ‘Packing of spheres in spaces of constant curvature’. *Acta Math. Acad. Sci. Hungar.* 32 (1978), pp. 243–261.
- [Cox54] H. Coxeter. ‘Arrangements of equal spheres in non-Euclidean spaces’. *Acta Math. Acad. Sci. Hungar.* 5 (1954), pp. 263–274.
- [DK21] S. T. Drewitz and R. Kellerhals. *The non-arithmetic cusped hyperbolic 3-orbifold of minimal volume*. 2021. arXiv: 2106.12279 [math.GT].
- [Dre21] S. T. Drewitz. ‘New contributions to groups of hyperbolic isometries’. PhD thesis. University of Fribourg, 2021.
- [Eve04] B. Everitt. ‘3-manifolds from Platonic solids’. *Topology Appl.* 138 (2004), pp. 253–263.
- [Fis+18] D. Fisher, J.-L. Lafont, N. Miller and M. Stover. ‘Finiteness of maximal geodesic submanifolds in hyperbolic hybrids’. *arXiv:math/1802.04619* (2018), 28 pp.
- [GMM09] D. Gabai, R. Meyerhoff and P. Milley. ‘Minimum volume cusped hyperbolic three-manifolds’. *J. Amer. Math. Soc.* 22.4 (2009), pp. 1157–1215. ISSN: 0894-0347. DOI: 10.1090/S0894-0347-09-00639-0.

-
- [Gug15] R. Guglielmetti. ‘CoxIter - Computing invariants of hyperbolic Coxeter groups’. *LMS J. Comput. Math.* 18 (2015), pp. 754–773.
- [Hil07a] T. Hild. ‘Cusped hyperbolic orbifolds of minimal volume in dimensions less than 11’. PhD thesis. no. 1567, University of Fribourg, 2007.
- [Hil07b] T. Hild. ‘The cusped hyperbolic orbifolds of minimal volume in dimensions less than ten’. *J. Algebra* 313 (2007), pp. 208–222.
- [HK07] T. Hild and R. Kellerhals. ‘The FCC lattice and the cusped hyperbolic 4-orbifold of minimal volume’. *J. Lond. Math. Soc. (2)* 75 (2007), pp. 677–689.
- [Joh+02] N. Johnson, R. Kellerhals, J. Ratcliffe and S. Tschantz. ‘Commensurability classes of hyperbolic Coxeter groups’. *Linear Algebra Appl.* 345 (2002), pp. 119–147.
- [Joh+99] N. Johnson, R. Kellerhals, J. Ratcliffe and S. Tschantz. ‘The size of a hyperbolic Coxeter simplex’. *Transform. Groups* 4 (1999), pp. 329–353.
- [Kel12] R. Kellerhals. ‘Scissors congruence, the golden ratio and volumes in hyperbolic 5-space’. *Discrete Comput. Geom.* 47 (2012), pp. 629–658.
- [Kel89] R. Kellerhals. ‘On the volume of hyperbolic polyhedra’. *Math. Ann.* 285 (1989), pp. 541–569.
- [Kel98] R. Kellerhals. ‘Volumes of cusped hyperbolic manifolds’. *Topology* 37 (1998), pp. 719–734.
- [Mey85] R. Meyerhoff. ‘The cusped hyperbolic 3-orbifold of minimum volume’. *Bull. Amer. Math. Soc. (N.S.)* 13 (1985), pp. 154–156.
- [Mey86] R. Meyerhoff. ‘Sphere-packing and volume in hyperbolic 3-space’. *Comment. Math. Helv.* 61 (1986), pp. 271–278.
- [MR03] C. Maclachlan and A. Reid. *The arithmetic of hyperbolic 3-manifolds*. Vol. 219. Graduate Texts in Mathematics. Springer-Verlag, New York, 2003.
- [NR92] W. Neumann and A. Reid. ‘Arithmetic of hyperbolic manifolds’. *Topology '90 (Columbus, OH, 1990)*. Vol. 1. Ohio State Univ. Math. Res. Inst. Publ. de Gruyter, Berlin, 1992, pp. 273–310.
- [Rat94] J. Ratcliffe. *Foundations of hyperbolic manifolds*. Vol. 149. Graduate Texts in Mathematics. Springer-Verlag, New York, 1994.
- [RHD07] R. Roeder, J. Hubbard and W. Dunbar. ‘Andreev’s theorem on hyperbolic polyhedra’. *Ann. Inst. Fourier (Grenoble)* 57 (2007), pp. 825–882.
- [Vin85] È. Vinberg. ‘Hyperbolic groups of reflections’. *Uspekhi Mat. Nauk* 40 (1985), pp. 29–66, 255.
- [VS93] È. Vinberg and O. Shvartsman. ‘Discrete groups of motions of spaces of constant curvature’. *Geometry, II*. Vol. 29. Encyclopaedia Math. Sci. Berlin: Springer, 1993, pp. 139–248.

IV. A Small Non-Arithmetic Hyperbolic 3-Manifold Covering a Coxeter Orbifold

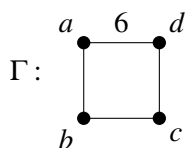
1. Introduction

In chapter III we identified the smallest non-compact non-arithmetic hyperbolic 3-orbifold. One natural question which arises is the one asking for the smallest non-compact non-arithmetic hyperbolic 3-manifolds. A first candidate might be a manifold covering the smallest orbifold.

As such we would have to find a torsion-free subgroup of the Coxeter group $\bullet \overset{5}{\text{---}} \bullet \overset{6}{\text{---}} \bullet$. However, this contains the finite subgroup $I_3 : \bullet \overset{5}{\text{---}} \bullet$ of order 120. As $\text{covol} \bullet \overset{5}{\text{---}} \bullet \overset{6}{\text{---}} \bullet \approx 0.1715 \dots$ (see section 2.3 of chapter III), the volume of a manifold covering $\mathbf{H}^3 / \bullet \overset{5}{\text{---}} \bullet \overset{6}{\text{---}} \bullet$ has to be at least

$$120 \text{covol} \left(\bullet \overset{5}{\text{---}} \bullet \overset{6}{\text{---}} \bullet \right) \approx 20.58.$$

The aim of this section is to describe a torsion-free subgroup of



having minimal possible index 24 in Γ . The covolume of Γ is bigger than the covolume of



$$\text{covol} \Gamma \approx 0.364 \dots > \text{covol} \bullet \overset{5}{\text{---}} \bullet \overset{6}{\text{---}} \bullet.$$

Despite the bigger covolume of Γ , the volume of the smallest covering manifolds is $24 \text{covol}(\Gamma) \approx 8.74$ and thus smaller than any covering manifold of $\mathbf{H}^3 / \bullet \overset{5}{\text{---}} \bullet \overset{6}{\text{---}} \bullet$.

Several people have considered small hyperbolic 3-manifolds. For example, Cao and Meyerhoff proved in [CM01] that the figure-eight knot complement is one of the two smallest orientable cusped hyperbolic 3-manifolds with volume ≈ 2.03 . Gabai, Meyerhoff, and Milley described in [GMM09] how the ten smallest orientable 1-cusped hyperbolic 3-manifolds can be obtained from Dehn filling on one of 21 cusped manifolds. Agol constructed in [Ago10] the smallest orientable 2-cusped hyperbolic 3-manifolds of volume ≈ 3.66 using topological arguments. Our approach of finding a covering manifold of a *non-arithmetic Coxeter orbifold* yields the only non-arithmetic example in this category known to the author.

2. Preliminaries

In order to describe a torsion-free subgroup of index 24 in Γ , we first explain a correspondence of (conjugacy classes of) subgroups of Coxeter groups and graphs with labelled edges. We learned the general principle of this chapter as a kind of ‘folklore’ from Brent Everitt.

2.1. Group Actions

Let Γ be a group. Our aim is to construct a transitive action of Γ on a suitable (finite) set V . Let us recall some facts. They can be found for example in Bosch [Bos09] or Smith [Smi16].

For a group Γ and a set V a group action of Γ on V is a group homomorphism

$$\rho : \Gamma \rightarrow \{f : V \rightarrow V \text{ bijection}\} =: \text{Sym}(V)$$

into the symmetric group of V . We will usually write it as

$$\begin{aligned} \Gamma \times V &\rightarrow V, \\ (\gamma, v) &\mapsto \gamma.v := \rho(\gamma)(v), \end{aligned}$$

and it satisfies the following properties:

- (i) The neutral element $e \in \Gamma$ induces the trivial map: $e.v = v$ for every $v \in V$.
- (ii) An associativity property holds: $(\gamma\delta).v = \gamma.(\delta.v)$ for every $v \in V$ and $\gamma, \delta \in \Gamma$.

A group action gives rise to subgroups of Γ and subsets of V . The *stabiliser* of an element $v \in V$ under the group action of Γ is the subgroup

$$\Gamma_v := \{\gamma \in \Gamma \mid \gamma.v = v\}$$

of elements in Γ fixing v . The *orbit* of a point $v \in V$ is the set of images under the group action

$$\Gamma.v := \{\gamma.v \mid \gamma \in \Gamma\}.$$

Orbits of different elements $v, w \in V$ are either the same or disjoint because a common element $\gamma.v = \delta.w$ implies that $w = \delta^{-1}\gamma.v$ is in the orbit of v and vice versa. For a given orbit $\Gamma.v$ there is a natural bijection between the elements of the orbit and the left cosets Γ/Γ_v . This map

$$\begin{aligned} \Gamma/\Gamma_v &\rightarrow \Gamma.v \\ \gamma\Gamma_v &\mapsto \gamma.v \end{aligned}$$

is well-defined and bijective. This proves a central theorem when studying group actions:

Theorem 1 (Orbit Stabiliser Theorem). *Let Γ a group acting on a set V . Then the cardinality of the orbit of an element $v \in V$ is the index of its stabiliser in the group Γ :*

$$|\Gamma.v| = [\Gamma : \Gamma_v].$$

The following consequence of the orbit stabiliser theorem will be helpful for finding a lower bound of the index for a torsion-free subgroup of Γ .

Lemma 2. *Let Γ be a group acting transitively on a finite set V . If $G < \Gamma$ is a finite subgroup such that no element of G fixes any element in V , then the order of G has to divide the cardinality of V .*

Proof. Restrict the group action of Γ to a group action of $G < \Gamma$ on V . Following the orbit stabiliser theorem, the orbit $G.v$ of any point $v \in V$ has to have cardinality $|G|$ since the stabilisers are trivial:

$$|G.v| = [G : G_v] = [G : \{e\}] = |G|.$$

Since the orbits partition V and have all the same size, $|G|$ has to divide $|V|$. \square

If there is only a single orbit for a group action, the action of Γ is called transitive. Equivalently, for any two $v, w \in V$ there is a $\gamma \in \Gamma$ with $\gamma.v = w$. This will be of most interest for us later. In this case all stabilisers Γ_v with $v \in V$ are conjugate subgroups with index $[\Gamma : \Gamma_v] = |V|$.

2.2. Torsion Elements in (Transitive) Group Actions of Coxeter Groups

In order to find a torsion-free subgroup in a given group Γ , we need to discern torsion elements. For this we assume Γ to be a Coxeter group generated by a finite set of generators S . An especially interesting kind of subgroup $G < \Gamma$ is a *visual* (sometimes called parabolic or special) subgroup generated by a subset $S' \subset S$ of the generators. The visual subgroup G is itself a Coxeter group. The visual subgroups help giving all torsion elements in Γ .

Theorem 3. *Let Γ be a hyperbolic Coxeter group and $w \in \Gamma$ an element of finite order. Then there is a finite visual subgroup of Γ which contains a conjugate of w .*

Proof. In the case of a hyperbolic Coxeter group we can consider the action of Γ on \mathbf{H}^n . The generators S of Γ correspond to the reflections in a fundamental polyhedron P . An element $w \in \Gamma$ with finite order is an elliptic element having at least one fixed point $p \in \mathbf{H}^n$. There is a group element $\gamma \in \Gamma$ such that $\gamma.p$ is in P and $\gamma w \gamma^{-1}$ fixes the point $\gamma.p$ in P . Since there cannot be a fixed point in the interior of P , $\gamma.p$ has to be a point on the boundary of P . Hence $\gamma w \gamma^{-1}$ is contained in the subgroup which is generated by all reflections in the hyperplanes containing $\gamma.p$. Since all elements in this subgroup fix $\gamma.p$, it is finite. This proves the theorem for the hyperbolic case. \square

Theorem 3 is also true in the case of abstract Coxeter groups. It is exercise 2) in §4 of chapter V in [Bou02]. There is a proof following roughly the ideas of the exercise in [BH93, Proposition 1.3], and a geometric proof in [Eve04, Theorem 4].

By giving all the maximal finite visual subgroups one can find all conjugates of elements of finite order. It is sufficient to consider elements of prime order. If an element of non-prime order fixes a point in \mathbf{H}^3 , then its powers of prime order do the same. Everitt [Eve04] gave a well-arranged recapitulation of a result of Carter [Car72] listing representatives of all conjugacy classes of elements of prime order in finite Coxeter groups. We will later list the representatives we need for our example in Table IV.1.

Together with Lemma 2 one can see that the orders of all finite visual subgroups of Γ have to divide the cardinality of a suitable finite set V on which Γ acts. A lower bound for the index of a torsion-free subgroup is given by the lowest common multiple of the orders of the maximal finite visual subgroups.

The following lemma will enable the reader to check that the subgroups described below are indeed torsion-free.

Lemma 4. *Let Γ be a Coxeter group acting transitively on a finite set V such that for each conjugacy class of torsion elements there is a representative which does not fix any element of V . Then the stabilisers of the elements in V are torsion-free.*

The following helps if one tries to find a group action by hand.

Proposition 5. *Let Γ be a group acting transitively on a finite set V with Γ_{v_0} torsion-free for some $v_0 \in V$. Then for any two distinct $\gamma_1, \gamma_2 \in \Gamma$ generating a finite subgroup of Γ , their action differs on every element in V .*

Proof. Assume that there was a $v \in V$ such that $\gamma_1.v = \gamma_2.v$. Then $\gamma_1^{-1}\gamma_2$ is an element of finite order fixing v . It cannot be the identity since we assumed γ_1 and γ_2 to be distinct. So Γ_{v_0} cannot be torsion-free. \square

2.3. Group Actions Given by Graphs

Let (Γ, S) be a Coxeter group. We will describe an action of Γ on the (finite) set V of vertices of a graph (V, E) with edges E . Each edge is labelled with a generator $s \in S$ (or appropriately marked). Two edges with the same label cannot have a common vertex. An edge (v, w) with the label s signifies that under the action of Γ the generator s swaps the two vertices v and w . This implies that for any generator s , s^2 acts as the identity. This is necessary because the generators of a Coxeter group are inversions. For this graph (V, E) to describe an action of Γ on V , we lastly need that all the relations $(s_i s_j)^{m_{ij}}$ act as the identity on (V, E) .

Example 6. One class of examples is the group action of a Coxeter group (Γ, S) on the Cayley graph of a visual subgroup $G < \Gamma$. The *Cayley graph* of a finite Coxeter group (G, S') is a graph with vertices $V = G$, the elements of the group G . There is an edge (g, h) with label $s \in S'$ between two elements $g, h \in G$ if and only if $sg = h$. This immediately gives an action of G on the Cayley graph of G : The relations of G are automatically fulfilled because for $s_i, s_j \in S'$, $(s_i s_j)^{m_{ij}} = e$ in G and it is easy to show that $(s_i s_j)^{m_{ij}}$ acts trivially on any vertex $v \in V = G$. If all weights m_{ij} for $s_i \in S \setminus S'$ and $s_j \in S'$ are even or ∞ , then the Cayley graph (V, E) of $G < \Gamma$ also describes an action of Γ on (V, E) (by assuming that any $s \in S \setminus S'$ acts trivially). If there are odd weights m_{ij} for $s_i \in S \setminus S'$ and $s_j \in S'$, one can often add appropriate edges to make it an action of Γ . However, this does not always work. For example, in the situation of $\Gamma = A_3$ and $G = \langle a, c \rangle$, where the generators are named as below in (2.1), it is not possible to create an action of Γ on the Cayley graph of G by just adding edges.

If the graph is connected, the action is transitive and the graph itself defines a conjugacy class of subgroups Γ_v of Γ with index $[\Gamma : \Gamma_v] = |V|$. A choice of a vertex $v_0 \in V$ is a choice of a representative of this conjugacy class.

If and only if an element $\gamma \in \Gamma$ does *not* fix any vertex of the graph, then neither γ nor any of its conjugates are in the stabiliser subgroup of any vertex. In general this implies that the Cayley graphs of the finite subgroups are included in the graph of the group action.

Some examples for group actions described by graphs are given in Figure IV.1. They are actions for the groups:

$$A_2 : \bullet \text{---} \bullet, \quad A_3 : \bullet \text{---} \bullet \text{---} \bullet, \quad G_2 : \bullet \overset{6}{\text{---}} \bullet. \quad (2.1)$$

The action of a is given by simple edges, the action of b by double edges, the action of c by dotted edges and the action of d by dashed/dotted edges. The first and last action are represented by the Cayley graphs of A_2 and G_2 , respectively.

Remark 7. Let Γ be a Coxeter group with a transitive action given by a finite graph (V, E) , and let $G < \Gamma$ be a finite visual subgroup. If the subgraph of (V, E) obtained by dropping all edges not labelled by generators of G is the Cayley graph of G (or a union thereof), then no element of G is contained in a stabiliser Γ_v of a vertex v in Γ . This is an alternative to look for the representatives of conjugacy classes of elements of prime order.

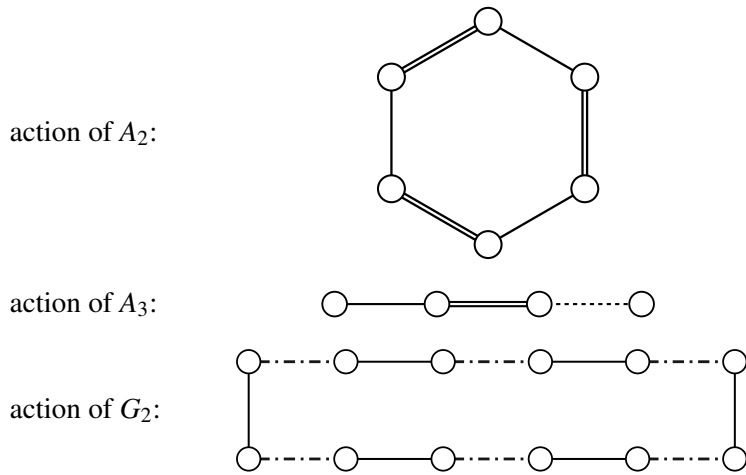


Figure IV.1.: Examples for Group Actions Given by Graphs

3. A Small Non-Arithmetic Hyperbolic 3-Manifold

3.1. The Base Orbifold

Consider the orbifold given by the quotient of \mathbf{H}^3 by the Coxeter group

$$\Gamma : \begin{array}{ccc} a & \overset{6}{\text{---}} & d \\ \bullet & \text{---} & \bullet \\ | & & | \\ \bullet & \text{---} & c \\ b & & \end{array} .$$

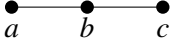
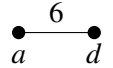
maximal finite subgroup	prime order	representatives of conjugacy classes
	2	$a \sim b \sim c$ ac
	3	$ab \sim bc$
	2	$b \sim c \sim d$ bd
	3	$bc \sim cd$
	2	a, d $(ad)^3$
	3	$(ad)^2$

 Table IV.1.: Conjugacy Representatives of Torsion Elements in Γ

Its fundamental polyhedron is a tetrahedron S_Γ with two ideal vertices. It has two cusps of type $\bullet \xrightarrow{6} \bullet \xrightarrow{6} \bullet$, and the maximal finite subgroups are of type $\bullet \xrightarrow{6} \bullet \xrightarrow{6} \bullet$ with $4! = 24$ elements ($\langle a, b, c \rangle$ and $\langle b, c, d \rangle$) or $\bullet \xrightarrow{6} \bullet$ with $2 \cdot 6 = 12$ elements ($\langle a, d \rangle$). Thus a torsion-free subgroup of Γ has at least index 24.

By [EH09] we can find representatives of all conjugacy classes of prime order elements (see IV.1).

Using Magma [BCP97] one detects four conjugacy classes of torsion-free subgroups with minimal index 24:

- (i) $\Gamma_1 := \langle abd, bacdca \rangle$
- (ii) $\Gamma_2 := \langle bdca, cbadab, cdacda, abacdbc \rangle = \langle bdca, abacdbc, abdabcb \rangle$
- (iii) $\Gamma_3 := \langle acd, abadc, cbadcb \rangle$
- (iv) $\Gamma_4 := \langle abd, bacdc, cbadcb \rangle = \langle bacdc, cbadcb, dcbdad \rangle$

The Magma code is in Appendix B. The corresponding manifolds \mathbf{H}^3/Γ_i have two, two, three, and four cusps, respectively, and they are all non-orientable. The detailed computations are described for Γ_1 below. For Γ_i ($i > 1$) the computations are similar.

3.2. The Manifold \mathbf{H}^3/Γ_1

Let us describe the first group Γ_1 in more detail. As the fundamental polyhedron of Γ is a simplex, we can also use the names of the generators for the reflecting hyperplanes and the vertices opposite those hyperplanes.

The subgroup Γ_1 can be described by the graph in Figure IV.2 as follows. The simple edges represent transpositions by the generator a , double edges stand for the generator b , dashed edges correspond to c and bold dotted/dashed edges represent d . Notice that the graph is based on the

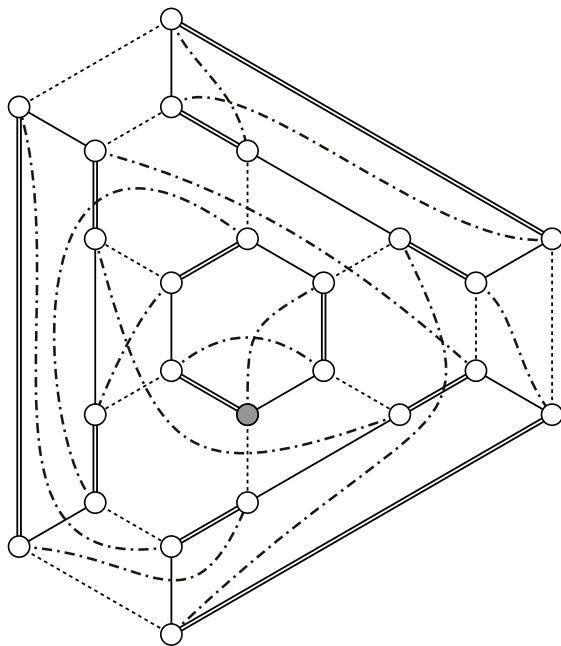


Figure IV.2.: Graph for Γ_1

Cayley graph of A_3 in the generators a , b , and c , which is a maximal finite subgroup of largest order of Γ . The subgroup $\Gamma_1 < \Gamma$ is the stabiliser of the grey vertex in Figure IV.2. Another subgroup of Γ is conjugate to Γ_1 if and only if it is the stabiliser of a vertex in the graph.

A fundamental polyhedron for Γ_1 can be found by gluing 24 copies of the simplex S_Γ around the vertex corresponding to generator d (being stabilised by a , b and c). Those copies are obtained by taking the images of the simplex S_Γ under the subgroup $\bullet \text{---} \bullet \text{---} \bullet$ generated by a , b , and c .

Recall the geometry of the simplex S_Γ (see Figure IV.3). There are two edges with angle $\frac{\pi}{3}$ and $\frac{\pi}{2}$ adjacent to vertex d . The hyperplane d opposite this vertex has one right angle, one angle $\frac{\pi}{3}$ and one angle $\frac{\pi}{6}$. Doubling the simplex along hyperplane b doubles side d due to the right angle. Those two copies of the simplex give a pyramid with quadrilateral base (see Figure IV.4). The two pairs of opposite side ridges have angles $\frac{2\pi}{3}$ and $\frac{\pi}{2}$. The two pairs of adjacent base ridges have angles $\frac{\pi}{3}$ and $\frac{\pi}{6}$.

When twelve of these pyramids are glued together around vertex d , we get a fundamental polyhedron for Γ_1 that has three kinds of vertices which are images of the vertices a , b , and c of the original simplex: ideal vertices with three adjacent faces (images of c), ideal vertices with four adjacent faces (images of b) and finite vertices with three adjacent faces (images of a). In its structure it looks like an ideal tetrahedron with subdivisions (see Figure IV.5). Each edge of the tetrahedron has an additional ideal vertex and each face has a finite vertex in its centre. Choosing one copy of the fundamental simplex S_Γ of Γ inside the fundamental domain gives side identifications by considering how the elements of the group Γ_1 act on it. In Figure IV.5 the simplex S_Γ is signified by its vertices a , b , and c . The necessary elements of Γ_1 can be found by

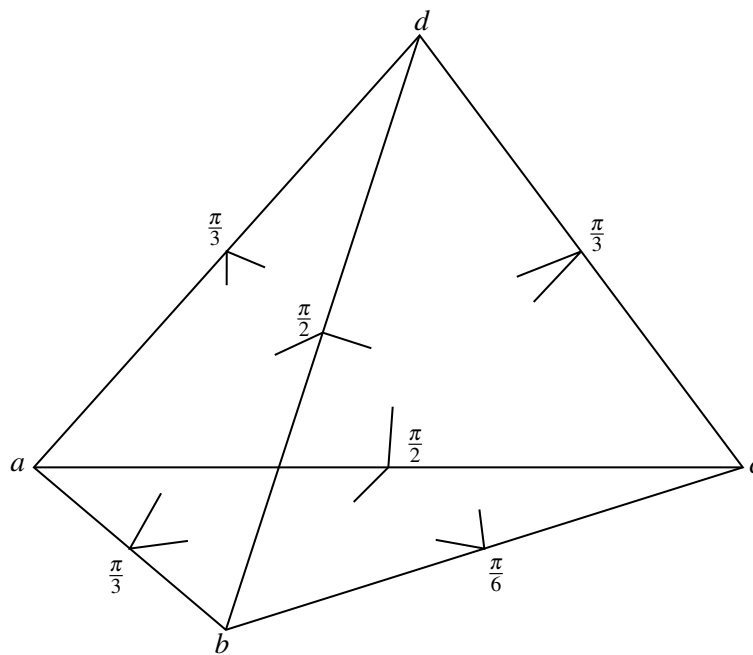


Figure IV.3.: Simplex Fundamental Region of Γ

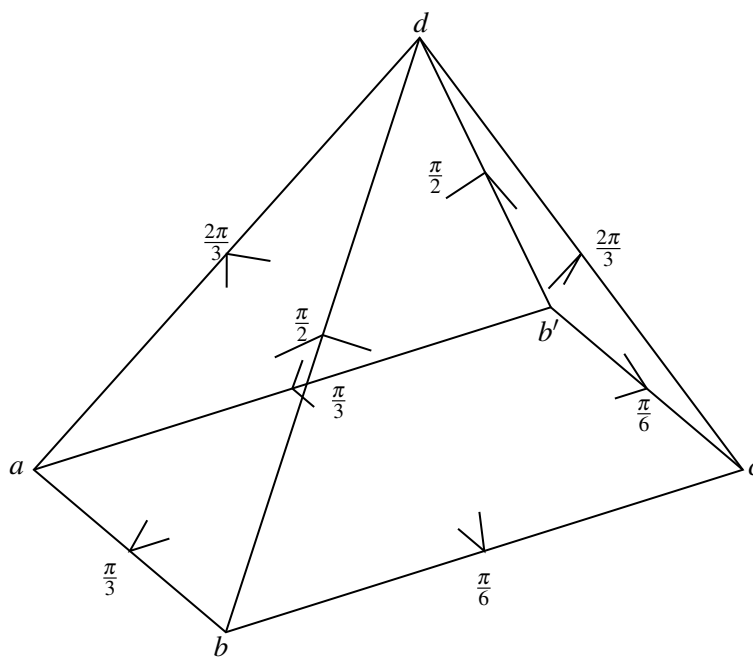


Figure IV.4.: Pyramid Obtained by Doubling the Simplex

side identification	element in Γ_1	orientation preserving
A	abd	no
B	$bacdca$	yes
C	$abadbcb$	no
D	$cdabcb$	yes
E	$abcdabc$	no
F	$abacdabcaba$	no

Table IV.2.: Side Identifications for Γ_1

looking for loops in the graph in Figure IV.2 containing exactly one edge with label d starting at the grey vertex. The side identifications can be seen in Figure IV.5. Their corresponding elements in Γ_1 are described in Table IV.2. The faces B and D are identified by orientation preserving isometries while all other side identifications are induced by orientation reversing isometries. With the side identifications one can check that there are two equivalence classes of ideal vertices modulo Γ_1 . The six images of the ideal vertex b form one class and the four images of the vertex c form the other. Hence, the manifold \mathbf{H}^3/Γ_1 has two cusps.

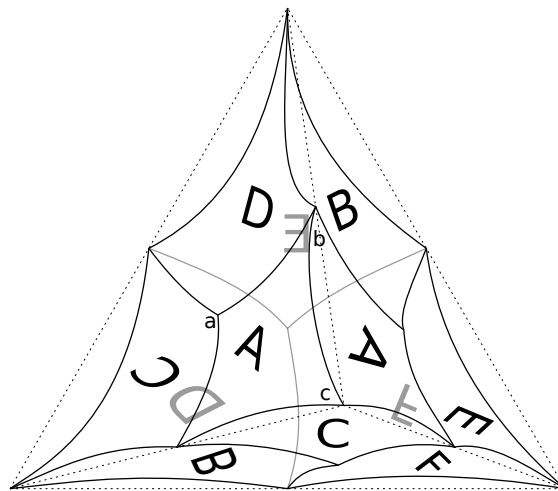


Figure IV.5.: Side Identifications for a Fundamental Domain of Γ_1

The other three manifolds \mathbf{H}^3/Γ_i , $2 \leq i \leq 4$, are given by the group actions depicted in Figure IV.6. By determining the side identifications in the same manner as before for Γ_1 , one can see that Γ_2 yields a manifold with two cusps, Γ_3 yields one with three cusps, and Γ_4 yields a manifold with four cusps.

To the best of the author's knowledge, the four isometry classes of non-compact, non-arithmetic 3-manifolds described above are the smallest known in \mathbf{H}^3 arising as cover manifolds of Coxeter orbifolds. It remains to find a proof that they are indeed the smallest of their kind or to find a smaller one.

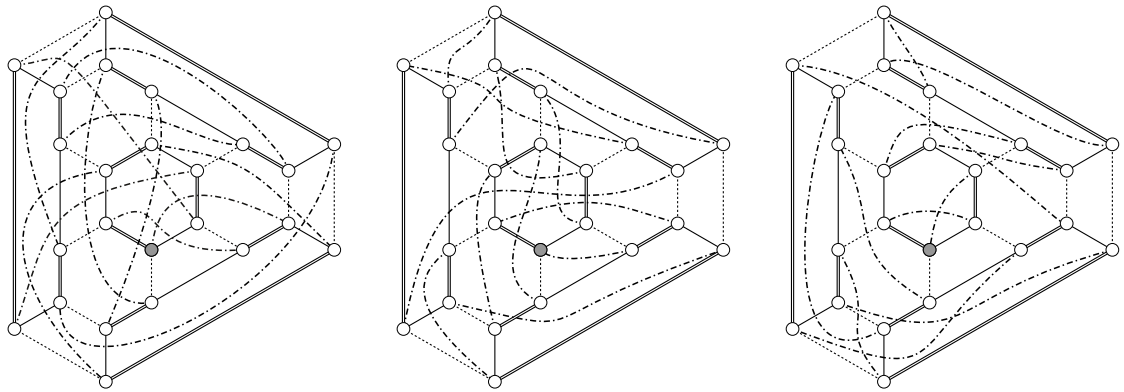


Figure IV.6.: Graphs for Γ_2 , Γ_3 , and Γ_4

References

- [Ago10] Ian Agol. ‘The minimal volume orientable hyperbolic 2-cusped 3-manifolds’. *Proc. Amer. Math. Soc.* 138.10 (2010), pp. 3723–3732. ISSN: 0002-9939. DOI: 10.1090/S0002-9939-10-10364-5.
- [BCP97] W. Bosma, J. Cannon and C. Playoust. ‘The Magma algebra system. I. The user language’. *J. Symbolic Comput.* 24.3-4 (1997). Computational algebra and number theory (London, 1993), pp. 235–265. DOI: 10.1006/jscs.1996.0125.
- [BH93] B. Brink and R. Howlett. ‘A finiteness property and an automatic structure for Coxeter groups’. *Math. Ann.* 296.1 (1993), pp. 179–190. DOI: 10.1007/BF01445101.
- [Bos09] S. Bosch. *Algebra*. Springer-Lehrbuch. Springer Berlin Heidelberg, 2009. DOI: 10.1007/978-3-540-92812-6.
- [Bou02] N. Bourbaki. *Lie groups and Lie algebras. Chapters 4–6*. Elements of Mathematics (Berlin). Translated from the 1968 French original by Andrew Pressley. Springer-Verlag, Berlin, 2002, pp. xii+300. DOI: 10.1007/978-3-540-89394-3.
- [Car72] R. Carter. ‘Conjugacy classes in the Weyl group’. *Compositio Math.* 25 (1972), pp. 1–59.
- [CM01] Chun Cao and G. Robert Meyerhoff. ‘The orientable cusped hyperbolic 3-manifolds of minimum volume’. *Invent. Math.* 146.3 (2001), pp. 451–478. ISSN: 0020-9910. DOI: 10.1007/s002220100167.
- [EH09] B. Everitt and R. Howlett. ‘Weyl groups, lattices and geometric manifolds’. *Geom. Dedicata* 142 (2009), pp. 1–21. DOI: 10.1007/s10711-009-9354-5.
- [Eve04] B. Everitt. ‘Coxeter groups and hyperbolic manifolds’. *Math. Ann.* 330.1 (2004), pp. 127–150. DOI: 10.1007/s00208-004-0543-0.

- [GMM09] David Gabai, Robert Meyerhoff and Peter Milley. ‘Minimum volume cusped hyperbolic three-manifolds’. *J. Amer. Math. Soc.* 22.4 (2009), pp. 1157–1215. ISSN: 0894-0347. DOI: 10.1090/S0894-0347-09-00639-0.
- [Smi16] Jonathan D. H. Smith. *Introduction to abstract algebra*. Second. Textbooks in Mathematics. CRC Press, Boca Raton, FL, 2016, pp. xii+340. ISBN: 978-1-4987-3161-4.

V. The Non-Compact Non-Arithmetic Hyperbolic 2-Orbifold of Minimal Area

1. Introduction

In the article [DK21], which is included as chapter III of this thesis, we proved that the hyperbolic 3-orbifold with fundamental group

$$\bullet \overset{5}{\text{---}} \bullet \text{---} \bullet \overset{6}{\text{---}} \bullet$$

yields the minimal volume orbifold among all non-compact non-arithmetic hyperbolic 3-orbifolds. In this chapter, we prove the analogue in \mathbf{H}^2 . A hyperbolic 2-orbifold is the quotient of \mathbf{H}^2 by a discrete subgroup $\Gamma < \text{Isom}\mathbf{H}^2$. By listing small cusped hyperbolic 2-orbifolds, we can reason that the smallest non-arithmetic cusped hyperbolic 2-orbifold has the fundamental group

$$\bullet \overset{5}{\text{---}} \bullet \overset{\infty}{\text{---}} \bullet$$

We use the results and notions as introduced in chapter III, but otherwise this chapter could be seen as a stepping stone for the result in three dimensions, because it helped us to finalise the arguments of chapter III.

The results about cross ratios and orthogonality of geodesics in chapter II were helpful for some calculations in this chapter. Specifically, they allow us to find orthogonal geodesics and to verify the orthogonality of geodesics which appear to be orthogonal in the horoball diagram.

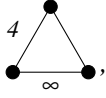
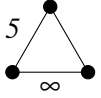
We consider the two-dimensional analogue of what we proved in three dimensions. Siegel [Sie45] found the smallest compact orbifold as the quotient of \mathbf{H}^2 by the Coxeter triangle group $\bullet \text{---} \overset{7}{\text{---}} \bullet$. Beardon [Bea95, §10.4.] used the signature of a Fuchsian group to prove that the smallest possible area of a hyperbolic polygon is $\frac{\pi}{42}$. It is straight-forward to use those results to prove that the minimal area $\frac{\pi}{6}$ of a non-compact hyperbolic 2-orbifold is related to the Coxeter group $\bullet \text{---} \overset{\infty}{\text{---}} \bullet$.

The following theorem provides not only an alternative proof of this fact, but it furthermore lists all possibilities for a small orbifold in \mathbf{H}^2 using elementary horoball geometry. This results in a detailed demonstration that $\bullet \overset{5}{\text{---}} \bullet \overset{\infty}{\text{---}} \bullet$ is the smallest non-arithmetic non-compact hyperbolic 2-orbifold. In this context, *small* means an area less than $\frac{\pi}{2}$. The methodology used in the proof improves the understanding of similar methods used in chapter III. Another possibility would be to use the signature of Fuchsian groups (compare [Bea95, §10.4.]).

Theorem 1. *Let \mathbf{H}^2/Γ be a non-compact hyperbolic 2-orbifold with $\text{area}(\mathbf{H}^2/\Gamma) < \frac{\pi}{2}$. Then Γ is*

(i) the reflection group of a right-angled triangle $\bullet \overset{n}{\text{---}} \bullet \overset{\infty}{\text{---}} \bullet$ with $n \geq 3$ and $\text{area}(\bullet \overset{n}{\text{---}} \bullet \overset{\infty}{\text{---}} \bullet) = \frac{\pi}{2} - \frac{\pi}{n}$,

(ii) a subgroup of index 2 of $\bullet \text{---} \bullet \overset{\infty}{\text{---}} \bullet$ with $\text{area}(\mathbf{H}^2/\Gamma) = \frac{\pi}{3}$, or

(iii) one of , or  with areas $\frac{5\pi}{12}$, or $\frac{7\pi}{15}$, respectively.

The orientable double cover of $\mathbf{H}^2/\bullet \text{---} \bullet \overset{\infty}{\text{---}} \bullet$ is the only orientable orbifold with area less than $\frac{\pi}{2}$.

Note that the area of the triangles $\bullet \overset{n}{\text{---}} \bullet \overset{\infty}{\text{---}} \bullet$ is ascending in n . This allows us to list small orbifolds in ascending order and to determine the smallest non-arithmetic 2-orbifold using Vinberg's criterion [VS93]. Any non-compact right-angled Coxeter triangle $\bullet \overset{n}{\text{---}} \bullet \overset{\infty}{\text{---}} \bullet$ with a weight $n \neq 2, 3, 4$, or 6 turns out to be non-arithmetic as well as the two Coxeter groups with triangular graphs in case (iii).

Corollary 2. *The smallest two-dimensional non-compact non-arithmetic hyperbolic orbifold is the quotient of \mathbf{H}^2 by the Coxeter group $\bullet \overset{5}{\text{---}} \bullet \overset{\infty}{\text{---}} \bullet$. It has area $\left(\mathbf{H}^2/\bullet \overset{5}{\text{---}} \bullet \overset{\infty}{\text{---}} \bullet\right) = \frac{3\pi}{10}$.*

The idea of the proof is based on horoball packings and their density. A cusp in an orbifold corresponds to a horoball packing in \mathbf{H}^2 by the action of its fundamental group on a horoball covering the cusp. Different horoball packings lead to different cusp sizes which allow us to estimate the area of the orbifold by virtue of the proposition below. The proof then consists of a case distinction on the number of cusps and on the number of equivalence classes of full-sized horoballs modulo the stabiliser subgroup associated to a cusp. Remember that in the upper half plane \mathbf{H}^2 the area of the cusp is equal to its euclidean width.

Proposition 3 ([Kel98, Lemma 3.2]). *If an orientable orbifold \mathbf{H}^2/Γ has n disjoint cusps C_1, \dots, C_n , with boundary widths d_1, \dots, d_n , then its area can be bounded from below by the quotient*

$$\text{area}(\mathbf{H}^2/\Gamma) \geq \frac{\sum_{i=1}^n \text{area}(C_i)}{d_2(\infty)} = \frac{\sum_i d_i}{d_2(\infty)} = \frac{\pi}{3} \sum_i d_i,$$

where $d_2(\infty) = \frac{3}{\pi}$ denotes the simplicial horoball density.

2. One cusp

For the proof of Theorem 1 let Γ be a discrete subgroup of $\text{Isom } \mathbf{H}^2$ whose quotient has at least one cusp. We can assume that one cusp is at ∞ , meaning $\Gamma_\infty \neq \{1\}$. To simplify the proof, we will mostly assume Γ to be orientation preserving. Then Γ_∞ has to be a group of translations isomorphic to \mathbb{Z} . Otherwise, Γ_∞ could also be a reflection group isomorphic to $\bullet \overset{\infty}{\text{---}} \bullet$. Every

orientable orbifold we construct will be the double cover of a non-orientable one. Mostly, it is easier to only consider orientation preserving isometries, but once the cusp area is close to 3, there are benefits to considering reflections.

We have to find the orientable orbifolds up to area π . Then we construct the non-orientable orbifolds which they are the double cover of. To sustain the horoball diagram, take a (small) horoball centred in ∞ , denoted by H_∞ , and its images under Γ . In this context a *small horosphere at ∞* is a Euclidean line on a height $h \gg 1$ over the boundary \mathbb{R} . Increase the size of the horoball (i. e. decrease h) until it touches at least one of its images. In the usual situation, it then touches infinitely many of its images. If there are multiple cusps, repeat the process for the other cusps one at a time until each horoball touches itself or one of the previous cusps. In our situation, one can normalise such that H_∞ is at height 1. We call a sketch of the relative position of horoballs a *horoball diagram*. Since it is impractical to draw all infinitely many horoballs, we usually draw just as many as necessary to sufficiently understand the geometry. By construction, there are horoballs of diameter 1 which touch the horoball H_∞ . Call these horoballs *full-sized horoballs*. This implies that the shortest possible translation length d (and hence the smallest possible cusp area in the oriented case) is ≥ 1 .

For the beginning we will assume that there is only one cusp. The case of two or more cusps can be easily excluded, but we will do this at the end of this chapter because a basic understanding of horoball geometry is helpful.

The smallest cusp area arises when there is one class of full-sized horoballs modulo Γ_∞ (see section 2.2). If neighbouring full-sized horoballs touch each other, we get the situation of Figure V.1. The Ford domain gives the triangular fundamental domain of the modular group $\mathrm{PSL}_2(\mathbb{Z})$ which is an index 2 subgroup of $\bullet \text{---} \bullet \overset{\infty}{\text{---}} \bullet$. In order to properly interpret this horoball diagram, we need [Ada92, Lemma 2.1]:

Lemma 4. *If all full-sized horoballs in the horoball diagram of an orientable cusped 2-orbifold are equivalent modulo Γ_∞ , then for any full-sized horoball H_p there is an order 2 rotation around the touching point of H_p and the horoball H_∞ at ∞ .*

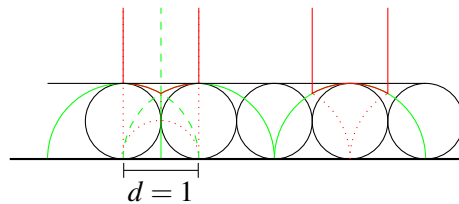


Figure V.1.: Touching Full-Sized Horoballs in Upper Half Plane

With Lemma 4, we can now analyse Figure V.1. The translation t with length 1 and a rotation r from this lemma are the well-known generators of the modular group $\mathrm{PSL}_2(\mathbb{Z})$. The classical fundamental domain is sketched on the right-hand side of the figure. If we allow for non-orientable orbifolds, the modular space $\mathbf{H}^2 / \mathrm{PSL}_2(\mathbb{Z})$ is the orientable double cover of the quotient $\mathbf{H}^2 / \bullet \text{---} \bullet \overset{\infty}{\text{---}} \bullet$.

There is also another (ultimately equivalent) way to interpret the diagram. The concatenation of the rotation r and the translation t is a rotation of order 3 as hinted at on the left-hand side of Figure V.1. Thus we can interpret $\mathrm{PSL}_2(\mathbb{Z})$ as the semi-direct product of a group yielding a tessellation of \mathbf{H}^2 with ideal triangles and the symmetry group of the ideal triangle. This helps in the more general case below. Recall the classification of hyperbolic isometries as it can be found in [Bea95] or [Rat06]. A hyperbolic isometry ρ is

- *elliptic*, if ρ has a fixed point in \mathbf{H}^2 ,
- *parabolic*, if ρ is not elliptic and has a unique fixed point in $\partial\mathbf{H}^2$, and
- *loxodromic*, if ρ is not elliptic and has two fixed points in $\partial\mathbf{H}^2$.

Lemma 5. *Under the same conditions as in Lemma 4 there is an isometry ρ whose nature depends on the shortest translation length d in Γ_∞ .*

- For $1 \leq d < 2$, ρ is an elliptic element,
- for $d = 2$, ρ is parabolic, and
- for $d > 2$, ρ is loxodromic.

Proof. Consider the horoball diagram where there are two full-sized horoballs at distance d centred at $\pm\frac{d}{2}$ as in Figure V.2. The representations of r and t in $\mathrm{PSL}_2(\mathbb{R})$ can be calculated as

$$r = \begin{pmatrix} -\frac{d}{2} & -\left(1 + \frac{d^2}{4}\right) \\ 1 & \frac{d}{2} \end{pmatrix}, \quad t = \begin{pmatrix} 1 & d \\ 0 & 1 \end{pmatrix}.$$

Then we define ρ as the concatenation

$$\rho := t \circ r = \begin{pmatrix} \frac{d}{2} & \frac{d^2}{4} - 1 \\ 1 & \frac{d}{2} \end{pmatrix}.$$

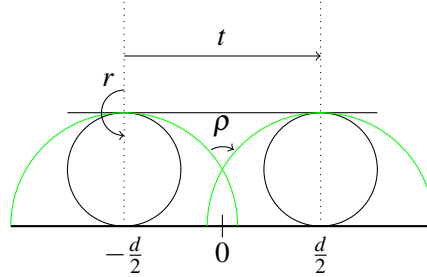


Figure V.2.: Basic Isometries in the Horoball Diagram

The nature of the isometry ρ can be read from the trace of the matrix (see for example [Bea95, Theorem 4.3.4]). For $1 \leq d < 2$ the fixed point in $\mathbf{H}^2 \subset \mathbb{C}_+$ of the elliptic isometry ρ is $i\sqrt{1 - \frac{d^2}{4}}$. The parabolic isometry ρ with $d = 2$ has ideal fixed point 0, and the loxodromic isometry ρ with $d > 2$ has the fixed points $\pm\sqrt{\frac{d^2}{4} - 1}$. \square

2.1. One Equivalence Class of Full-Sized Horoballs

If the full-sized horoballs do not touch each other, there is another class of smaller horoballs. Denote the shortest distance between two full-sized horoballs (in this case also the shortest translation length in Γ_∞) by d . We will determine all possible values for d with $d < 2$ which is essentially a different proof for [Bea75, Theorem 3]. Take a full-sized horoball H_p and the order 2 rotation r around the touching point between H_p and H_∞ according to Lemma 4. Then r maps a neighbouring full-sized horoball H_q with distance d to H_p to a horoball touching $H_p = r(H_\infty)$. The new horoball has distance $\frac{1}{d}$ from H_p and diameter $\frac{1}{d^2}$. In the same manner as in chapter III and [Ada92], we consider $\frac{1}{d}$ -balls. Compare Figure V.3. There are three cases about the relative

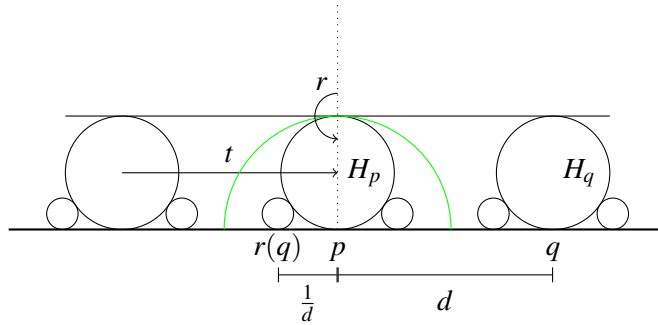


Figure V.3.: $\frac{1}{d}$ -Balls Touching Full-Sized Horoballs

position of the $\frac{1}{d}$ -balls:

- (i) Each $\frac{1}{d}$ -ball touches *two* full-sized horoball,
- (ii) each $\frac{1}{d}$ -ball touches *one* full-sized horoball and one $\frac{1}{d}$ -ball,
- (iii) each $\frac{1}{d}$ -ball touches *one* full-sized horoball and no $\frac{1}{d}$ -ball.

The first case implies $\frac{d}{2} = \frac{1}{d}$ or $d = \sqrt{2}$.

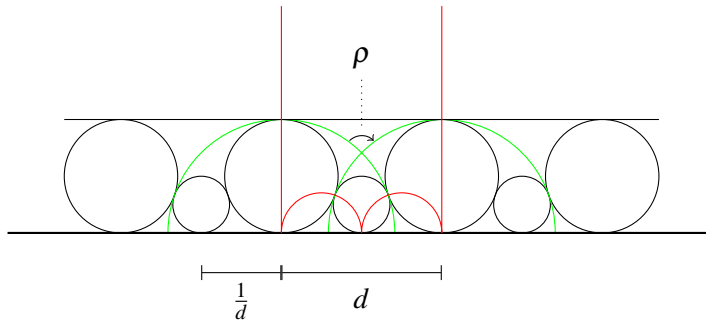


Figure V.4.: One $\frac{1}{d}$ -Ball Touches Two Full-Sized Balls

For the second case, where two $\frac{1}{d}$ -balls touch each other, it is convenient to first consider the action of r on each horoball. The horoball H_p gets exchanged with H_∞ , and its neighbouring

full-sized balls H_q and H_s are mapped onto $\frac{1}{d}$ -balls touching H_p . The two $\frac{1}{d}$ -balls H_x and H_y in-between, which touch H_s and H_q respectively, have to be sent to each other by r . Compare Figure V.5. Due to the symmetry of the situation this implies that the distance between H_p and H_y has to be 1. Hence d has to obey $d = 1 + \frac{1}{d}$ which implies that $d = \frac{1}{2} + \frac{1}{2}\sqrt{5}$ is the golden ratio.

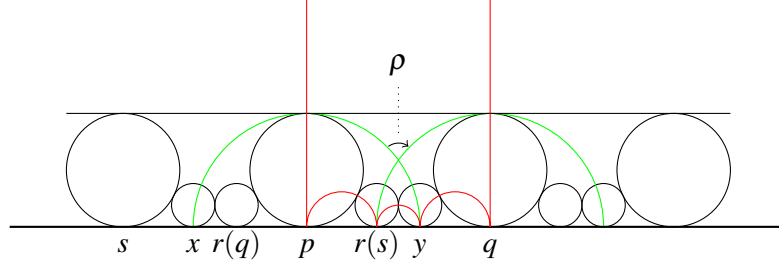


Figure V.5.: Two $\frac{1}{d}$ -Balls Touching Each Other

In the third case, the $\frac{1}{d}$ -ball touching H_q is mapped to a horoball touching the other $\frac{1}{d}$ -ball (see Figure V.6). With the same argument as before, this new $\frac{1}{w}$ -ball has to be in distance $\frac{1}{w}$ of H_p where $w = d - \frac{1}{d}$ is the distance from H_p to the next $\frac{1}{d}$ -ball *not* touching H_p . This $\frac{1}{d}$ -ball is the (pre-) image of the $\frac{1}{w}$ -ball under the map r . (The notation is again following [Ada92].)

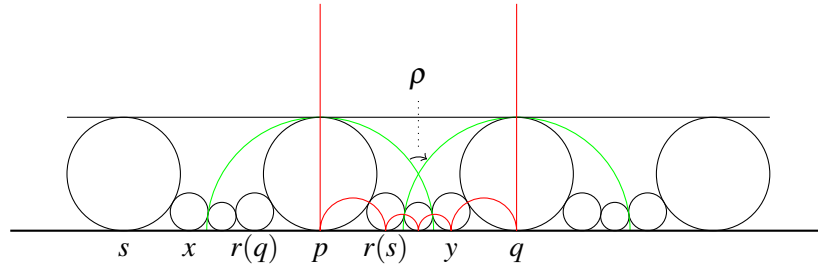


Figure V.6.: One $\frac{1}{d}$ -Ball Touching Neither Full-Sized nor Another $\frac{1}{d}$ -Ball

With this $\frac{1}{w}$ -ball, there are again the three cases from above, where $\frac{1}{d}$ -balls are exchanged with $\frac{1}{w}$ -balls and full-sized balls are exchanged with $\frac{1}{d}$ -balls. This argument is then repeated. Denote $d_1 := d$, $d_2 := d - \frac{1}{d_1}$ and replace $\frac{1}{d}$ -balls with $\frac{1}{d_1}$ -balls and $\frac{1}{w}$ -balls with $\frac{1}{d_2}$ -balls. Then

$$d_k := d - \frac{1}{d_{k-1}} \tag{2.1}$$

leads to the general case distinction:

- (i) The $\frac{1}{d_k}$ -balls touch *two* $\frac{1}{d_{k-1}}$ -balls,
- (ii) the $\frac{1}{d_k}$ -balls touch *one* $\frac{1}{d_{k-1}}$ -balls, and one other $\frac{1}{d_k}$ -ball,
- (iii) the $\frac{1}{d_k}$ -balls touch *one* $\frac{1}{d_{k-1}}$ -ball and no $\frac{1}{d_k}$ -ball.

The same arguments as above lead to the equalities

$$\frac{d}{2} = \frac{1}{d_k} \text{ in the first case, and} \quad (2.2)$$

$$d = 1 + \frac{1}{d_k} \text{ in the second case.} \quad (2.3)$$

The equation (2.1) leads to the representation

$$d_k = \frac{p_k(d)}{p_{k-1}(d)}, \quad (2.4)$$

where the polynomials p_k are given by

$$p_0(d) = 1, \quad p_1(d) = d, \quad p_{k+1}(d) = d p_k(d) - p_{k-1}(d). \quad (2.5)$$

The following explicit calculation of p_k can be proven by induction:

$$p_k(d) = \sum_{i=0}^k (-1)^i \binom{k-i}{i} d^{k-2i}.$$

Note that the recursion (2.5) looks very similar to the Chebyshev polynomials. The Chebyshev polynomials of the first kind are given by

$$T_0(x) = 1, \quad T_1(x) = x, \quad T_{k+1}(x) = 2x T_k(x) - T_{k-1}(x).$$

The set of zeros of the k -th Chebyshev polynomial T_k is $\left\{ \cos\left(\frac{(2i-1)\pi}{2k}\right) \mid i = 1, \dots, k \right\}$. The Chebyshev polynomials of the second kind are given by

$$U_0(x) = 1, \quad U_1(x) = 2x, \quad U_{k+1}(x) = 2x T_k(x) - T_{k-1}(x).$$

The set of zeros of the k -th Chebyshev polynomial U_k is $\left\{ \cos\left(\frac{i\pi}{k+1}\right) \mid i = 1, \dots, k \right\}$.

In the first case, where two $\frac{1}{d_k}$ -balls coincide or one $\frac{1}{d_k}$ -ball touches two $\frac{1}{d_{k-1}}$ -balls, the equations (2.2) and (2.4) yield

$$0 = d p_k(d) - 2 p_{k-1}(d) = p_{k+1}(d) - p_{k-1}(d).$$

One can see that $p_{k+1}(d) - p_{k-1}(d) = 2 T_{k+1}\left(\frac{d}{2}\right)$, where T_{k+1} is the Chebyshev polynomial of degree $2k+1$. Using the facts that $d > 1$ and $d_{k+1} > d_k$ this implies that

$$d_k = 2 \cos\left(\frac{\pi}{2k+2}\right). \quad (2.6)$$

In the second case, where two $\frac{1}{d_k}$ -balls touch, the equations (2.3) and 2.4 yield

$$0 = d p_k(d) - p_k(d) - p_{k-1}(d) = p_{k+1}(d) - p_k(d).$$

In order to analyse the zeros of $q_k := p_{k+1} - p_k$, it is not difficult to prove the following by a simultaneous induction:

Proposition 6.

$$q_k(x) \cdot q_k(-x) = (-1)^{k+1} U_{2k+2} \left(\frac{x}{2} \right) \quad (2.7)$$

$$q_k(x) \cdot q_{k-1}(-x) - q_k(-x) \cdot q_{k-1}(x) = (-1)^k 2 U_{2k+1} \left(\frac{x}{2} \right) \quad (2.8)$$

The zeros of $q_k(x) \cdot q_k(-x)$ are hence $2 \cos \left(\frac{i\pi}{2k+3} \right)$ with $i = 1, \dots, 2k+2$. By noting that

$$-\cos \left(\frac{(2i+3)\pi}{2k+3} \right) = \cos \left(\pi - \frac{(2i+3)\pi}{2k+3} \right) = \cos \left(\frac{2(k-i)\pi}{2k+3} \right),$$

one can see that the k zeros of q_k are $2 \cos \left(\frac{i\pi}{2k+3} \right)$ with $1 \leq i \leq 2k+2$ either even or odd. Again we can argue using $d_{k+1} > d_k$. This implies that

$$d_k = 2 \cos \left(\frac{\pi}{2k+3} \right). \quad (2.9)$$

Either way, the group Γ pertaining to the horoball diagram is a semi-direct product of a group yielding a tessellation of the hyperbolic plane by regular ideal n -gons with the orientable symmetry group of such an ideal n -gon where $n = 2k+2$ or $n = 2k+3$ depending on the case. Essential to this point of view are the translation t and the rotation ρ from Lemma 5. The generators of the tessellation group can (for example) be chosen as the rotations in each side of the n -gon:

$$\left\{ \rho^{-(l+1)} t \rho^l \mid l = 0, \dots, n-1 \right\}.$$

The symmetries of the n -gon are the rotations generated by ρ . Compare the sketches in Figure V.7 and the previous ones. The orbifolds can be interpreted as the orientable double covers of the quotients of \mathbf{H}^2 by $\bullet \xrightarrow{n} \bullet \xrightarrow{\infty} \bullet$ with area $\frac{(n-2)\pi}{n}$.

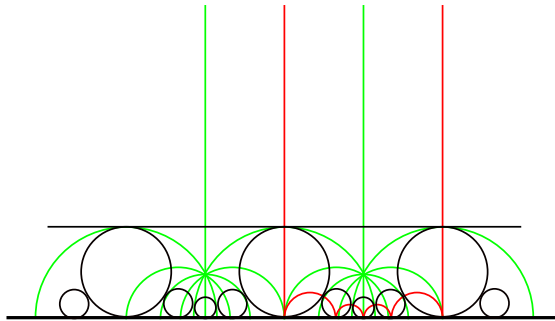
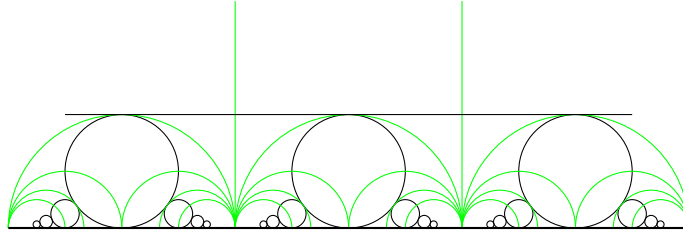


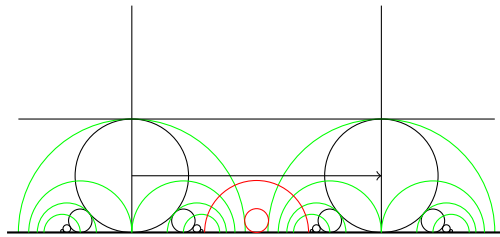
Figure V.7.: Ideal n -gon in the Horoball Diagram (here $n = 6$)

In the case where n tends to ∞ or equivalently d converges to 2, there emerges a second cusp. See Figure V.8 for a sketch. The resulting orbifold is based on an ideal triangle where two sides are identified by the translation t and the third side gets identified with itself by the rotation r by Lemma 4. It is the orientable double cover of $\mathbf{H}^2 / \bullet \xrightarrow{\infty} \bullet \xrightarrow{\infty} \bullet$. The Coxeter triangle $\bullet \xrightarrow{\infty} \bullet \xrightarrow{\infty} \bullet$ has area $\frac{\pi}{2}$ and yields as such the smallest possible 2-dimensional hyperbolic orbifold with more than one cusp (confer Lemma 9 further down).

Figure V.8.: Second Cusp for $d = 2$ **Distance $d > 2$ and $d \leq 2\sqrt{2}$**

Usually we considered the Ford-Dirichlet cell bounded by the bisectors of the horoballs in the diagram as a fundamental polygon for Γ . If the distance d between two neighbouring full-sized horoballs is bigger than 2, then this polygon will not have finite area.

The isometry ρ of Lemma 5 is loxodromic with fixed points $\pm\sqrt{\frac{d^2}{4} - 1}$. By using the orthogonality results of [DD19], it can be immediately seen that the axis of ρ is orthogonal to the bisecting geodesics of two neighbouring full-sized horoballs. See Figure V.9 where the small red horosphere signifies the image of H_∞ under the reflection in the invariant axis of ρ (also marked in red). Please do note that this horoball does not necessarily appear in the horoball diagram, but we can prove that this would lead to the minimal possible area.

Figure V.9.: $d > 2$

Apply an isometry to the objects in Figure V.9 that sends $-\sqrt{\frac{d^2}{4} - 1}$ to 0 and $\sqrt{\frac{d^2}{4} - 1}$ to ∞ . The result is illustrated in Figure V.10, where the horoballs on the left are the horoballs whose existence we previously established in Figure V.9. The red line is the loxodromic axis of ρ and on the right the dotted balls are potential horoballs below the loxodromic axis of ρ in Figure V.9. As said before, they could be different to what you see in the figure but the balls could not be bigger. In fact, the loxodromic isometry ρ acts as a multiplication which sends each ball on the left to its neighbour. By construction, the stretching factor equals

$$\frac{d^2}{2} - 1 + d\sqrt{\frac{d^2}{4} - 1}.$$

If the balls on the right of Figure V.10 were bigger than drawn, then their images would not line up with the balls themselves. They could potentially be smaller. Then on the right the isometry would not send the horoballs to their direct neighbours but to horoballs further away.

This implies that the loxodromic axis of ρ is included in the polygon (if not on the inside then on the boundary).

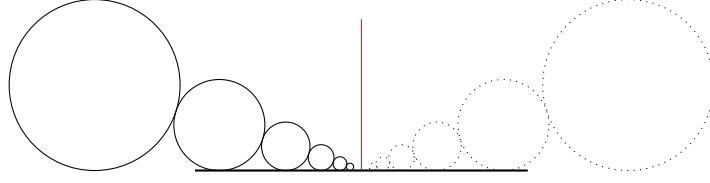


Figure V.10.: Horoballs along the Loxodromic Axis

Having established that the addition of the common perpendicular of two neighbouring bisectors yields the minimal possible area, we see that for $d > 2$ the minimal area is achieved by a pentagon P with one ideal vertex and four right angles. This has

$$\text{area}(P) = 3\pi - 4\frac{\pi}{2} = \pi.$$

The addition of the loxodromic axis works as long as the radius of the semicircle is less than one:

$$\sqrt{\frac{d^2}{4} - 1} \leq 1 \Rightarrow d \leq 2\sqrt{2}.$$

If the radius was bigger than 1, it would intersect with the horosphere H_∞ .

Distance $d > 2\sqrt{2}$

With the density argument of Proposition 3, we need to consider only distances $d \leq 3$, so it is necessary to treat the possibility $2\sqrt{2} < d \leq 3$. The same idea we used in chapter III for large cusp volumes of a $\{2, 3, 6\}$ -cusp does help here. Assume that Γ is a group such that Γ_∞ had translation distance $d > 2\sqrt{2}$ between full-sized horoballs. If Γ_∞ is a translation group, then

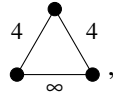
$$\text{area}(\mathbf{H}^2/\Gamma) \geq \frac{d}{d_2(\infty)} = d\frac{\pi}{3} \geq \frac{2\sqrt{2}}{3}\pi > \frac{\pi}{2}$$

independently of Γ being orientation preserving or not. Since we are only interested in orbifolds with area $< \frac{\pi}{2}$ after all, we can directly assume that Γ_∞ contains reflections, and then prove that the coarea of Γ is bigger than $\frac{\pi}{2}$. This is easier than considering orientable orbifolds and then prove that their area is bigger than π because reflection axes can only intersect horoballs orthogonally or not at all.

If Γ_∞ contains reflections, they have to be across vertical lines cutting the full-sized horoballs in half and across vertical lines in the middle between two neighbouring full-sized horoballs. See Figure V.11. With the same argument as in Lemma 4 there has to be a rotation or a reflection r that maps a full-sized horoball H_p to H_∞ and vice versa. If r was a rotation, then we could concatenate it with a reflection in Γ_∞ through the geodesic (p, ∞) and hence assume that r is a reflection in the bisector of H_p and H_∞ .

Assume there is a horoball based in $q \in \partial\mathbf{H}^2$, where q is the midpoint between the centres of H_p and a neighbouring full-sized horoball. The full-sized horoball H_q can at most have diameter

1. Then it is a representative of a second equivalence class of full-sized horoballs, which will be treated later in section 2.2. The angle α of the bisectors with H_∞ belonging to the horoballs H_p and H_q is in this case $\frac{\pi}{2}$ yielding a subgroup of



with coarea $\frac{\pi}{2}$. If the diameter of H_q shrinks or the distance d increases, the angle α decreases and the area gets bigger. Hence, with $d \geq 2\sqrt{2}$ and horoballs in the centres between the full-sized horoballs, the minimal possible area is $\frac{\pi}{2}$.

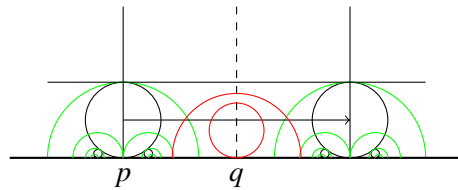


Figure V.11.: $d > 2\sqrt{2}$ with Horoball on Midpoint

If there is no horoball centred in the midpoint of two neighbouring full-sized horoballs, the biggest possible horoballs touch the vertical reflection geodesic and the reflecting bisector of H_∞ with a full-sized horoball (see Figure V.12). The bisectors of H_p with H_∞ and H_q with H_∞ intersect perpendicularly. The intersection of the bisector of H_q and H_∞ with the vertical reflection geodesic is an acute angle. So in this case, the coarea of Γ can be bounded by

$$\text{area}(\mathbf{H}^2/\Gamma) > 2\pi - 3\frac{\pi}{2} = \frac{\pi}{2}$$

and it is too big for our interest.

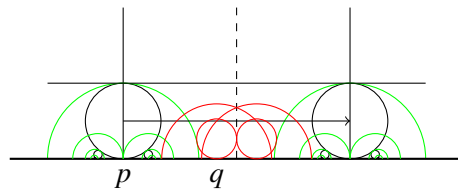


Figure V.12.: $d > 2\sqrt{2}$ with Horoball not on Midpoint

2.2. Two Equivalence Classes of Full-Sized Horoballs

From now on we will go back to regarding orientation preserving isometries, and we assume that there are two equivalence classes of full-sized horoballs with regard to the action of Γ_∞ . In Lemma 4 a central hypothesis was that there is only a single equivalence class of full-sized horoballs. We start by analysing the situation if representatives of the two equivalence classes of

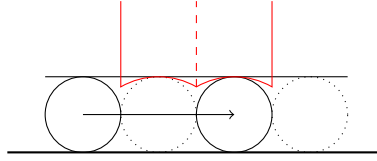


Figure V.13.: Two Equivalence Classes of Full-Sized Horoballs with $d_1 = d_2 = 1$

full-sized horoballs touch, as depicted in Figure V.13. Similarly to Lemma 4 there could be a rotation r of order 2 in Γ which swaps a full-sized horoball with H_∞ . If there is such a rotation for every full-sized horoball, then Γ identifies sides of the red quadrilateral in Figure V.13 by identifying the left vertical side with the right vertical side and each of the other two sides with itself. As such, we find the fundamental quadrilateral with

$$\text{area}(\mathbf{H}^2/\Gamma) = 2\pi - 4\frac{\pi}{3} = \frac{2\pi}{3},$$

and Γ has to be a subgroup of index 4 in $\bullet \text{---} \bullet \overset{\infty}{\text{---}} \bullet$. This yields case (ii) of Theorem 1.

In the case where we do not have the rotations of order 2 as in Lemma 4, we will conclude that there must be a rotation of three pairwise touching horoballs instead. Call the equivalence classes A and B . There is an isometry sending a horoball of class A to H_∞ . This isometry cannot send H_∞ to a ball of class A because we assumed that there is no such symmetry (compare the proof of Lemma 4). So it has to map H_∞ to a horoball of class B . After applying an appropriate translation in Γ_∞ we can assume that those three horoballs touch pairwise. The horoball of class B has to get mapped to the horoball of class A , because of the pairwise touching points. By assuming orientability, this isometry is a rotation of order three. Considering the finite index subgroup of Γ generated by this rotation and a translation of length 3, we see again that the group Γ is a subgroup of $\bullet \text{---} \bullet \overset{\infty}{\text{---}} \bullet$ yielding the same case (ii) of Theorem 1.

Now to the case where the full-sized horoballs do not all touch. If horoballs of the two equivalence classes touch on one side of a full-sized ball and not on the other, the situation represents itself as in Figures V.14 and V.15. We define distances d_1 and d_2 as in Figure V.14. In this case $d_1 = 1$ and $d_2 > 1$. As long as $d_2 < 2$, there cannot be a rotation as in Lemma 4 because of the asymmetry of the situation. It would mean that the images of the full-sized horoballs overlap. For $d_2 \geq 2$ the cusp area is $d_1 + d_2 \geq 3$ meaning the orbifold has area $\geq \pi$.

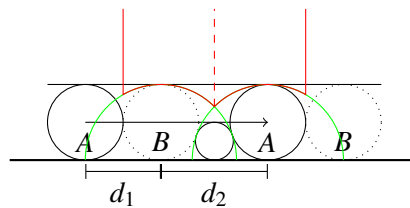


Figure V.14.: Two Equivalence Classes of Full-Sized Horoballs with $d_1 = 1, d_2 = \sqrt{2}$

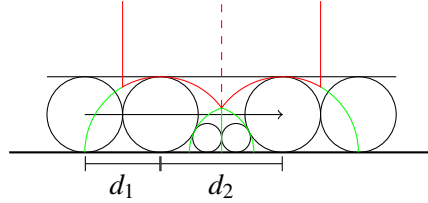


Figure V.15.: Two Equivalence Classes of Full-Sized Horoballs with $d_1 = 1, d_2 = \frac{1}{2}(1 + \sqrt{5})$

Due to the asymmetry of the diagram, there cannot be a rotation around a point of tangency between two horoballs as in Lemma 4 because otherwise the image of the $\frac{1}{d}$ -ball would intersect with a full-sized horoball. There will be a rotation ρ similar to Lemma 5 involving two full-sized horoballs, H_∞ , and potentially some $\frac{1}{d}$ -balls.

Lemma 7. *If there are two equivalence classes of full-sized horoballs in the translation group Γ_∞ with asymmetric distances $d_1 \neq d_2$, then there are rotations ρ_1 , and $\rho_2 \in \Gamma$ such that*

$$d_i = 2 \cos\left(\frac{\pi}{\text{ord } \rho_i}\right), i = 1, 2.$$

Proof. The basic ideas of Lemma 4 can be adapted for this asymmetric situation. Since we assume that the orbifold is orientable, Γ_∞ is a translation group. Consider the full-sized horoballs H_p and H_q with distance d_1 as in Figure V.16. There is a symmetry ρ which send H_p to H_∞ . This symmetry ρ has to map H_∞ to a full-sized horoball which is equivalent to H_q modulo Γ_∞ because otherwise there would be an order 2 rotation swapping H_∞ and H_p . We excluded the latter due to the asymmetry of the diagram. Assume that ρ maps H_∞ to H_q (this we can do without loss of generality after applying a translation in Γ_∞). This means that H_q gets mapped to a horoball of diameter $\frac{1}{d_1}^2$ to the right of H_q . If the isometry ρ has finite order, the same considerations as in Section 2.1 apply and H_p , and H_q have to be part of a regular ideal polygon with $\text{ord } \rho$ vertices. The distance d_1 has to satisfy $d_1 = 2 \cos\left(\frac{\pi}{\text{ord } \rho_1}\right)$ because in the diagram the sizes of the horoballs are given by equations (2.6), (2.9) from Section 2.1. With the same considerations, $d_1 \geq 2$ if ρ has infinite order.

The analogue argument proves the existence of a rotation where d_1 and d_2 are exchanged.

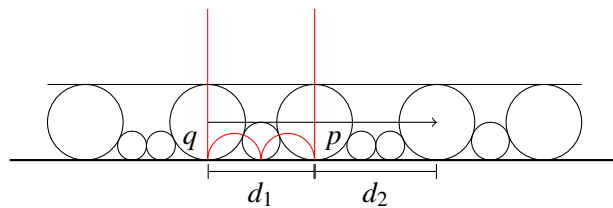
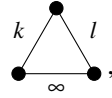


Figure V.16.: Rotation between full-sized horoball and H_∞ in asymmetric diagram

□

If we now are in the situation with two equivalence classes of full-sized horoballs, then in the asymmetric case Lemma 7 applies, and in the symmetric case one of the Lemmas 7 or 4 applies. In either case we can deduce that the group Γ is a subgroup of order 2 of



with $k, l \geq 3$ (possibly $= \infty$). It is easy to see that these have coarea smaller than $\frac{\pi}{2}$ if and only if $k = 3$ and $l \in \{3, 4, 5\}$ (or vice versa). As long as $d_1, d_2 \leq 2$, the horoball diagram leads to an index 2 subgroup of such a triangular reflection group. If $d_1 > 2$ or $d_2 > 2$, then $d = d_1 + d_2 > 3$ and with Proposition 3, the area of \mathbf{H}^2/Γ gets bigger than π .

2.3. At Least Three Equivalence Classes of Full-Sized Horoballs

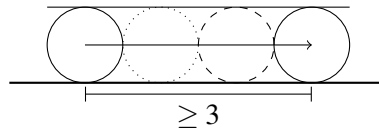


Figure V.17.: Minimal Area with Three Equivalence Classes of Full-Sized Horoballs

If there are at least 3 equivalence classes of full-sized horoballs, then the minimal translation length $d \geq 3$ and also the minimal cusp area is at least 3. With Proposition 3 we can find a lower bound for the orbifold area as:

$$\text{area}(\mathbf{H}^2/\Gamma) \geq \frac{d}{d_2(\infty)} = d \frac{\pi}{3} \geq \pi.$$

Hence, this case is not of concern for us.

3. Two or More Cusps

In order to eliminate the case where the orbifold \mathbf{H}^2/Γ has two or more cusps when considering small area, recall the concept of a *disc of no tangency* as discussed by Adams in [Ada88] and already used in chapter III.

Definition 8. A disc of no tangency in a horoball diagram is

- a disc with radius 1 on the horosphere at ∞ where no equivalent full-sized horoballs touch H_∞ , or equivalently,
- the upper hemisphere of a non-full-sized horoball ($\neq H_\infty$) which does not touch any bigger equivalent horoball.

Here, the equivalence is meant modulo Γ . We only consider horoballs of a single cusp. If the orbifold \mathbf{H}^2/Γ contains more cusps than one, horoballs of other cusps are ignored.

The first interpretation is helpful to get a lower bound on the cusp area after one has argued about the existence of a disc of no tangency in the horoball diagram using the second definition. The equivalence can be seen in Figure V.18. If there is a non-full-sized horoball H_p which does not touch any bigger horoball, one can consider the reflection in a geodesic which swaps H_p and the horosphere H_∞ on height 1. Then the disc of no tangency on H_p is mapped to a disc of radius 1 on H_∞ . Adams uses this concept in several papers like [Ada92; Ada88].

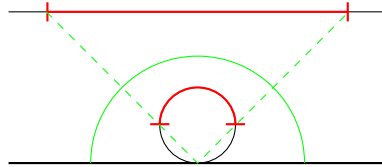


Figure V.18.: Disc of no Tangency

We prove an analogue statement to [Ada88, Lemma 4.1] which then shows that the area of an orbifold with two (or more) cusps is at least $\frac{\pi}{2}$ (in the non-orientable case).

Lemma 9. *For an (orientable) orbifold with at least 2 cusps, the first cusp has area ≥ 1 (or ≥ 2 in the orientable case).*

Proof. Assume an orbifold has two cusps C_1 and C_2 . When drawing the horoball diagram by maximising the cusp C_1 and afterwards C_2 , the maximal horoballs in the cusp C_1 have to touch each other, and the maximal horoballs of C_2 touch the maximal horoballs of C_1 or C_2 (or both).

If we consider the horoball diagram where a horoball covering the cusp C_2 is based at ∞ , then the horoballs of C_1 have a maximal diameter of 1. This implies that there is a horoball H covering cusp C_1 which does not touch any bigger equivalent horoball, meaning H has a disc of no tangency. Note that the same argument does *not* have to hold for C_2 , because the assumption that the maximal cusp C_1 touches itself is essential. In Figure V.19 one can see an example that the cusp area of C_2 can actually be as small as 1 (in the oriented case).

Having a disc of no tangency (of radius 1) in cusp C_1 means that the area of this cusp is at least 2 if the orbifold is orientable and at least 1 otherwise. \square

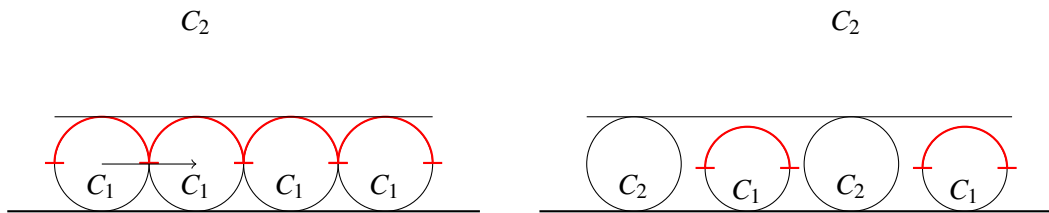


Figure V.19.: Discs of no Tangency in C_2

This Lemma implies that the cusp area in an orientable orbifold with two cusps is at least $2 + 1 = 3$. Using the density argument of Proposition 3, the minimal area of an orbifold with two cusps is area $(\mathbf{H}^2/\Gamma) \geq 3\frac{\pi}{3} = \pi$ which is in fact obtained by the orientable double cover of $\mathbf{H}^2/\bullet \xrightarrow{\infty} \bullet \xrightarrow{\infty} \bullet$. This concludes the proof of Theorem 1. \square

References

- [Ada88] C. Adams. ‘Volumes of N -cusped hyperbolic 3-manifolds’. *J. London Math. Soc. (2)* 38.3 (1988), pp. 555–565. ISSN: 0024-6107. DOI: 10.1112/jlms/s2-38.3.555.
- [Ada92] C. Adams. ‘Noncompact hyperbolic 3-orbifolds of small volume’. *Topology '90 (Columbus, OH, 1990)*. Vol. 1. Ohio State Univ. Math. Res. Inst. Publ. de Gruyter, Berlin, 1992, pp. 1–15.
- [Bea75] A. F. Beardon. ‘On the isometric circles of elements in a Fuchsian group’. *J. London Math. Soc. (2)* 10 (1975), pp. 329–337. DOI: 10.1112/jlms/s2-10.3.329.
- [Bea95] A. Beardon. *The geometry of discrete groups*. Vol. 91. Graduate Texts in Mathematics. Corrected reprint of the 1983 original. Springer-Verlag, New York, 1995, pp. xii+337. ISBN: 0-387-90788-2.
- [DD19] E. Dotti and S. T. Drewitz. ‘On right-angled polygons in hyperbolic space’. *Geometriae Dedicata* 200.1 (June 2019), pp. 45–59. DOI: 10.1007/s10711-018-0357-y.
- [DK21] S. T. Drewitz and R. Kellerhals. *The non-arithmetic cusped hyperbolic 3-orbifold of minimal volume*. 2021. arXiv: 2106.12279 [math.GT].
- [Kel98] R. Kellerhals. ‘Volumes of cusped hyperbolic manifolds’. *Topology* 37.4 (1998), pp. 719–734. ISSN: 0040-9383. DOI: 10.1016/S0040-9383(97)00052-9.
- [Rat06] J. Ratcliffe. *Foundations of hyperbolic manifolds*. Second. Vol. 149. Graduate Texts in Mathematics. Springer, New York, 2006, pp. xii+779.
- [Sie45] C. Siegel. ‘Some Remarks on Discontinuous Groups’. *Annals of Mathematics* 46.4 (1945), pp. 708–718. URL: <http://www.jstor.org/stable/1969206>.
- [VS93] È. Vinberg and O. Shvartsman. ‘Discrete groups of motions of spaces of constant curvature’. *Geometry, II*. Vol. 29. Encyclopaedia Math. Sci. Berlin: Springer, 1993, pp. 139–248.

VI. Minimal Fundamental Polygons

1. Introduction

As an application of the methods from chapter IV, we consider and complete the work of Matthieu Jacquemet [Jac15, chapter 4.3.2] about extremal fundamental polygons. He uses Poincaré's polyhedron theorem to provide an alternative proof of Siegel's theorem which he cites as:

Theorem 1 (Siegel [Sie45]). *Let $H \subset \text{Isom}(\mathbf{H}^2)$ be a discrete group, and let $\bullet \text{---} \bullet \overset{7}{\text{---}} \bullet$ be the Coxeter group generated by the reflections in the sides of the triangle with angles $\frac{\pi}{2}$, $\frac{\pi}{3}$, and $\frac{\pi}{7}$. Then, $\text{covol}(H) \geq \text{covol}\left(\bullet \text{---} \bullet \overset{7}{\text{---}} \bullet\right)$ with equality if and only if H is conjugate to $\bullet \text{---} \bullet \overset{7}{\text{---}} \bullet$ in $\text{Isom}(\mathbf{H}^2)$.*

By considering all possible side identifications, he finds the smallest polygons \mathcal{P}_N with $3 \leq N \leq 6$ edges which are the fundamental polygons of the fundamental groups of hyperbolic 2-orbifolds. For $N > 6$ he just gave a lower bound for the area:

$$\text{area}(\mathcal{P}_N) \geq \frac{\pi}{3}(N-6). \quad (1.1)$$

The orbifolds in the cases $N \leq 6$ are unique up to isometry. The group realising the minimal quadrilateral actually also realises the minimal pentagon and is in fact an index 2 subgroup of the Coxeter group $\bullet \text{---} \bullet \overset{7}{\text{---}} \bullet$ with coarea $\frac{\pi}{42}$.

We will show that the bound (1.1) is sharp for $N > 6$ by giving examples for orbifolds having N -gons \mathcal{P}_N with $\text{area}(\mathcal{P}_N) = \frac{\pi}{3}(N-6)$ as fundamental polygons. In contrast to the polygons with up to 6 edges, for $N > 6$ the orbifolds will *not* be unique up to isometry since there will be orientable and non-orientable examples. In fact, two closed surfaces of equal Euler characteristic cannot be homeomorphic if one is orientable but the other is not (see [Rat06, Theorem 9.1.2]).

After having discussed mainly cusped orbifolds throughout this thesis, we now discuss the compact case. In chapter V we saw that small cusped polygons are indeed bigger than the small compact polygons that Matthieu Jacquemet found.

2. Minimal Hyperbolic N -gon for $N > 6$

Notice that the area of a hyperbolic N -gon with angles α_i , $1 \leq i \leq N$, is given by

$$\text{area}(\mathcal{P}(\alpha_1, \dots, \alpha_N)) = \pi(N-2) - \sum_1^N \alpha_i. \quad (2.1)$$

VI. Minimal Fundamental Polygons

The regular N -gon $\mathcal{P}_N := \mathcal{P}(\frac{2\pi}{3}, \dots, \frac{2\pi}{3})$ with angles $\frac{2\pi}{3}$ is a realiser of the minimal area:

$$\text{area}(\mathcal{P}_N) = \pi(N-2) - N \frac{2\pi}{3} = \frac{\pi}{3}(N-6). \quad (2.2)$$

It can be obtained by gluing together $2N$ copies of a right angled triangle \mathcal{T}_N with angles $\frac{\pi}{3}$ and $\frac{\pi}{N}$ around the vertex with the smallest angle. The associated Coxeter group

$$\Gamma_N : \bullet \xrightarrow{c} \bullet \xrightarrow{b} \bullet \xrightarrow{a} \bullet \xrightarrow{N} \bullet \quad (2.3)$$

with relations $(ab)^N, (bc)^3, (ac)^2$ has the triangle \mathcal{T}_N as fundamental polygon and the generating reflections yield a tessellation of \mathbf{H}^2 by triangles isometric to \mathcal{T}_N . The copies of \mathcal{T}_N around vertex c (with angle $\frac{\pi}{N}$) are generated by the dihedral subgroup $D_{2N} = \langle a, b \rangle : \bullet \xrightarrow{N} \bullet$ in Γ_N . Compare Figure VI.1. One can identify the copies of \mathcal{T}_N around vertex c with the elements of $D_{2N} < \Gamma_N$, that is, with the nodes of the Cayley graph of D_{2N} .

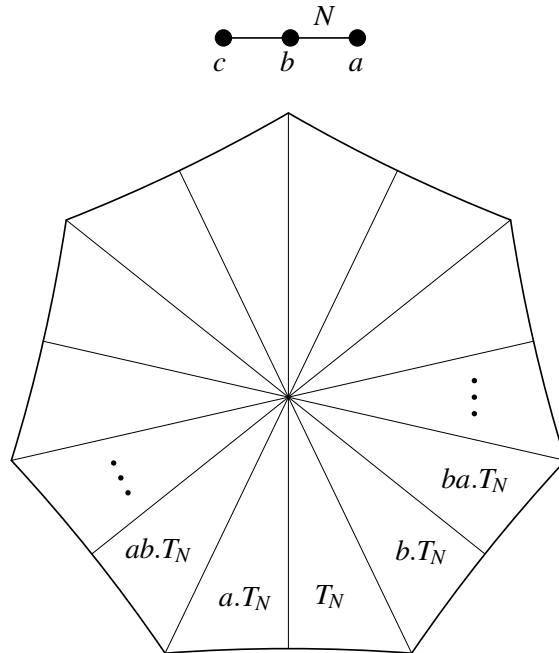


Figure VI.1.: Polygon \mathcal{P}_N and Triangle \mathcal{T}_N

If a subgroup G of Γ_N has index $2N$ and does not contain any element of D_{2N} , then \mathcal{P}_N is a fundamental polygon for G because the elements of D_{2N} are a system of representatives for the cosets of G in Γ_N .

Proposition 2. *For every $N > 6$, there is a group $G_N < \text{Isom}(\mathbf{H}^2)$ that has the regular polygon \mathcal{P}_N as a fundamental polygon and hence realising the minimal area N -gon as a fundamental polygon.*

Proof. The proof is based on Figures VI.2, VI.3, and VI.4. For $N = 7, 8,$ and $9,$ the graphs $(V, E),$ with $|V| = 2N,$ in Figure VI.2 are directly giving an action of Γ_N as described below. For $N = 7 + 3k, 8 + 3k,$ and $9 + 3k,$ the respective graph has to be taken and k copies of Figure VI.3 have to be added in the position indicated by a dotted line. Confer to Section 2.3 of Chapter IV for the correspondence between graph and group action. The labels are colour coded, that is blue edges encode the action of generator $a,$ green edges are labelled $b,$ and red edges describe $c.$ The names of the generators are as in (2.3).

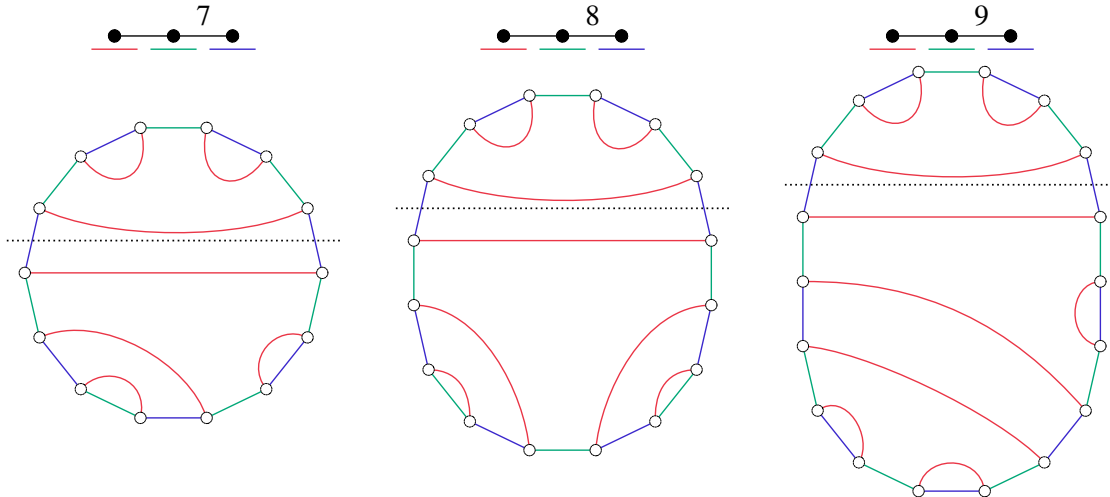


Figure VI.2.: 7-, 8-, and 9-gon

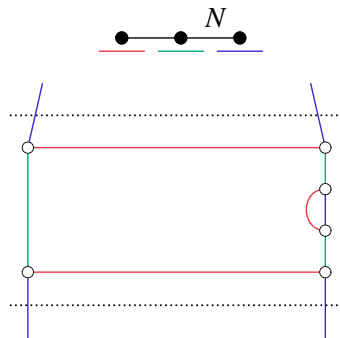


Figure VI.3.: Additional Piece for $N > 9$

The graphs contain the Cayley graphs of D_{2N} (by dropping the red edges corresponding to c), so the elements of the dihedral group have no fixed points. The fundamental polyhedron of the stabiliser subgroup G_N of a vertex can be obtained by gluing together $2N$ copies of \mathcal{T}_N around vertex $c.$ Those copies are the images of \mathcal{T}_N under the dihedral group $D_{2N}.$ Since the stabiliser subgroups of different vertices are conjugate, it does not matter which vertex is chosen.

It remains to check that the relations $(ab)^N, (bc)^3,$ and $(ac)^2$ of the Coxeter group Γ_N are met. This then proves that the graphs are actually giving group actions. All the generators act correctly

as involutions since the edges of the graphs are not directed and any vertex has at most one edge of a given colour. The word $(ab)^N$ acts as the identity on any vertex since it is the complete rotation of the graph (V, E) . The relation $(ac)^2$ is respected because any connected subgraph spanned by the edges with labels a and c is a square or two vertices connected by a double edge with both labels. The element $(bc)^3$ gives the identity since any connected subgraph spanned by the edges with labels b and c is either a hexagon giving the Cayley graph of $\bullet \text{---} \bullet$ or a double edge with both labels. \square

Remark 3. The elements of the stabiliser subgroups $G_N < \Gamma_N$ correspond to loops in the graphs. All the graphs so far only have loops of even length. This implies that the resulting subgroups G_N are orientation preserving. By replacing the top section as hinted in Figure VI.4, we can pass on to a subgroup $G'_N < \Gamma_N$ with the same fundamental polygon as G_N . The new graph contains loops of length 3 creating orientation reversing elements in G'_N . Due to [Rat06, Theorem 9.1.2], the two orbifolds \mathbf{H}^2/G_N and \mathbf{H}^2/G'_N are not homeomorphic. Hence, they cannot be isometric.

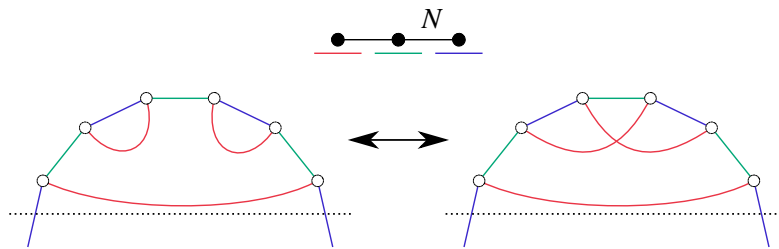


Figure VI.4.: Graph Replacements to Obtain Non-Conjugate Subgroups

3. Surfaces Realising Minimal Polygons

We can use the methods from chapter IV to find minimal area (smooth) hyperbolic surfaces based on certain polygons. Such a surface corresponds to a torsion-free subgroup of the Coxeter group Γ_N . If we find a torsion-free subgroup of index $2N$ of the same type as in the previous section, it results in a regular polygon \mathcal{P}_N with N vertices which yields a manifold. That is, we are looking for an alternative for the subgroup $G_N < \Gamma_N$, that is torsion-free and also of index $2N$. A necessary condition for a torsion-free subgroup is that its index is divisible by all orders of finite subgroups in Γ_N . There are the three maximal finite subgroups $\bullet \bullet$, $\bullet \text{---} \bullet$, and $\bullet \text{---}^N \bullet$ with orders 4, 6, and $2N$, respectively. In order to be able to obtain a torsion-free subgroup of index $2N$, the lowest common multiple must be $2N$. This gives the necessary condition $2|N$ and $3|N$.

Proposition 4. *There is a hyperbolic surface Σ_N having the regular N -gon \mathcal{P}_N with angles $\frac{2\pi}{3}$ as a fundamental polygon if and only if $N > 6$ is a multiple of 6.*

Proof. The necessity of N being a multiple of 6 was discussed above. For $N = 6k$ the graph in Figure VI.5 gives an action of Γ_N . The middle section has to be repeated $(k - 1)$ times. By the same argument as in Lemma 2, the graph yields a group action.

For each maximal finite subgroup, the subgraph consisting of all edges corresponding to the respective generators is a (disjoint) union of the Cayley graphs. This implies that the action of any finite order element is non-trivial and the stabiliser subgroup of any vertex is torsion-free. Compare Remark 7 in chapter IV. \square

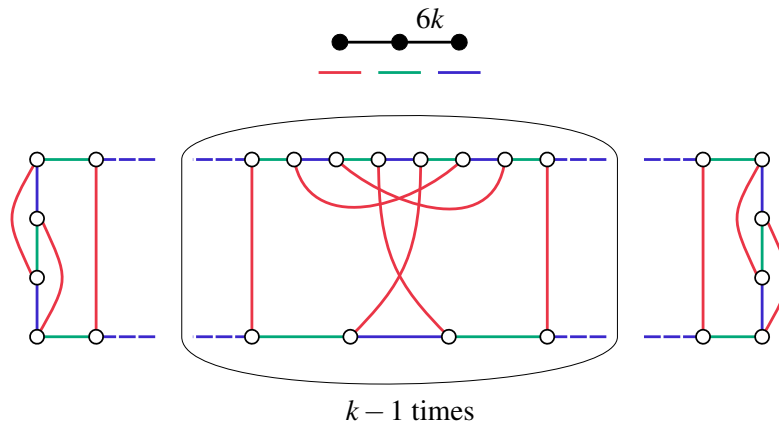


Figure VI.5.: Group Action in Order to Obtain a Surface Σ_N

References

- [Jac15] M. Jacquemet. ‘New contributions to hyperbolic polyhedra, reflection groups, and their commensurability’. PhD thesis. University of Fribourg, 2015. DOI: 10.13140/RG.2.1.2418.8248.
- [Rat06] J. Ratcliffe. *Foundations of hyperbolic manifolds*. Second. Vol. 149. Graduate Texts in Mathematics. Springer, New York, 2006, pp. xii+779.
- [Sie45] C. Siegel. ‘Some Remarks on Discontinuous Groups’. *Annals of Mathematics* 46.4 (1945), pp. 708–718. URL: <http://www.jstor.org/stable/1969206>.

Appendices

A. On Right-Angled Polygons in Hyperbolic Space

This appendix is a reprint of the joint paper [DD19] with Edoardo Dotti, where we generalise results of Delgove and Retailleau [DR14]. My contribution is the algorithm along with its realisability and counterexamples to the Theorem in [DR14].

Abstract We study oriented right-angled polygons in hyperbolic spaces of arbitrary dimensions, that is, finite sequences $(S_0, S_1, \dots, S_{p-1})$ of oriented geodesics in the hyperbolic space \mathbf{H}^{n+2} such that consecutive sides are orthogonal.

It was previously shown by Delgove and Retailleau [DR14] that three quaternionic parameters define a right-angled hexagon in the 5-dimensional hyperbolic space. We generalise this method to right-angled polygons with an arbitrary number of sides $p \geq 5$ in a hyperbolic space of arbitrary dimension.

Introduction

For $n \geq 0$, let \mathbf{H}^{n+2} denote the real hyperbolic $(n+2)$ -space. The boundary of this space can be described with Clifford vectors. These are special elements of the Clifford algebra \mathcal{C}_n , which is the unitary associative algebra generated by n elements i_1, \dots, i_n such that $i_j i_l = -i_l i_j, i_l^2 = -1$ for $l \neq j$. The group of orientation preserving isometries $\text{Isom}^+(\mathbf{H}^{n+2})$ of the hyperbolic space \mathbf{H}^{n+2} can be expressed with Clifford matrices. These are 2×2 matrices with coefficients in the multiplicative group generated by Clifford vectors and with Ahlfors determinant 1.

In this context, we describe hyperbolic right-angled polygons for which we mean right-angled closed edge paths in $n+2$ dimensions. We show how to construct a hyperbolic right-angled polygon Π_p of p sides, $p > 4$, by prescribing a parameter set consisting of $p-3$ Clifford vectors in $\partial\mathbf{H}^{n+2}$. Such a construction is achieved in an arbitrary dimension. No connection between the dimension of the space and the number of sides of the polygon is required.

Similar objects have already been studied in dimension 2 and 3 by Thurston [FLP79] and by Fenchel [Fen89], who studied right-angled hexagons. Costa and Martínez [CM95] studied right-angled polygons with an arbitrary number of sides in the hyperbolic plane. More recently Delgove and Retailleau [DR14] classified right-angled hexagons in \mathbf{H}^5 . In their work, 2×2 quaternionic matrices having Dieudonné determinant 1 are used in order to describe the direct isometries of \mathbf{H}^5 . While this approach based on quaternions is very convenient, it can not be extended to arbitrary dimensions. By using Clifford matrices instead, we are able to generalise the construction to any dimension. Particularly, 2×2 quaternionic Clifford matrices are used to describe direct isometries of \mathbf{H}^4 .

In the first section we develop more precisely the connection between hyperbolic space and the Clifford algebra. Then we discuss the role of the cross ratio for Clifford vectors and its geometrical interpretation. Our main result, the algorithmic construction of Π_p , is presented in the second section. In the last part we treat the case when the convex hull of the p vertices of the polygon Π_p give rise to a hyperbolic $(p - 1)$ -simplex. A necessary condition for its realisation is stated. As a conclusion we discuss in more details a special case in 4 dimensions, supposing that all the edges of the edge path have equal length. By exploiting the work of Dekster and Wilker [DW91] we explicitly state a necessary and sufficient condition for realisability depending on such a side length. Surprisingly, it turns out that the side length must be related to the golden ratio $\gamma = \frac{1+\sqrt{5}}{2}$.

1. The real Clifford Algebra and Hyperbolic Space

In this section we present the notion of Clifford algebra and its relation to isometries of hyperbolic space. For a more complete description we refer to the works of Ahlfors [Ahl85], [Ahl86], Vahlen [Vah02] and Waterman [Wat93] (see also [Par07, §7]).

1.1. The Real Clifford Algebra \mathcal{C}_n

Consider the real Clifford algebra \mathcal{C}_n generated by i_1, \dots, i_n , that is

$$\mathcal{C}_n = \langle i_1, \dots, i_n \mid i_j i_l = -i_l i_j, i_l^2 = -1 \text{ for } l \neq j \rangle,$$

which is a unitary associative real algebra. Every element x of the algebra \mathcal{C}_n can be uniquely written as $x = \sum x_I I$, where $x_I \in \mathbb{R}$ and the sum is taken over all the products $I = i_{k_1} \cdots i_{k_m}$, with $1 \leq k_1 < \cdots < k_m \leq n$ and $1 \leq m \leq n$. Here the empty product I_0 is included and identified with $i_0 := 1$. Hence \mathcal{C}_n is a 2^n -dimensional real vector space. In particular we can identify \mathcal{C}_0 with \mathbb{R} , \mathcal{C}_1 with \mathbb{C} and \mathcal{C}_2 with \mathbb{H} , the Hamiltonian quaternions. To each element $x = \sum x_I I$ we associate a norm as given by $|x|^2 = \sum x_I^2$, inducing a Euclidean structure on \mathcal{C}_n . Denote with $\Re(x)$ the coefficient x_0 , called the *real part* of x , while $\Im(x) = x - \Re(x)$ is called the *non-real part* of x . If $\Re(x) = 0$ we will refer to x as a *pure element* of \mathcal{C}_n .

On \mathcal{C}_n there are three well-known involutions. Let $x \in \mathcal{C}_n$, $x = \sum x_I I$. Then:

- (i) $x^* = \sum x_I I^*$, where I^* is obtained from $I = i_{k_1} \cdots i_{k_m}$ by reversing the order of the factors, that is $I^* = i_{k_m} \cdots i_{k_1}$;
- (ii) $x' = \sum x_I I'$, where I' is obtained from $I = i_{k_1} \cdots i_{k_m}$ by replacing each factor i_k with $-i_k$, that is $I' = (-i_{k_1}) \cdots (-i_{k_m}) = (-1)^m I$;
- (iii) $\bar{x} = (x^*)' = (x')^*$.

The involutions i) and iii) are anti-automorphisms, while the involution ii) is an automorphism.

Of particular interest are Clifford elements of the form $x = x_0 + x_1 i_1 + \cdots + x_n i_n$, called *Clifford vectors*. The set

$$\mathbb{V}^{n+1} = \{x_0 + x_1 i_1 + \cdots + x_n i_n \mid x_0, \dots, x_n \in \mathbb{R}\}$$

of all Clifford vectors is an $(n + 1)$ -dimensional real vector space, naturally isomorphic to the Euclidean space \mathbb{R}^{n+1} . Notice that for an element $x \in \mathbb{V}^{n+1}$ we have $x^* = x$ and hence $\bar{x} = x'$ as well as $x + \bar{x} = 2\Re(x)$ and $x\bar{x} = \bar{x}x = |x|^2$. Moreover every non-zero vector x has an inverse given by $x^{-1} = \frac{\bar{x}}{|x|^2}$. Hence finite products of non-zero vectors are invertible and they form the so-called Clifford group Γ_n . Observe that we have $\Gamma_n = \mathcal{C}_n \setminus \{0\}$ only for $n \in \{0, 1, 2\}$.

1.2. Square Root of a Clifford Vector

Next we introduce the notion of the square root of a Clifford vector. It will be a generalisation of the square root of quaternions (see [Par06] for example) in the following way:

Proposition 1. *Let $y \in \mathbb{V}^{n+1} \setminus \{0\}$ be a Clifford vector. If $y \notin \mathbb{R}_{<0}$, then there exist exactly two elements $x_1, x_2 \in \mathbb{V}^{n+1}$ such that $x_1^2 = x_2^2 = y$; x_1 and x_2 are both called a square root of y . If $y \in \mathbb{R}_{<0}$, we have the three following situations depending on n :*

- *If $n = 0$, then there is no element $x \in \mathbb{V}^1$ such that $x^2 = y$,*
- *If $n = 1$, then there are exactly two elements $x_1, x_2 \in \mathbb{V}^2$ such that $x_1^2 = x_2^2 = y$,*
- *If $n \geq 2$, then there are uncountably many square roots of y .*

Proof. Suppose that $x^2 = y$, with $x, y \in \mathbb{V}^{n+1} \setminus \{0\}$. Then $\bar{x}^2 = \bar{y}$ and $|x|^2 = |y|$. We have the following two equations:

$$x(\bar{x} + x) = x\bar{x} + x^2 = |y| + y, \quad (1.1)$$

$$(x + \bar{x})^2 = x^2 + 2x\bar{x} + \bar{x}^2 = y + 2|y| + \bar{y} = 2(\Re(y) + |y|). \quad (1.2)$$

Observe that the term $2(\Re(y) + |y|) \geq 0$.

Now let $y \notin \mathbb{R}_{<0}$, then we have $\Re(y) + |y| > 0$, and the element

$$x := \frac{|y| + y}{\sqrt{2(\Re(y) + |y|)}} \in \mathbb{V}^{n+1} \quad (1.3)$$

satisfies $x^2 = y$. Indeed,

$$x^2 = \frac{|y|^2 + 2|y|y + y^2}{2\Re(y) + 2|y|} = \frac{(\bar{y} + 2|y| + y)y}{2\Re(y) + 2|y|} = y.$$

Notice that in the special case if $y \in \mathbb{R}_{>0}$, the identity (1.3) yields $x = \pm\sqrt{y}$ as desired. For $y \notin \mathbb{R}$ the square roots of y have to lie in the plane spanned by 1 and y which is isomorphic to \mathbb{C} , ensuring the non-existence of more than two roots. By abuse of notation the square root x of y is denoted by $\sqrt{y} := x$.

Let $y \in \mathbb{R}_{<0}$. For $n = 1$ or 2 the assertion is trivial. Let $n \geq 2$. We can write $y = -z^2$ for some $z \in \mathbb{R}_{>0}$. In this case consider $x := z \cdot u$ where u is a pure Clifford vector with norm 1. In general for any pure Clifford vector we have

$$0 = (u + \bar{u})u = u\bar{u} + u^2 = |u|^2 + u^2,$$

which implies $u^2 = -|u|^2$. Hence $x^2 = z^2u^2 = -z^2|u|^2 = -z^2$. □

Remark 2. Notice that Proposition 1 remains true for $y \in \Gamma_2 = \mathbb{H} \setminus \{0\}$ since $y + \bar{y} = 2\Re(y)$ still holds. However, it does not hold for a general element of \mathcal{C}_n or even Γ_n , $n \geq 3$. Indeed, for an arbitrary $y \in \Gamma_n$ one has $y + \bar{y} \neq 2\Re(y)$. For example let $y = i_1 i_2 i_3 \in \Gamma_n$, $n \geq 3$. Then $y + \bar{y} = 2i_1 i_2 i_3$. Hence equation (1.2) does not hold.

Remark 3. For the square root \sqrt{y} of a Clifford vector $y \in \mathbb{V}^{n+1} \setminus \mathbb{R}_{\leq 0}$ we have:

- For all positive $\mu \in \mathbb{R}_{>0}$, $\sqrt{\mu y} = \sqrt{\mu} \sqrt{y}$,
- For the inverse $\sqrt{y^{-1}} = \sqrt{y}^{-1} = \frac{1}{|y|} \sqrt{y}$.
- The square root of $-y$ can be found by a rotation of 90° : $\sqrt{-y} = i \sqrt{y}$ for some pure Clifford vector i with $i^2 = -1$. This also holds for negative $y \in \mathbb{R}_{<0}$.

1.3. Clifford Matrices and Hyperbolic Isometries

We now take a look at matrices having entries in the extended Clifford group $\Gamma_n \cup \{0\}$. These matrices will be used to explicitly represent direct isometries of the hyperbolic space \mathbf{H}^{n+2} (see for example [Wat93] and [Par07, §7]).

A *Clifford matrix* is a 2×2 matrix $A = \begin{pmatrix} a & b \\ c & d \end{pmatrix}$ with

$$a, b, c, d \in \Gamma_n \cup \{0\}, ab^*, cd^*, c^*a, d^*b \in \mathbb{V}^{n+1}, ad^* - bc^* \in \mathbb{R} \setminus \{0\},$$

where $ad^* - bc^*$ is the *Ahlfors determinant* of A . Denote the set of such matrices by $\text{GL}(2, \mathcal{C}_n)$. By a result of Vahlen and Maass [Ahl86, p. 221] the set

$$\text{SL}(2, \mathcal{C}_n) = \left\{ A = \begin{pmatrix} a & b \\ c & d \end{pmatrix} \in \text{GL}(2, \mathcal{C}_n) \mid ad^* - bc^* = 1 \right\} \quad (1.4)$$

of Clifford matrices with Ahlfors determinant 1 is a multiplicative group.

Each element $T = \begin{pmatrix} a & b \\ c & d \end{pmatrix} \in \text{SL}(2, \mathcal{C}_n)$ has the inverse matrix $T^{-1} = \begin{pmatrix} d^* & -b^* \\ -c^* & a^* \end{pmatrix}$.

Furthermore $\text{SL}(2, \mathcal{C}_n)$ is generated by the matrices

$$\begin{pmatrix} 1 & t \\ 0 & 1 \end{pmatrix}, \begin{pmatrix} 0 & -1 \\ 1 & 0 \end{pmatrix}, \begin{pmatrix} a & 0 \\ 0 & a^{*-1} \end{pmatrix},$$

where $t \in \mathbb{V}^{n+1}$ and $a \in \Gamma_n$ (see for example [Par07, §7]).

The group $\text{SL}(2, \mathcal{C}_n)$ plays an important role in our investigation since it is closely related to the group of orientation preserving isometries of the hyperbolic $(n+2)$ -space realised in the upper half-space according to

$$\begin{aligned} \mathbf{H}^{n+2} &= \{x = (x_0, x_1, \dots, x_{n+1}) \in \mathbb{R}^{n+2} \mid x_{n+1} > 0\} \\ &\cong \mathbb{V}^{n+1} \times \mathbb{R}_{>0}. \end{aligned}$$

The compactification $\overline{\mathbf{H}^{n+2}}$ is given by the union of \mathbf{H}^{n+2} with the boundary set $\partial\mathbf{H}^{n+2} = \mathbb{V}^{n+1} \cup \{\infty\}$ of points at infinity of \mathbf{H}^{n+2} .

Consider the projective group

$$\mathrm{PSL}(2, \mathcal{C}_n) = \mathrm{SL}(2, \mathcal{C}_n) / \{\pm I\}.$$

It is known that this group acts bijectively on $\mathbb{V}^{n+1} \cup \{\infty\}$ by

$$T(x) = (ax + b)(cx + d)^{-1} \quad (1.5)$$

with $T(-c^{-1}d) = \infty$, $T(\infty) = ac^{-1}$ if $c \neq 0$, and $T(\infty) = \infty$ otherwise. By Poincaré extension, the action (1.5) can be extended to the upper half-space \mathbf{H}^{n+2} . In this way we obtain an isomorphism between $\mathrm{PSL}(2, \mathcal{C}_n)$ and the group $\mathrm{Möb}^+(n+1)$ of orientation preserving Möbius transformations of $\mathbb{V}^{n+1} \cup \{\infty\}$ (see [Wat93], [CW98]). Since the group $\mathrm{Isom}^+(\mathbf{H}^{n+2})$ of orientation preserving isometries of \mathbf{H}^{n+2} is isomorphic to $\mathrm{Möb}^+(n+1)$, we get the following identification:

$$\mathrm{Isom}^+(\mathbf{H}^{n+2}) \cong \mathrm{Möb}^+(n+1) \cong \mathrm{PSL}(2, \mathcal{C}_n). \quad (1.6)$$

Therefore any direct isometry of \mathbf{H}^{n+2} can be represented by a Clifford matrix in $\mathrm{PSL}(2, \mathcal{C}_n)$.

Finally, we remark that Möbius transformations act triply transitively on $\mathbb{V}^{n+1} \cup \{\infty\}$ (see [Wil81, §6], for example). That is, given two triplets $\{x_1, x_2, x_3\}$ and $\{x'_1, x'_2, x'_3\}$ of distinct points in the boundary x_1, x_2, x_3 and x'_1, x'_2, x'_3 respectively, there always exists a transformation $T \in \mathrm{Möb}(n+1)$ with $T(x_i) = x'_i$. For $n = 0$ this map is unique and for $n = 1$ it is unique if one demands that it preserves the orientation. In higher dimensions this map is not unique anymore.

1.4. The Cross Ratio

As in the classical case, we shall use the cross ratio to study configurations of points in $\mathbb{V}^{n+1} \cup \{\infty\}$.

Definition 4. Let x, y, z, w be four pairwise different Clifford vectors in \mathbb{V}^{n+1} . Then

$$[x, y, z, w] := (x - z)(x - w)^{-1}(y - w)(y - z)^{-1} \in \Gamma_n \setminus \{0\} \quad (1.7)$$

is called the cross ratio of x, y, z and w .

We extend the definition (1.7) by continuity to $\mathbb{V}^{n+1} \cup \{\infty\}$, allowing x, y or w to be ∞ , by

$$[\infty, y, z, w] = (y - w)(y - z)^{-1} \text{ for } x = \infty, \quad (1.8)$$

and similarly for $y = \infty$ and $w = \infty$. Moreover in an analogous way we put

$$[x, y, \infty, w] = (x - w)^{-1}(y - w).$$

The cross ratio satisfies the following transformation behaviour (see [CW98] [Lemma 6.2]):

$$[T(x), T(y), T(z), T(w)] = (cz + d)^{*-1} [x, y, z, w] (cz + d)^*, \quad (1.9)$$

$$\forall T = \begin{pmatrix} a & b \\ c & d \end{pmatrix} \in \mathrm{SL}(2, \mathcal{C}_n).$$

Hence, the real part and the norm of the cross ratio $[x, y, z, w]$ of four vectors are invariant under the action of T . However, the cross ratio itself is not an invariant.

We specialise the cross ratio in the following way: Consider two oriented geodesics s, t in \mathbf{H}^{n+2} whose endpoints s^-, s^+ and t^-, t^+ are four distinct points in $\mathbb{V}^{n+1} \cup \{\infty\}$.

Definition 5. *The cross ratio $\Delta(s, t)$ of s and t is defined by*

$$\Delta(s, t) := [s^-, s^+, t^-, t^+]. \quad (1.10)$$

Lemma 6. *Let s and t be two geodesics as above. If s and t intersect then $\Delta(s, t) = \Delta(t, s)$. If s and t are disjoint, then $\Delta(s, t) = \Delta(t, s)$ if one of the endpoints is ∞ or if the cross ratios are real, otherwise the two cross ratios are conjugate.*

Proof. Assuming one of the endpoints to be infinity, let $s = (x, \infty)$ with $x \in \mathbb{V}^{n+1}$. We can apply a translation $\begin{pmatrix} 1 & -x \\ 0 & 1 \end{pmatrix}$ such that s is mapped to $(0, \infty)$. By (1.9), any translation leaves the cross ratio unchanged. Using (1.8) it is easy to see that $\Delta(s, t) = \Delta(t, s)$.

Let now s and t be two arbitrary geodesics with no endpoint at infinity. We know that we can always find an isometry $T = \begin{pmatrix} a & b \\ c & d \end{pmatrix} \in \mathrm{SL}(2, \mathcal{C}_n)$ mapping the two endpoints of one of the geodesics to 0 and ∞ . Using (1.9) and what we have just discussed above we get

$$\begin{aligned} (ct^- + d)^{* -1} [s^-, s^+, t^-, t^+] (ct^- + d)^* &= [T(s^-), T(s^+), T(t^-), T(t^+)] \\ &= [T(t^-), T(t^+), T(s^-), T(s^+)] \\ &= (cs^- + d)^{* -1} [t^-, t^+, s^-, s^+] (cs^- + d)^*. \end{aligned}$$

Hence the two cross ratios $\Delta(s, t)$ and $\Delta(t, s)$ are conjugate. This implies that if the cross ratios are real, then the equality $\Delta(s, t) = \Delta(t, s)$ holds. In particular, if two geodesics intersect, then $\Delta(s, t) = \Delta(t, s)$ by Proposition 9 below. \square

Now consider three geodesics r, s and t in \mathbf{H}^{n+2} with pairwise different endpoints r^-, r^+, s^-, s^+ and t^-, t^+ in $\mathbb{V}^{n+1} \cup \{\infty\}$.

Definition 7. *The quantity*

$$\Delta(r, s, t) := [s^+, s^-, r^+, t^+] \quad (1.11)$$

is called the double bridge cross ratio of (r, s, t) .

Definition 8. *The ordered triple (r, s, t) is called a double bridge if s is orthogonal to r and t such that $r \neq t$. If $|\Delta(r, s, t)| > 1$, then the intersections $r \cap s$ and $s \cap t$ do not coincide and we call the double bridge properly oriented.*

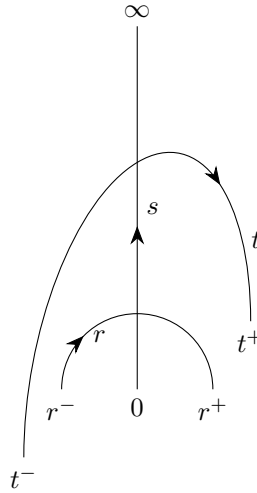


Figure A.1.: Double Bridge

Consider a properly oriented double bridge (r, s, t) . The norm of $\Delta(r, s, t)$ encodes the hyperbolic length of the geodesic segment $[r, t]$ on s between r and t . Indeed, assume w.l.o.g. that the endpoints of s in the double bridge (r, s, t) are $s^- = 0$ and $s^+ = \infty$ (see Figure A.1). The hyperbolic distance δ of two points $p, q \in s$ in \mathbf{H}^{n+2} with $p_{n+2} > q_{n+2}$ is equal to (see [Bea12, p. 131])

$$\delta = \log \left(\frac{p_{n+2}}{q_{n+2}} \right).$$

On the other hand, by (1.7) we get

$$|\Delta(r, s, t)| = |[\infty, 0, r^+, t^+]| = \frac{|t^+|}{|r^+|}.$$

If we take $p = s \cap t$ and $q = r \cap s$, we conclude that $\delta = \log(|\Delta(r, s, t)|)$.

The following results will be of importance:

Proposition 9. *Two hyperbolic geodesics s and t intersect if and only if their cross ratio $\Delta(s, t) \in \mathbb{R}_{<0}$. Furthermore s and t are perpendicular if and only if $\Delta(s, t) = -1$.*

Proof. Since hyperbolic isometries act triply transitively, there is an isometry represented by $A \in \text{SL}(2, \mathcal{C}_n)$ mapping s and t into $(0, \infty)$ and $(1, x)$, $x \in \mathbb{V}^{n+1}$. Then, by (1.7) and (1.8), the cross ratio of $A(s)$ and $A(t)$ equals $\Delta(A(s), A(t)) = [0, \infty, 1, x] = x^{-1}$, and the assertions follow for $A(s)$ and $A(t)$. Moreover, by (1.9), a real cross ratio stays invariant under isometry. \square

Proposition 10. *Let $s = (0, \infty)$ and $t = (1, y)$ with $y \neq 0, \infty$ be two disjoint geodesics in \mathbf{H}^{n+2} . Then the common perpendicular l is $(-\sqrt{y}, \sqrt{y})$. This perpendicular is unique up to orientation.*

Proof. Let $l = (z, w)$ denote the common perpendicular between s and t . By Proposition 9 and by (1.8), we get

$$\Delta(s, l) = [0, \infty, z, w] = -1. \tag{1.12}$$

and

$$\Delta(t, l) = [1, y, z, w] = -1. \quad (1.13)$$

Equation (1.12) yields $z = -w$. The equation (1.13) states that

$$(1 - z)(1 + z)^{-1} = -(y - z)(y + z)^{-1}. \quad (1.14)$$

It is easy to see that $(1 - z)(1 + z)^{-1} = (1 + z)^{-1}(1 - z)$, so that

$$(1 - z)(y + z) = -(1 + z)(y - z).$$

By expanding the above equation we obtain $y = z^2$. Notice that by construction, since s and t are disjoint, we have $y \notin \mathbb{R}_{<0}$. Hence, by applying Proposition 1, the result follows for $l = (\pm\sqrt{y}, \mp\sqrt{y})$. \square

2. The Main Theorem

2.1. Preliminaries

Our aim is to construct oriented right-angled polygons in hyperbolic space from a minimal number of prescribed parameters.

Definition 11. *An oriented right-angled polygon with p sides in \mathbf{H}^{n+2} (or p -gon for short), $n \geq 0$, is a p -tuple of oriented geodesics $(S_0, S_1, \dots, S_{p-1})$ with $S_{i-1} \neq S_{i+1}$ for $i \pmod{p}$ and such that S_i is orthogonal to S_{i+1} for $0 \leq i \leq p - 2$ and S_{p-1} is orthogonal to S_0 .*

We usually denote it by Π_p .

We call such a p -gon Π_p non-degenerate if consecutive intersections do not coincide (that is $S_{i-1} \cap S_i \neq S_i \cap S_{i+1}$ for $i \pmod{p}$) and the double bridges (S_{i-1}, S_i, S_{i+1}) , $i \pmod{p}$, are properly oriented.

We can take $p \geq 5$ since the simplest case of a right-angled polygon is the pentagon. There cannot be a hyperbolic rectangle since the common perpendicular of two geodesics S_0 and S_2 is unique. Hence if there was a hyperbolic rectangle (S_0, S_1, S_2, S_3) , two geodesics would have to be identical.

Note that it is no restriction to only consider p -gons in \mathbf{H}^{p-1} since the convex hull of p geodesics can at most have dimension $p - 1$. Hence, we will always refer to this case.

Recall that the one-point compactified vector space $\mathbb{V}^{p-2} \cup \{\infty\}$ forms the boundary of hyperbolic $(p - 1)$ -space

$$\mathbf{H}^{p-1} = \{(x, y) \in \mathbb{V}^{p-2} \times \mathbb{R}_{>0}\}.$$

Consider the standard configuration double bridge (r, s, t) similar to Section 1.4 with $r = (-1, 1)$, $s = (0, \infty)$ and $t = (-x, x)$ for $x \in \mathbb{V}^{p-2} \setminus \{-1, 0, 1\}$ (see Figure A.2).

A small computation shows that the double bridge cross ratio is given by

$$\Delta((-1, 1), (0, \infty), (-x, x)) = [\infty, 0, 1, x] = x. \quad (2.1)$$

If conversely the first two geodesics of this double bridge and a desired double bridge cross ratio q are given, one can construct the third geodesic as $(-q, q)$. In the general case this is not easy

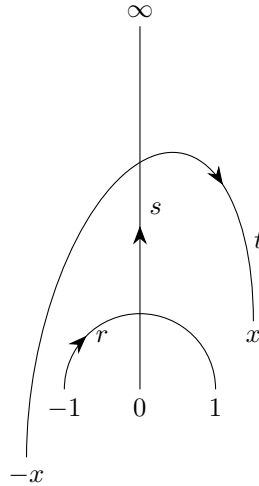


Figure A.2.: Standard Configuration Double Bridge

since the Clifford vectors do not commute. In view of (2.1) we shall start with the configuration given by the geodesics $(-1, 1)$, $(0, \infty)$ and $(-x, x)$. If the double bridges are supposed to be properly oriented, this poses the immediate restriction $|x| > 1$.

To construct more geodesics we will have to apply certain isometries to achieve this configuration from a general double bridge. These isometries depend on the double bridge cross ratios in the right-angled polygon Π_p they are part of.

Definition 12. For a set of given Clifford vectors $\{q_1, \dots, q_{p-3}\} \subset \mathbb{V}^{p-2} \setminus \{0\}$ define the isometries ϕ_i of upper half-space by the following Möbius transformations:

$$\phi_i : x \mapsto \sqrt{-2q_i}^{-1} (x + q_i) (x - q_i)^{-1} \sqrt{-2q_i}, \quad 1 \leq i \leq p-3. \quad (2.2)$$

If $q_i \in \mathbb{R}_{>0}$, choose $\sqrt{-2q_i} := \sqrt{2q_i} i_1$.

Let Φ_i be the concatenation $\Phi_i := \phi_i \circ \phi_{i-1} \circ \dots \circ \phi_1$.

Note that the isometries ϕ_i carry the two geodesics $(0, \infty)$ and $(-q_i, q_i)$ into the geodesics $(-1, 1)$ and $(0, \infty)$ of a double bridge in the aforementioned setting. However, these isometries are not uniquely defined by this property. We will always apply these ϕ_i if we need an isometry which maps given geodesics to specific other geodesics in a polygon Π_p .

The Clifford matrix corresponding to ϕ_i is

$$\begin{pmatrix} \sqrt{-2q_i}^{-1} & q_i \sqrt{-2q_i}^{-1} \\ \sqrt{-2q_i}^{-1} & -q_i \sqrt{-2q_i}^{-1} \end{pmatrix}. \quad (2.3)$$

The inverse $\phi_i^{-1}(x) = \sqrt{-q_i} (1+x)(1-x)^{-1} \sqrt{-q_i}$ is represented by the matrix

$$\begin{pmatrix} q_i \sqrt{-2q_i}^{-1} & q_i \sqrt{-2q_i}^{-1} \\ \sqrt{-2q_i}^{-1} & -\sqrt{-2q_i}^{-1} \end{pmatrix}. \quad (2.4)$$

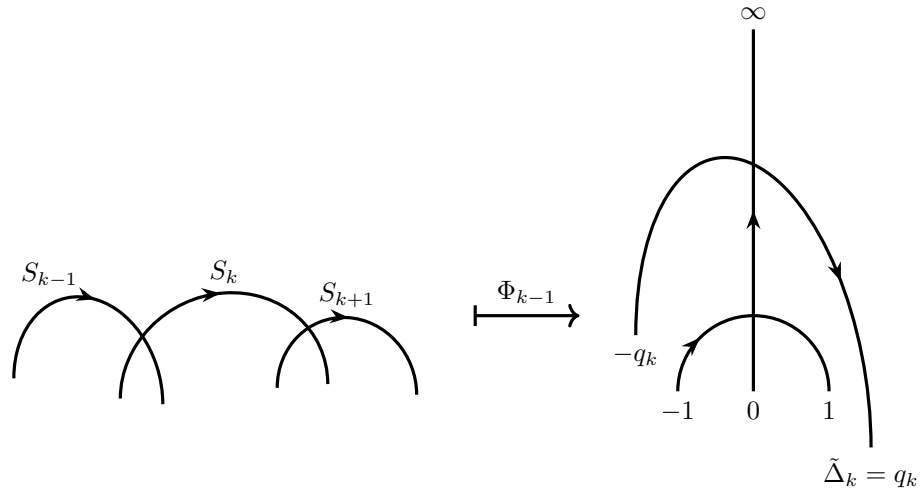


Figure A.3.: Gauging by an Isometry

Repeatedly applying these isometries to geodesics in a Π_p enables us to standardise the cross ratio of a double bridge in a p -gon and eliminate the problem of the cross ratio not being invariant under isometries.

2.2. The Theorem

Definition 13. Let (S_0, \dots, S_{p-1}) be a right-angled p -gon. Define the gauged double bridge cross ratios $\tilde{\Delta}_i$ for $i = 1, \dots, p-3$ by the following recursive definition:

$$\tilde{\Delta}_1 := \Delta(S_0, S_1, S_2), \quad (2.5)$$

$$\tilde{\Delta}_{i+1} := \Delta(\Phi_i(S_i), \Phi_i(S_{i+1}), \Phi_i(S_{i+2})). \quad (2.6)$$

The Clifford vectors q_i which are needed to define the maps Φ_i are calculated along the way as

$$q_i = \tilde{\Delta}_i. \quad (2.7)$$

These gauged double bridge cross ratios will be the parameters describing the non-degenerate right-angled p -gons in \mathbf{H}^{p-1} in the Theorem 14 below. Hence consider the set

$$\mathcal{P}_p := \{(q_1, \dots, q_{p-3}) \mid q_i \in \mathbb{V}^{p-2}, |q_i| > 1, 1 \leq i \leq p-3\} \quad (2.8)$$

of $(p-3)$ -tuples of non-zero Clifford vectors. Denote by

$$\text{RAP}_p := \left\{ (S_0, \dots, S_{p-1}) \text{ non-degenerate right-angled polygon in } \mathbf{H}^{p-1} \right. \\ \left. \text{with } S_0 = (-1, 1), S_1 = (0, \infty) \right\} \quad (2.9)$$

the set of non-degenerate right-angled polygons with p sides. The calculation of the gauged double bridge cross ratios gives a map $\tilde{\Delta} : \text{RAP}_p \rightarrow \mathcal{P}_p$. Denote the image of this map by

$\mathcal{P}_p^* := \tilde{\Delta}(\text{RAP}_p) \subset \mathcal{P}_p$. This is the set of parameters which will yield a non-degenerate Π_p in the construction below.

Theorem 14. *The map $\tilde{\Delta} : \text{RAP}_p \rightarrow \mathcal{P}_p^*$ is a bijection. The inverse map can be given as an explicit construction of a right-angled p -gon Π_p from a tuple of $p-3$ parameters in \mathcal{P}_p^* .*

2.3. Proof of Theorem 14

Bijectivity It is sufficient to prove the injectivity of $\tilde{\Delta}$ since it is surjective by definition. Note that in the standard configuration double bridge of Figure A.2, there is a one-to-one correspondence of Clifford vectors x and geodesics $t = (-x, x)$ as given by equation (2.1). Now assume there are two p -gons $\Pi_p = (S_0, \dots, S_{p-1})$, $\Pi'_p = (S'_0, \dots, S'_{p-1}) \in \text{RAP}_p$ such that $\tilde{\Delta}(\Pi_p) = \tilde{\Delta}(\Pi'_p) = (q_1, \dots, q_{p-3})$. By definition $S_0 = S'_0$ and $S_1 = S'_1$. By the above correspondence we also have $S_2 = S'_2$. Furthermore the maps $\phi_1, \dots, \phi_{p-3}$ are the same for both Π_p and Π'_p since these maps are defined by q_1, \dots, q_{p-3} as given in equation (2.2). Therefore the map Φ_i yields the same one-to-one correspondence between geodesics and Clifford vectors in both p -gons.

Construction of the Polygon Π_p The inverse map $\tilde{\Delta}^{-1}$ is given by the construction of a Π_p from $p-3$ parameters $q_1, \dots, q_{p-3} \in \mathbb{V}^{p-2}$.

Assume we are given $p-3$ parameters $(q_1, \dots, q_{p-3}) \in \mathcal{P}_p^*$.

Start The first two geodesics are fixed as $S_0 = (-1, 1)$ and $S_1 = (0, \infty)$. Since this is the standard configuration double bridge considered above, we find $S_2 = (-q_1, q_1)$ if we demand $\Delta(S_0, S_1, S_2) = q_1$.

The Geodesic S_3 To find the endpoints of S_3 , we benefit from the isometry ϕ_1^{-1} above which maps $(-1, 1)$ to $(0, \infty)$ and $(0, \infty)$ to S_2 . If q_2 was the cross ratio of a double bridge involving $(-1, 1)$ and $(0, \infty)$, the third geodesic would be $(-q_2, q_2)$. Since S_3 is part of the double bridge starting with $(0, \infty)$ and S_2 , S_3 can be found by applying ϕ_1^{-1} to $(-q_2, q_2)$, that is $S_3 = (\phi_1^{-1}(-q_2), \phi_1^{-1}(q_2))$.

The Next Geodesic in the General Case The further procedure expands the previous idea. First we note that the next geodesic is given by the parameter q_3 . The geodesic S_4 would then be the image of $(-q_3, q_3)$ under the isometry Φ_2^{-1} mapping $(-1, 1)$ and $(0, \infty)$ to S_2 and S_3 , respectively.

In general, assuming we have calculated the geodesics S_0, \dots, S_k for some k with $2 \leq k \leq p-3$, we can use Φ_{k-1}^{-1} in order to obtain $S_{k+1} = (\Phi_{k-1}^{-1}(-q_k), \Phi_{k-1}^{-1}(q_k))$.

Existence of the Last Geodesic After using all the parameters q_1, \dots, q_{p-3} , we have determined the geodesics S_0, \dots, S_{p-2} . As a consequence of Proposition 9 the last common perpendicular between S_0 and S_{p-2} exists and is unique as long as

$$\Delta(S_0, S_{p-2}) \notin \mathbb{R}_-. \quad (2.10)$$

This is ensured by the set $\mathcal{P}^* \subset \mathcal{P}$. □

Remark 15. Since the Clifford vectors do not commute, one cannot directly compute the common perpendicular S_{p-1} using the equations

$$\Delta(S_{p-1}, S_0) = -1, \quad \Delta(S_{p-1}, S_{p-2}) = -1. \quad (2.11)$$

However, one can use an isometry to obtain a nice configuration where the terms in the equations above commute. Writing $S_{p-2} = (a, b)$, consider the isometry

$$\psi : x \mapsto \alpha^{-1} (1+x)(1-x)^{-1} \alpha^{-1} \quad (2.12)$$

where $\alpha := \sqrt{-(1+a)(1-a)^{-1}}$. This isometry maps S_0 to $(0, \infty)$ and S_{p-2} to $(1, c)$ where $c := \alpha^{-1} (1+b)(1-b)^{-1} \alpha^{-1}$.

Hence, by Proposition 10

$$S_{p-1} = (\psi^{-1}(-\sqrt{c}), \psi^{-1}(\sqrt{c})) \quad (2.13)$$

modulo orientation where ψ^{-1} is given by

$$\psi^{-1}(x) = (\alpha x \alpha - 1)(\alpha x \alpha + 1)^{-1}. \quad (2.14)$$

Remark 16. A major drawback is that we cannot explicitly describe \mathcal{P}_p^* . One can take a set of parameters $(q_1, \dots, q_{p-3}) \in \mathcal{P}_p$, apply the above construction and afterwards check whether the created object actually is a non-degenerate right-angled p -gon.

If all the parameters q_i have norm $|q_i| > 1$ the proper orientation of the geodesics S_1, \dots, S_{p-3} is automatically guaranteed. So one needs to check the orientation of S_0, S_{p-2} and S_{p-1} . This can be done by calculating the norm of the double bridge cross ratios with the respective geodesic as the central one. Since the norm of the cross ratio is invariant under isometry we do not have to use the gauged double bridge cross ratios at this point. If the orientation of S_{p-1} is wrong, one can just invert it. If the orientation of S_{p-2} is wrong, one needs to replace the parameter q_{p-3} by $-q_{p-3}$ and the construction yields the same Π_p just with the inverted orientation of S_{p-2} . If the orientation of S_0 is wrong, one can replace the parameter q_1 by $-q_1$. This introduces a factor i to the left and to the right of the map ϕ_1^{-1} , where i is a root of -1 in the plane spanned by 1 and q_1 ; respectively $i = i_1$ if q_1 is real. Such a map is a rotation of 180° in the plane spanned by 1 and i .

After some exemplary calculations, we conjecture that for $p = 5$ the set

$$\{(q_1, q_2) \in \mathcal{P}_5 \mid \Re(q_1) \neq 0, q_1 \not\perp q_2\} \quad (2.15)$$

yields non-degenerate right-angled 5-gons up to orientation.

3. Right-Angled Polygons with Full Span

One natural question which arises when studying right-angled polygons is the question of the dimension of the resulting object. In this section we consider right-angled p -gons which have the highest possible dimension. This is the case if the p intersection points are the vertices of a $(p-1)$ -simplex. Thus the parameters will be taken from a $(p-2)$ -dimensional Clifford vector space $\mathbb{V}^{p-2} \subset \mathcal{C}_{p-3}$.

3.1. A Necessary Condition for the Realisation of $(p - 1)$ -Simplices

If we want some set of parameters to yield a simplex, we need to pass to a new dimension with every new geodesic in the construction. This basic idea results in the following theorem:

Theorem 17. *If the parameters $q_1, \dots, q_{p-3} \in \mathcal{C}_{p-3}$ give rise to a right-angled polygon Π_p whose intersection points are the vertices of a simplex, then the parameters together with 1 have to form a basis of the Clifford vectors according to $\langle 1, q_1, \dots, q_{p-3} \rangle = \mathbb{V}^{p-2}$.*

This theorem is a consequence of the following lemma:

Lemma 18. *Let (S_0, S_1, \dots, S_k) , $k \geq 2$ be a finite sequence of geodesics in upper-half space \mathbf{H}^{p-1} such that $S_0 = (-1, 1)$, $S_1 = (0, \infty)$ and $S_{i-1} \perp S_i$ for $i = 1, \dots, k$. Furthermore denote by $q_i := \tilde{\Delta}(S_{i-1}, S_i, S_{i+1})$ the gauged double bridge cross ratios of the respective double bridges for $i = 1, \dots, k-1$ and write $S_i = (S_i^-, S_i^+)$ for all geodesics.*

Then the linear subspace of \mathbb{V}^{p-2} spanned by the endpoints of the geodesics is the same as the subspace spanned by $\{1, q_0, q_1, \dots, q_{k-1}\}$. In symbols this means

$$\langle S_0^\pm, S_2^\pm, S_3^\pm, \dots, S_k^\pm \rangle = \langle 1, q_1, q_2, \dots, q_{k-1} \rangle. \quad (3.1)$$

The geodesic S_1 is left out since $\infty \notin \mathbb{V}^{p-2}$.

Proof. We prove this by induction over k . For $k = 2$ the lemma is plain, since $S_2 = (-q_1, q_1)$.

Hence, we have to prove $\langle 1, q_1, q_2, \dots, q_{k-1}, S_{k+1}^\pm \rangle = \langle 1, q_1, q_2, \dots, q_k \rangle$. We know that S_{k+1} is given as the image of $(-q_k, q_k)$ under the isometry Φ_{k-1}^{-1} . This isometry is given as a concatenation of the maps $\phi_i^{-1} : x \mapsto \sqrt{-q_i}(1+x)(1-x)^{-1}\sqrt{-q_i}$, $1 \leq i \leq k-1$. If $q_i \notin \mathbb{R}$, ϕ_i^{-1} restricts to an isometry on \mathbf{H}^3 where the boundary is given as $\partial\mathbf{H}^3 = \langle 1, q_i \rangle \cup \{\infty\}$. Likewise, ϕ_i restricts to an isometry on \mathbf{H}^4 where the boundary is given as $\partial\mathbf{H}^4 = \langle 1, q_i, q_k \rangle \cup \{\infty\}$. The case $q_i \in \mathbb{R}$ follows in the same manner, by yielding isometries leaving corresponding subspaces \mathbf{H}^2 and \mathbf{H}^3 invariant. Thus follows the statement. \square

Notice that the theorem above does not give a sufficient condition. If the parameters q_i are pairwise orthogonal to each other and pure Clifford vectors then the geodesics S_0 and S_{p-2} will contribute sides of length 0.

3.2. Hyperbolic 4-Simplices with an Orthogonal Cyclic Edge Path

In the end, it would be nice to have an *a priori* condition on the parameters of at least some family of pentagons. Dekster and Wilker [DW91] proved a criterion for the existence of n -simplices with vertices p_1, \dots, p_{n+1} with given side and diagonal lengths $l_{ij} = d(p_i, p_j)$, $1 \leq i < j \leq n+1$ in a Euclidean, spherical or hyperbolic space $X \in \{\mathbf{E}^n, \mathbf{S}^n, \mathbf{H}^n\}$. They call a symmetric $(n+1) \times (n+1)$ -matrix $L = (l_{ij})$ allowable if $l_{ii} = 0$ and $l_{ij} > 0$ for $i \neq j$. The matrix L is called *realisable* in the space X if there are $n+1$ points p_1, \dots, p_{n+1} in X with the given distances $d(p_i, p_j) = l_{ij}$. They gave a criterion for realisability in each of the three above cases. We are especially interested in the hyperbolic case.

Theorem 19 ([DW91, Theorem 1 (hyperbolic case)]). *Let $L = (l_{ij})$ be an allowable $(n + 1) \times (n + 1)$ -matrix and let its entries be used to form the $(n \times n)$ -matrix $S = (s_{ij})$ where*

$$s_{ij} = \cosh l_{i,n+1} \cosh l_{j,n+1} - \cosh l_{ij}.$$

Then L is realisable if and only if the eigenvalues of S are non-negative. If L is realisable then the dimension of each realisation is equal to the rank of S .

Now we can easily treat the case of a hyperbolic pentagon having a cyclic edge path along which all sides have the same length. With [DW91] we can get a criterion on the side lengths and due to symmetry it might be possible to find the corresponding orientations of the sides.

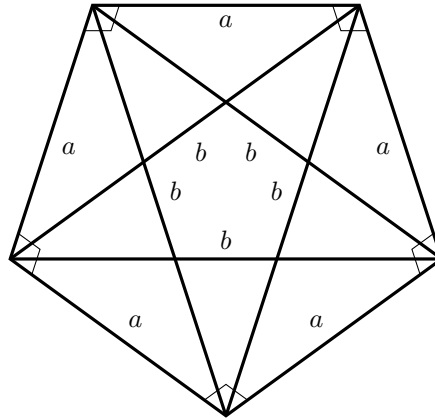


Figure A.4.: Hyperbolic Pentagon with Right-Angled Cyclic Edge Path

Lemma 20. *A right-angled hyperbolic pentagon $\Pi_5 = (S_0, \dots, S_4)$ with all side lengths equal to $a > 0$ is realisable as a 4-simplex if and only if $\cosh(a) < \gamma$, where $\gamma = \frac{1+\sqrt{5}}{2}$ denotes the golden ratio.*

Proof. By using hyperbolic trigonometry (see for example [Rat06, §3.5]) we obtain the relation $\cosh(b) = \cosh^2(a)$. We can now construct the two matrices L and S as in [DW91, Theorem 1].

We get

$$L = \begin{pmatrix} 0 & a & b & b & a \\ a & 0 & a & b & b \\ b & a & 0 & a & b \\ b & b & a & 0 & a \\ a & b & b & a & 0 \end{pmatrix}.$$

Let us define $x := \cosh(a)$. We then have

$$S = \begin{pmatrix} x^2 - 1 & x^3 - x & x^3 - x^2 & 0 \\ x^3 - x & x^4 - 1 & x^4 - x & x^3 - x^2 \\ x^3 - x^2 & x^4 - x & x^4 - 1 & x^3 - x \\ 0 & x^3 - x^2 & x^3 - x & x^2 - 1 \end{pmatrix}.$$

By Dekster's and Wilker's Theorem, the matrix L is realisable as a 4-simplex if and only if all the eigenvalues of S are positive. This is true if and only if S is positive definite. By Sylvester's criterion, it is enough to check that all the top left minors of S have positive determinant:

$$\begin{aligned}\det_1 &= x^2 - 1, \\ \det_2 &= x^4 - 2x^2 + 1 = (x^2 - 1)^2 = (x + 1)^2(x - 1)^2, \\ \det_3 &= -x^8 + 2x^7 + x^6 - 2x^5 - 2x^4 + 3x^2 - 1, \\ \det_4 &= \det(S) = 2x^{10} - 10x^9 + 15x^8 - 15x^6 + 2x^5 + 10x^4 - 5x^2 + 1.\end{aligned}$$

Notice that $x > 1$ since a must be greater than 0. Hence \det_1 and \det_2 are always greater than 0. Furthermore, \det_3 is positive whenever $-1 < x < \frac{1-\sqrt{5}}{2}$ or $1 < x < \frac{1+\sqrt{5}}{2}$, hence only the latter has to be considered. The determinant of S is positive everywhere except in $\frac{1-\sqrt{5}}{2}, 1, \frac{1+\sqrt{5}}{2}$, where it vanishes. Combining everything we obtain that S is positive definite whenever $1 < x < \gamma$, giving us the desired result. \square

Acknowledgements Both authors would like to thank their PhD supervisor Prof. Ruth Kellerhals for her encouragement and valuable advice throughout the work on this paper and for her constant support.

References

- [Ahl85] L. V. Ahlfors. 'Möbius Transformations and Clifford Numbers'. *Differential geometry and complex analysis*. Springer, 1985, pp. 65–73.
- [Ahl86] L. V. Ahlfors. 'Möbius transformations in \mathbb{R}^n expressed through 2×2 matrices of Clifford numbers'. *Complex Variables and Elliptic Equations* 5.2-4 (1986), pp. 215–224.
- [Bea12] A. F. Beardon. *The geometry of discrete groups*. Vol. 91. Springer Science & Business Media, 2012.
- [CM95] A. F. Costa and E. Martínez. 'On hyperbolic right-angled polygons'. *Geom. Dedicata* 58.3 (Dec. 1995), pp. 313–326. ISSN: 1572-9168. DOI: 10.1007/BF01263459.
- [CW98] C. Cao and P. L. Waterman. 'Conjugacy Invariants of Möbius Groups'. *Quasiconformal Mappings and Analysis* (1998), pp. 109–139.
- [DD19] E. Dotti and S. T. Drewitz. 'On right-angled polygons in hyperbolic space'. *Geometriae Dedicata* 200.1 (June 2019), pp. 45–59. DOI: 10.1007/s10711-018-0357-y.
- [DR14] F. Delgove and N. Retailleau. 'Sur la classification des hexagones hyperboliques à angles droits en dimension 5'. eng. *Ann. de la fac. des sci. de Toulouse Math.* 23.5 (2014), pp. 1049–1061. DOI: 10.5802/afst.1435.
- [DW91] B. V. Dekster and J. B. Wilker. 'Simplexes in spaces of constant curvature'. *Geom. Dedicata* 38.1 (1991), pp. 1–12. ISSN: 0046-5755. DOI: 10.1007/BF00147732.

- [Fen89] W. Fenchel. *Elementary geometry in hyperbolic space*. Vol. 11. De Gruyter Studies in Mathematics. Walter de Gruyter & Co., Berlin, 1989, pp. xii+225. ISBN: 3-11-011734-7. DOI: 10.1515/9783110849455.
- [FLP79] A. Fathi, F. Laudenbach and V. Poénaru. ‘Travaux de Thurston sur les surfaces’. *Astérisque* 66-67 (1979). Séminaire Orsay.
- [Par06] J. Parizet. *Quaternions et Géométrie*. http://www.math.unicaen.fr/lmno/semana/documents/parizet/Quaternions_A.pdf. Accessed: 2017-07-11. Feb. 2006.
- [Par07] J. Parker. *Hyperbolic Spaces. The Jyväskylä Notes*. <http://maths.dur.ac.uk/~dma0jrp/img/HSjyvaskyla.pdf>. Accessed: 2017-07-11. 21st Nov. 2007.
- [Rat06] J. G. Ratcliffe. *Foundations of hyperbolic manifolds*. Second. Vol. 149. Graduate Texts in Mathematics. Springer, New York, 2006, pp. xii+779. DOI: 10.1007/978-1-4757-4013-4.
- [Vah02] K. T. Vahlen. ‘Über bewegungen und complexe Zahlen’. *Mathematische Annalen* 55.4 (1902), pp. 585–593.
- [Wat93] P. L. Waterman. ‘Möbius Transformations in Several Dimensions’. *Adv. in Math.* 101.1 (1993), pp. 87–113. DOI: 10.1006/aima.1993.1043.
- [Wil81] J. B. Wilker. ‘Inversive geometry’. *The geometric vein*. Springer, 1981, pp. 379–442.

B. Magma Code

```
G<a, b, c, d> := Group< a, b, c, d | \
    a^2, b^2, c^2, d^2, (a*b)^3, (b*c)^3, (c*d)^3, (a*d)^6, (a*c)^2, (b*d)^2>;
torsion := [a, a*b, a*c, (a*d)^2, (a*d)^3, b*c, b*d, c*d];

candidates := LowIndexSubgroups(G, 24);

torsionfree := [];

k := 0;

for g in candidates do
    foundtorsion := false;
    ind := Index(G, g);
    repr := CosetAction(G, g);
    for t in torsion do
        for x in [1..ind] do
            if x eq x^repr(t) then
                foundtorsion := true;
                break;
            end if;
        end for;
        if foundtorsion then
            break;
        end if;
    end for;
    if not foundtorsion then
        torsionfree := Append(torsionfree, g);
        k := k+1;
        print "Gruppe ", k, ":\n";
        print g;
        Rewrite(G, g);
        print "\n";
    end if;
end for;
```


Simon Tobias Drewitz

Birthday 19 September 1991
Place of Birth Bad Dürkheim (Germany)
Nationality German

Education

since 09/2015 **Doctorate in Mathematics**
“*New Contributions to Groups of Hyperbolic Isometries*”
Université de Fribourg (Switzerland)

09/2014 – 09/2015 **Master of Science in Mathematics**
“*Hyperbolic Polytopes and the Polylogarithms*”
Durham University (United Kingdom)

04/2011 – 02/2014 **Bachelor of Science in Mathematics**
“*Hopfalgebren, Birkhoffzerlegung und Renormierung*”
Johannes Gutenberg-Universität Mainz (Germany)

2002 – 2011 **Abitur**
Werner-Heisenberg-Gymnasium Bad Dürkheim

Papers

The non-arithmetic cusped hyperbolic 3-orbifold of minimal volume, *Drewitz, S.T. & Kellerhals, R.*, submitted, arXiv:2106.12279

Cusp density and commensurability of non-arithmetic hyperbolic Coxeter orbifolds, *Dotti, E. & Drewitz, S.T. & Kellerhals, R.*, submitted

On right-angled polygons in hyperbolic space, *Dotti, E. & Drewitz, S.T.*, *Geom Dedicata* (2019) 200: 45., DOI:10.1007/s10711-018-0357-y

Invited Talks

06/2019 **Strategies to Find Hyperbolic Manifolds**, *SMS Annual Meeting and Conference*

01/2019 **On Right-Angled Polygons in Hyperbolic Space**, *Geometry and Topology Seminar*, Durham

03/2017 **On Right-Angled Polygons in Hyperbolic Space**, *Journée de Géométrie Hyperbolique*, Fribourg, with Edoardo Dotti

11/2016 **On Right-Angled Polygons in Hyperbolic Space**, *Oberseminar Geometrie*, Fribourg, with Edoardo Dotti

10/2015 **Volumes of Hyperbolic Orthoschemes in 3 and 5 Dimensions**, *Oberseminar Geometrie*, Fribourg

Attended Workshops and Conferences

06/2019 **Géométrie, topologie et arithmétique de façon hyperbolique**, *CUSO summer school*, Les Diablerets (Switzerland)

- 06/2019 **SMS Annual Meeting and Conference**, Neuchâtel (Switzerland)
- 12/2018 **Topology and Dynamics in the Swiss Alps**, *Borel Seminar*, Les Diablerets (Switzerland)
- 07/2018 **Growth in Topology and Number Theory: Volumes, Entropy, and L2-torsion**, *Workshop*, Hausdorff Center for Mathematics, Bonn (Germany)
- 02/2018 – 03/2018 **Subgroups and lattices of Lie groups**, *GAP-PARI-Sage days 93*, Faber Residency, Olot (Spain)
- 11/2017 **Géométrie et Topologie**, *Conférence en l'honneur de Christophe Bavard*, Institut de Mathématiques de Bordeaux (France)
- 08/2017 **Growth in Geometry and Topology**, *Borel Seminar*, Les Diablerets (Switzerland)
- 06/2017 **Geometric topology in Cortona**, *INdAM meeting*, Palazzone di Cortona (Italy)
- 03/2017 **Journée de Géométrie Hyperbolique**, *Workshop*, Fribourg (Switzerland)
- 01/2017 **Atelier PARI/GP 2017**, *Workshop*, Institut Camille Jordan, Lyon (France)
- 09/2016 **Geometry Days**, *Workshop*, Fribourg (Switzerland)
- 01/2016 **Seminar on Matroids in Algebra, Representation theory and Topology (SM'ART)**, *Borel Seminar*, Les Diablerets (Switzerland)
- 03/2015 **Cluster algebras and integrable systems**, *LMS Invited Lectures*, Durham University (United Kingdom)
- 03/2013 **Feynman Graphs and Motives**, *Spring School*, Bingen (Germany)

Research Visits

- 01/2018 **Dr. Brent Everitt**, *University of York*, United Kingdom
- 09/2018 **Dr. Brent Everitt**, *University of York*, United Kingdom

Professional Experience

- 03/2016 – 06/2021 **IT Correspondant**, *University of Fribourg*
- 09/2015 – 06/2021 **Teaching Assistant**, *Université de Fribourg*
- 05/2014 – 08/2014 **IT internship rollout planning**, *Accenture GmbH*, Frankfurt am Main
- 10/2011 – 03/2014 **Student Assistant**, *Johannes Gutenberg-Universität Mainz*

Outreach

- 09/2020 **Goûter Scientifique**, *Fribourg (Switzerland)*, support
- 09/2019 **MatheFest**, *Fribourg (Switzerland)*, organisational support
- 2016 – 2017 **Organisation of the Mathematikon**

TecDays

- 11/2017 **Cryptographie et codage: protéger vos secrets**, *Collège Saint-Michel*, Fribourg
- 10/2017 **Spiele in der Mathematik oder wo steht meine Bar?**, *Gymnasium Lerbermatt*, Bern

Summer Schools for Pupils

- until 2014 Assistance in the organisation of several summer schools of the Deutsche Schüler-Akademie and the Mainzer Mathe Akademie